ASSESSMENT OF RISK OF DISPROPORTIONATE COLLAPSE OF STEEL BUILDING STRUCTURES EXPOSED TO MULTIPLE HAZARDS

A Dissertation
Presented to
The Academic Faculty

by

Guoqing Xu

In Partial Fulfillment
of the Requirements for the Degree
Doctor of Philosophy in the
School of Civil and Environmental Engineering

Georgia Institute of Technology

August, 2011

ASSESSMENT OF RISK OF DISPROPORTIONATE COLLAPSE OF STEEL BUILDING STRUCTURES EXPOSED TO MULTIPLE HAZARDS

Approved by:

Dr. Bruce R. Ellingwood, Advisor
School of Civil and Environmental Engineering
Georgia Institute of Technology

Dr. Donald W. White
School of Civil and Environmental Engineering
Georgia Institute of Technology

Dr. Abdul-Hamid Zureick
School of Civil and Environmental Engineering
Georgia Institute of Technology

Dr. George A. Kardomateas
School of Aerospace Engineering
Georgia Institute of Technology

Dr. Kenneth M. Will
School of Civil and Environmental Engineering
Georgia Institute of Technology

Date Approved: May 5, 2011

ACKNOWLEDGEMENTS

First and foremost I offer my sincerest gratitude to my advisor, Dr. Bruce Ellingwood, for his technical expertise, professionalism, excellent guidance, and providing me with an excellent atmosphere for doing research. I would like to extend my gratitude to my thesis committee members: Dr. Abdul-Hamid Zureick, Dr. Kenneth Will, Dr. Donald White and Dr. George Kardomateas without whose insightful advice and guidance this study would not have been successful.

I would like to thank the help from the student colleagues and research engineers in the SEMM group: Naiyu, Chuang-Sheng, Andrew, Curtis, Eun and Soravit. The SEMM group is comprised of individuals with amazing talent all of whom are dedicated to sharing their knowledge with others. Thank you for the inspirational discussions and friendship you offered.

I am truly grateful for the unconditional support of my family, which made this work possible. My parents and brother have offered love, support and encouragement. Finally, I would like to thank my wife, Qiben. Her endless love and understanding have meant the world to me throughout the past few years and always.

TABLE OF CONTENTS

LIST OF TABLES

LIST OF FIGURES

SUMMARY

Vulnerability of buildings to disproportionate (or progressive) collapse has become an increasingly important performance issue following the collapses of the Alfred P. Murrah Federal Building in Oklahoma City in 1995 and the World Trade Center in 2001. Although considerable research has been conducted on this topic, there are still numerous unresolved research issues. This dissertation is aimed at developing structural models and analysis procedures for robustness assessment of steel building structures typical of construction practices in the United States, and assessing the performance of these typical structures.

Beam-column connections are usually the most vulnerable elements in steel buildings structures suffering local damage. Models of three typical frame connections for use in robustness assessment have been developed with different techniques, depending on the experimental data available to support such models. A probabilistic model of a pre-Northridge moment-resisting connection was developed through finite element simulations, in which the uncertainties in the initial flaw size, beam yield strength and fracture toughness of the weld were considered. A macro-model for a bolted T-stub connections was developed by considering the behavior of each connection element individually (i.e. T-stub, shear tab and panel zone) and assembling the elements to form a complete connection model, which was subsequently calibrated to experimental data. For modeling riveted connections in older steel buildings that might be candidates for rehabilitation, a new method was proposed to take advantage of available experimental data from tests of earthquake-resistant connections and to take into account

the effects of the unequal compressive and tensile stiffnesses of top and bottom parts in a connection and catenary action.

These connection models were integrated into nonlinear finite element models of structural systems to allow the effect of catenary and other large-deformation action on the behavior of the frames and their connections following initial local structural damage to be assessed. The performance of pre-Northridge moment-resisting frames was assessed with both mean-centered deterministic and probabilistic assessment procedures; the significance of uncertainties in collapse assessment was examined by comparing the results from both procedures. A deterministic assessment of frames with full and partial-strength bolted T-stub connections was conducted considering three typical beam spans in both directions. The vulnerability of an older steel building with riveted connections was also analyzed deterministically. The contributions from unreinforced masonry infill panels and reinforced concrete slabs on the behavior of the building were investigated.

To meet the need for a relatively simple procedure for preliminary vulnerability assessment, an energy-based nonlinear static pushdown analysis procedure was developed. This procedure provides an alternative method of static analysis of disproportionate collapse vulnerability that can be used as an assessment tool for regular building frames subjected to local damage. Through modal analysis, dominant vibration modes of a damaged frame were first identified. The structure was divided into two parts, each of which had different vibration characteristics and was modeled by a single degree-of-freedom (SDOF) system separately. The predictions were found to be sufficiently close to the results of a nonlinear dynamic time history analysis (NTHA) that the method

would be useful for collapse-resistant design of buildings with regular steel framing systems.

CHAPTER 1 INTRODUCTION

1.1 BACKGROUND

A disproportionate (or progressive) collapse is initiated by local damage to the structure that cannot be contained and propagates throughout the entire structure or a large portion of it, to the point where the extent of final damage is disproportionate to the initiating local damage. The partial collapse in 1968 of the multi-story large-panel apartment building at Ronan Point in the UK brought disproportionate collapse to the attention of the structural engineering community as a potential building performance issue. Interest in enhancing structural robustness through design to prevent or mitigate disproportionate collapse intensified following the bombing of the Alfred P. Murrah Federal Building in Oklahoma City in 1995, and again following the World Trade Center collapse in 2001. In the past decade, the literature on disproportionate collapse and extreme events has expanded significantly. The United States Federal government now is requiring an assessment of collapse susceptibility as part of design of new buildings as well as major renovation projects (GSA 2003; DoD 2009). With the need to address the imminent risk of terrorist attack, there has been a natural tendency to adapt exist existing technology to problems of risk reduction. However, research published to date only addresses a limited number of the issues involved in building vulnerability assessment and risk mitigation, and is insufficient to provide the technical support needed for improving building standards and achieving cost-effective solutions. This dissertation is aimed at providing some of that technical support for assessment of steel-frame buildings.

1.2 RESEARCH OBJECTIVES AND SCOPE

The research in this dissertation is aimed at developing practical structural models and an assessment framework for evaluating risk of disproportionate collapse for steel-framed building structures exposed to multiple hazards. To achieve this objective, the following research tasks are required and will be undertaken:

- Review and critically appraise current disproportionate collapse risk assessment frameworks.
- Collect and synthesize applicable test data with finite element models for estimating the behavior of damaged structural components and systems during disproportionate collapse.
- Investigate the behavior of typical beam-column connections under extreme conditions through finite element analysis.
- Develop a nonlinear static disproportionate collapse analysis procedure which is consistent with current design practice, and validate this procedure through nonlinear time-domain finite element analysis.
- Investigate the effects of uncertainties in the collapse-resisting capacity of structures and gravity loads on the performance of structures.
- Assess the disproportionate collapse risk of typical steel building structures.

The focus herein is on the behavior of steel frames immediately following initial damage, rather than on the development of disproportionate collapse following damage. This is because the focus of the *GSA* and *UFC* guidelines is on the containment of damage following notional element removal and preservation of life safety. Accordingly, sequential failures of structural columns and debris loading are not considered

1.3 OUTLINE OF THE DISSERTATION

The present chapter has introduced the motivation for this research. The remainder of this dissertation consists of 5 chapters, followed by a list of references.

Chapter 2 reviews the start-of-the-art of current research and practice on disproportionate collapse. Chapter 3 summarizes a methodology for modeling the behavior of connections for use in the analysis of structures following initial local damage, and presents models of three typical connections in steel frames. In Chapter 4, the connection models summarized in Chapter 3 are integrated into nonlinear finite element models of steel structural frames to allow the effect of catenary and other large-deformation action on the behavior of the frames and their connections to be examined. The robustness of typical steel building structures is assessed with these models. In Chapter 5, an energy-based nonlinear static pushdown analysis procedure is developed to provide an alternative method of static analysis of disproportionate collapse vulnerability that can be used as an assessment tool for regular building frames suffering local damage. Finally, Chapter 6 summarizes the major contributions of this research and makes suggestions for future inquiry.

CHAPTER 2 REVIEW OF PREVIOUS WORK

This chapter reviews current research on disproportionate collapse. Abnormal loads, which have the potential to cause initial damage to structures, structural models and analysis methods for modeling structures following initial damage, are summarized first. Following that review, strategies for mitigating the risk of disproportionate collapse are discussed. Risk assessment methods and cost-benefit analysis procedures are also summarized. Finally, a critical appraisal of current research is conducted following the review to discuss some of the existing issues that have yet to be resolved.

2.1 MODELING DISPROPORTIONATE COLLAPSE

To predict the response of steel building structures following local damage due to abnormal loads, the characteristics of abnormal loads, the nonlinear relation between forces and displacements in structural components and systems, finite element formulations of structural members under large deformations, and analysis procedures consistent with dynamic response need to be considered carefully.

2.1.1 Characteristics of Abnormal Loads

Abnormal loads may be categorized as impact loads (e.g., debris, missile impact, vehicular collision), pressure loads (e.g., natural gas explosions, bomb blasts), or deformation-related actions (fire, foundation subsidence). A few examples follow.

Natural gas explosions are potential hazards to commercial and residential buildings and can lead to severe direct and indirect damage to structures as shown by the Ronan Point collapse in 1968. The pressures of the explosions, depending on the

compartment venting and resonance of the air mass in the compartment, are usually less than 2.5 psi (17 kPa). The pressures from a natural gas explosion act mainly on the compartment boundaries, and its effects on a structure are basically static. According to the early study by Leyendecker and Burnett (1976), the mean rate of occurrence in residential buildings was approximately 2×10^{-6}/dwelling unit/year. More recent studies (NIST 2007) have confirmed this value.

Detonations of high explosives initially create a positive incident and reflective shock wave pressure by highly compressed air decaying rapidly in milliseconds. Following the positive pressure, a negative pressure phase, which usually is less important in structural design than the positive pressure, occurs with longer duration. The pressure-time history often can be modeled as a triangular impulse with essentially instantaneous rise time and linear decay. Although the transient pulse of an explosive detonation often has little impact on the overall structural system due to its short duration and localized effect, it can cause severe local damage to some individual elements in close proximity to the explosion. The average annual incidence of bomb explosions in the building population at large is very small (0.34×10^{-6}) (Leyendecker and Burnett 1976). However, certain buildings such as government buildings, major financial institutions, or public assembly buildings, may have a higher risk exposure.

Buildings are exposed to fire hazards. Also, fire can follow explosions and frequently follows earthquakes when building utilities are disrupted. Elevated temperatures caused by fire in a building will lead to changes to internal forces of structural elements as well as the reduction of the failure criterion due to deterioration of strength and stiffness of structural materials (Poh 2001). The whole building structure

may collapse following the buckling of columns in the case of increasing temperature. For instance, the fires that followed the impact of debris from the collapse of World Trade Center Building 1 led to the collapse of World Trade Center 7 (NIST 2008). The annual mean occurrence rate of fully developed fires in buildings in urban areas which pose a significant risk of structural damage is, in-order-of-magnitude, 10^{-8} per square meter of occupied space (Ellingwood and Dusenberry 2005).

2.1.2 Structural Models and Modeling Issues

While there are some similarities in the philosophies of modeling building frames for earthquake resistance and disproportionate collapse resistance, there are some significant differences as well. Perhaps most significant, the emphasis in the analysis of vulnerability to disproportionate collapse following local damage is on the behavior of the structure in resisting gravity loads instead of lateral loads (Powell 2005), while in earthquake-resistant design, the emphasis is on lateral force resistance. For earthquake analysis, floor slabs of a building often are assumed as rigid diaphragms and are not included in the analysis model that determines the distribution of lateral forces throughout the frame. Moreover, the gravity frames of the buildings, whose lateral stiffness is essentially assumed to be negligible, typically are not modeled in earthquake analysis, except that the gravity loads on the gravity frames are included to take into account the so-called P-Delta effects. The steel moment-resisting frames (SMRF), which in modern construction in the United States often are situated at the building perimeter, are modeled in a two-dimensional way unless the building plan is highly irregular, and the masses are lumped at the levels of the beams. For disproportionate collapse analysis,

in contrast, the interaction between the beams and the floor slabs in the building has a substantial effect on the behavior of the frame. The gravity frames, which are less ductile and more vulnerable than SMRF, are susceptible to local damage incurred by abnormal loads as well as the perimeter SMRFs. To assess the behavior of the whole structure system of the building to resist disproportionate collapse, the gravity frames need to be taken into account in the analysis model as well.

As with earthquake-resistant design, in checking the capacity of a frame to withstand local damage without disproportionate collapse, economic costs make it impractical to design all structural elements to remain in the elastic range following a local damage. On the other hand, the assessment of disproportionate collapse susceptibility generally will not be meaningful if the nonlinear behavior of the structural elements is not considered, either directly or indirectly. Catenary action plays a significant role in resisting gravity loads when large deflections of horizontal members develop, provided that tension anchorage can be provided. Hence, the behavior of connections and beams under large deformations from gravity loads must be investigated. A significant amount of experimental and analytical research has been accomplished on the behavior of connections under seismic loading as part of the SAC Project (FEMA 1997b). However, the effect of tensile forces, which may be substantial if the catenary effect can be developed, was not considered in this body of connection research.

To address this problem, the behavior of steel connections during disproportionate collapse has been examined using high-fidelity (detailed) finite element models in recent research. For example, the behavior of seismically designed steel special moment frames with post-Northridge moment-resisting connections has been investigated by Khandelwal

and El-Tawil (2007), who modeled two-bay frame subassemblies with spans of 30 ft (9.14 m) using the computer program LS-DYNA (Hallquist 2005). The subassemblies were analyzed by imposing prescribed vertical displacements on the top of the removed center column to represent the scenario of a sudden column loss (the motivation for this approach is discussed in more detail in the following section). The connections were modeled using shell elements, and the connection failure mode was assumed to be ductile. The predicted structural behavior was found to be influenced substantially by factors such as the ratio of yield to ultimate strength in the beams and columns and beam web-to-column details; catenary action in these frames provided substantial capacity in resisting collapse.

The behavior of shear connections in the interior gravity frames in buildings with steel framing systems designed for Seismic Design Category C and D (ASCE 2006) following sudden interior column removal was investigated using high-fidelity finite element analyses (LS-DYNA) (Sadek et al. 2008). A macro-model representing the simple single-plate shear connections in these frames was also developed as part of this research. This investigation revealed that following notional column removal, gravity loads are primarily resisted by catenary action leading to increasing tensile forces in beams and connections. These tensile forces are the main cause of failure in shear connections.

Kaewkulchai and Williamson (2004) presented a modified beam element formulation based on the beam element developed by Kim (1995) for disproportionate collapse analysis of planar frames. The P-Δ effect was considered by the geometric stiffness matrix. The beam element lumped the plasticity at the beam ends and the effect

of axial force on yield moment was also incorporated. A damage index was used to determine the onset of structural element failure. A damage model depending linearly on the maximum deformation and the accumulated plastic energy was proposed. Liu (2007) developed a generic beam-column finite element formulation with stiffness degradation based on an analytical elliptic force-deformation model. While elastic-plastic bending, shearing and axial deformations were considered in the formulation, the model was based on an assumption of small deformation. A corotational approach (Crisfield 1991) was found to be appropriate to describe the behavior of frames under large displacements. Beam-column elements based on the moderate rotation and small strain assumptions within the corotational framework are capable of capturing the large displacement and rotation behavior required for post-damage assessment of the frame (Alemdar and White 2005).

2.1.3 Methods for Analyzing Disproportionate Collapse Susceptibility

Detailed simulation of post-damage responses of structures under abnormal loads raises significant research issues. First, it is difficult to model abnormal loads such as blast, vehicular impact and fire due to lack of available data and analytical models. Secondly, modeling responses involves certain advanced techniques including fluid-solid interaction, arbitrary Lagrangian-Eulerian (ALE) formulation, etc., which are not easily adapted to routine structural design analysis. Moreover, even if the data and techniques are available, simulation requires advanced finite element analysis software (e.g. LS-DYNA) and is very time-consuming because of the refined finite element mesh required in such models. Hence, it is not practical to apply such kind of analyses in routine

building evaluation. The alternative load path method (APM) of analysis (Ellingwood and Leyendecker 1978; Breen and Siess 1979), in which the capability of a structure to sustain local damage is evaluated by notionally removing major gravity load-bearing elements (columns, bearing walls), one at a time, and determining, through analysis, whether the damaged structure can reach a state of equilibrium without further propagation of damage, is an appropriate approach to analyze disproportionate collapse of structures in a threat-independent way. The *GSA* guidelines (GSA 2003; DoD 2009) permit this structural analysis to be performed by either static or dynamic analysis and permit the use of either linear or nonlinear structural analysis methods, while in the *UFC* guidelines (DoD 2009), linear dynamic analysis is not allowed.

The scenario of sudden member removal usually leads to a conservative assessment of disproportionate collapse vulnerability, in that the damaged members usually have some residual structural capacity. Furthermore, the beneficial effects of arching or catenary action following local damage are seldom considered in traditional safety checks. The sudden removal of structural members has the same effect as the sudden application of the structural forces in those members in the opposite direction (Powell 2005). Following sudden element removal, the structure undergoes transient dynamic response, forces redistribute in the system, and the damaged structure either comes to a new equilibrium point or the collapse process progresses further. While nonlinear dynamic time history analysis (NTHA) is believed to be the most realistic method to obtain the forces and deformation demands that develop in the system subsequent to initial damage (Marjanishvili 2004), its application requires considerable skill, the computational demands are significant, and information necessary to perform

the analysis correctly might not be available. The *UFC* stipulate that when the static analysis option is selected, the structural response must be amplified by a load increase factor for linear analysis and a dynamic increase factor for nonlinear analysis to account for dynamic effects. The value of the load increase factor depends on the structure type and the way that damage is controlled (i.e. deformation controlled or force controlled). Linear static analysis, while being the simplest, seldom captures the structural behavior in the inelastic range accurately. The value of the dynamic increase factor specified in the *UFC* depends on the structure type and plastic rotation limit; other factors, such as axial forces in beams (i.e. catenary effect) and structural configuration, which are known to have a significant effect on the nonlinear dynamic response, are not considered.

A nonlinear quasi-static computational procedure to predict the failure sequence of disproportionate collapse was developed by Grierson et al. (2005). Gravity loads and debris loads were incrementally applied to the damaged structure, and the failure of structural elements was tracked sequentially. The dynamic effect of debris loads was taken into account indirectly by an amplification factor. This approach simulates the highly dynamic behavior of a damaged structure through a highly simplified analysis procedure which may lead to misleading results.

Improved nonlinear static analysis approaches based on achieving an energy balance in the damaged structural system have been developed recently (Dusenberry and Hamburger 2006; Izzuddin et al. 2008). In these approaches, the energy balance between work done by the external loads and the strain energy stored in structural members is checked. Dusenberry and Hamburger (2006) presented two practical methods of performing the subsequent structural analysis, one consistent with linear elastic analysis

and the other requiring elastic-plastic analysis. In the former, the structure must be re-analyzed to obtain the internal forces and the corresponding displacements every time that a plastic hinge is formed. In the latter, each floor is treated independently and only a simplified model involving a single beam with a concentrated force applied in the middle and one spring at each end to simulate the boundary conditions is considered. In both methods, the strain energy is calculated directly from the internal forces and the corresponding displacements. Izzuddin, et al. (2008) developed a multi-level simplified assessment framework for disproportionate collapse, in which the nonlinear static response (i.e. the total gravity load and the deflection of beams above the removed column denoted as system deformation) can be obtained from either detailed structural model or simplified model. In the simplified model, the nonlinear static response of a high level model (e.g. a floor system) is assembled from the nonlinear static responses of low level models for each component (e.g. beams) using a work-related factor to account for the effect of load distribution type and a deformation compatibility factor to describe the relationship between the system and component deformation. The maximum dynamic response can be obtained by calculating the equivalence between external work (i.e. the product of the actual total gravity load and the system deformation) and internal energy (i.e. the integration of the nonlinear response).

To illustrate detailed conceptual disproportionate collapse analysis procedures using common structural analysis software, Marjanishvili and Agnew (2006) studied a nine-story SMRF building using SAP2000 (Computers & Structures Inc. 2002), providing a step-by-step explanation of all four methods permitted by the *GSA* guidelines. Although they stated that dynamic analysis procedures are easy to perform

and can produce more accurate results, they noted that the most difficult part of disproportionate collapse analysis is how to model the nonlinear force-displacement relationships of structural components and the interaction between components. For instance, the aforementioned behavior of slabs and connections have not been clearly investigated until now due to lack of test data.

Kaewkulchai and Williamson (2004) presented a dynamic analysis procedure to update the state of a structure following member failure for disproportionate collapse analysis of planar frames. To account for the impact effect of debris loading, they proposed a modeling strategy using rigid body impact theory. A two-node element condensed from a three-node element with the third node to represent the behavior of impact point was introduced. A five-story, two-bay frame was analyzed to show the importance of impact. With proposed macro connection models (Khandelwal et al. 2008), a two-dimensional, ten-story SMRF designed according to moderate and high seismic requirements was studied using the APM by nonlinear dynamic analysis in LS-DYNA. Khandelwal, et al noted that the improvement in disproportionate collapse-resistant performance of SMRF designed according to high seismic requirement was not due to improved ductile detailing but rather from layout and system strength. Foley et al. (2006) studied the robustness of the pre-Northridge moment-resisting frames using the APM but assumed that connection failure could be described by a simple interaction relationship among moment, axial and shear forces and did not develop a physics-based connection model. Finally, Sadek et al. (2008) showed that an interior gravity frame with single-plate shear tab connections and a composite floor system could not withstand the sudden removal of one column without collapse developing.

2.2 MITIGATION STRATEGIES FOR DISPROPORTIONATE COLLAPSE

A mathematical framework of disproportionate collapse risk analysis was proposed by Ellingwood(2006), defining the annual probability of collapse as

$$P[Collapse] = \sum_H \sum_D P[Collapse \mid D]P[D \mid H]\lambda_H \quad (2\text{-}1)$$

where H is the possible hazard event set, D is the set of events involving local damage, λ_H is the annual mean rate of occurrence of one specific event in H, $P[D \mid H]$ is the conditional probability of one damage state in D, given one event in H and $P[Collapse \mid D]$ is the conditional probability of disproportionate collapse, given one damage state in D. Cost-benefit analysis to minimize disproportionate collapse risk involves taking specific actions to change one or more terms in Equation (2-1) with constraints (e.g. certain amount of funding). Accordingly, there are basically three mitigation strategies for mitigating disproportionate collapse: (1) to reduce hazard occurrence rates (i.e. event control); (2) to prevent collapse through integrity and ductility requirements, retrofit, active and passive measures, etc. (Ellingwood and Dusenberry 2005); and (3) to prevent severe local damage which may lead to a disproportionate collapse (i.e. direct design).

2.2.1 Event Control Methods

The risk of disproportionate collapse to a building or other structure can be reduced by controlling the hazard occurrence through non-engineering means including installing protective barriers, limiting access to the building, requiring minimum stand-off distance, etc. If the annual mean hazard occurrence rate can to be less than the target threshold, the risk of collapse may not need to be considered. If there is no economically

effective way to reduce the mean occurrence rate to below the target threshold, the structure must be strengthened to prevent or absorb local damage.

2.2.2 Direct Design Methods

The direct design method involves strengthening key structural elements to withstand local damage or designing for alternative load paths (GSA 2003; ASCE 2006; DoD 2009) to permit local damage without collapse, or a combination of the two. In the specific local resistance method, critical load bearing structural components are designed to resist specified abnormal loads (e.g., blast, vehicular collision, etc.). This approach is quite difficult to implement in practice, in that the response of critical components to each kind of specific abnormal load needs to be identified and designed against through sophisticated analysis. As discussed previously, the threat-independent APM can simplify analysis and has been used widely in disproportionate collapse resistance design.

2.2.3 Indirect Design Methods

In the indirect design methods (GSA 2003; ASCE 2006; DoD 2009), the capacity of structures to resist disproportionate collapse is enhanced through minimum requirements of structural continuity, integrity, strength and ductility without consideration of specific abnormal loads. The approach is similar to earthquake-resistant design in regions of low to moderate seismicity. In structural systems, it is usually achieved by providing beam-column connections, column splices, and horizontal and vertical ties to transfer forces between structural elements. Other indirect design methods include installation of steel cables under slabs (Astaneh-Asl 2003), use of energy absorbing devices (Zhou and Yu 2004), etc.

2.3 RISK ASSESSMENT AND COST-BENEFIT ANALYSIS

The incidence and magnitude of various abnormal and extreme environmental events that might lead to disproportionate collapse of structures are uncertain. At the present time, assessment methods found in existing Federal guidelines are entirely deterministic; the types of extreme events and corresponding uncertainties are not taken into account, and a threat-independent scenario (i.e. sudden column removal), is usually adopted to assess the robustness of a structural system. In a probabilistic assessment, the uncertainties are modeled through assigning probability distributions to the demands and capacities. Until recently, uncertainties in structural demands or properties of structural materials could not be considered. However, based on the probabilistic assessment frameworks, disproportionate collapse risk mitigation strategies can be optimized with specified risk-informed decision-making criteria.

2.3.1 Deterministic Performance Assessment Frameworks

In the *UFC* and *GSA* guidelines (GSA 2003; DoD 2009), structural vulnerability is assessed through one of four approved methods. The limit of demand to capacity ratio is checked if a linear analysis procedure is used, while for a nonlinear analysis procedure, the ductility limit is the criterion to determine whether the structure can sustain local damage. Izzuddin et al.(2008) proposed to use the system pseudo-static response as the unique robustness measure, defined by the relationship between the gravity loads and the maximum dynamic displacement of connections above the removed column calculated from the proposed energy-based static analysis. Other factors (e.g. energy absorption capacity, redundancy and ductility) affecting structural robustness are implicitly included

in the response of a structure following a sudden column removal. In the deterministic assessment methods, the spatial uncertainties in damage are considered by removing columns at different locations of a structure (e.g. perimeter columns and interior columns at all floors).

2.3.2 Probabilistic Risk Assessment and Cost-benefit Analysis

Baker et al. (2008) proposed an index of robustness, which is the ratio of the direct risk to total risk (i.e. the direct and indirect risk) caused by abnormal loads. The direct risk is defined as the summation of the product of the direct consequence of each extreme event and its occurrence probability. The indirect risk is the summation of the product of the indirect consequence of each extreme event, its conditional probability given that the corresponding direct consequence happens and the occurrence probability of the corresponding extreme event. The assessed structure is completely robust when the robustness index is equal to 1, implying means that there are no indirect consequences. There are some deficiencies of the robustness index. First, it is difficult to quantify the indirect risk in that the indirect consequences including indirect economic loss, social impact, etc. cannot easily to be evaluated. Second, it does not properly account for the effects of the event control methods. For example, suppose that two structures are exposed to a bomb blast; one structure loses one column initially but does not collapse, while the second structure is undamaged as a result of a protective barrier. Although the robustness index is equal to 1 for both structures, the second structure is obviously more robust than the first one. Third, the condition of initial local damage is not considered in

the index. For example, the index does not change if one or more structural components are lost due to the same abnormal load, provided that no collapse occurs.

Cost-benefit analysis offers a method to minimize risk and maximize the robustness index. One such probabilistic assessment framework and corresponding cost-benefit analysis of installing reinforced window glazing was presented by Stewart and Netherton (2008), who developed fragility and blast reliability curves for window glazing subjected to blast loading to assess the risk to occupants. In another technical note (Stewart 2008), a preliminary cost-benefit analysis of risk mitigation strategies (e.g. blast resistant glazing, strengthening perimeter columns, etc.) to reduce the risk of terrorist attack for commercial buildings in the United States was conducted. The probability of attack was calculated directly from the number of the terrorist attacks which had already happened and the number of commercial buildings that are vulnerable to attack. The cost of protective measures and cost consequence of failure were also characterized. It was concluded that it is not cost-effective to reduce the risk of terrorist attack through commonly used protective measures for typical large commercial buildings in the case of nonspecific threats, while for buildings with high damage cost or facing a specific threat, it may be economical to adopt such protective measures.

2.4 CRITICAL APPRAISAL OF CURRENT RESEARCH

Assessment of disproportionate collapse vulnerability involves highly nonlinear dynamic response under loads caused by abnormal or extreme environmental events which have low probability of occurrence and high consequence. Despite the amount of

research that has been done on this topic recently, a number of significant research issues remain unanswered:

1. The behavior of damaged structures is poorly understood.

The nonlinear behavior of structural components during collapse is complicated and not easily derived solely from analytical models. Experimental testing is the most effective way to capture the behavior; unfortunately, most existing test data have been developed for other reasons (e.g., seismic) and are not easily adaptable to the problem at hand. An alternative way of investigation is to analyze structural components with detailed finite element models. However, the constitutive relationships of materials and failure modes are very difficult to determine. For example, while the behavior of post-Northridge steel moment-resisting connections and simple shear connections during earthquakes has been studied extensively using high-end finite element analysis software (Khandelwal and El-Tawil 2007; Sadek et al. 2008), the behavior of other connections which are commonly used in non-seismic zones of the country under extreme loading conditions has not been examined. Slabs may have important effects on the capacity of buildings to prevent disproportionate collapse according to finite element analysis results and limited test data (Astaneh-Asl et al. 2001; Sadek et al. 2008); most existing analytical studies do not include the slab. Moreover, failure criteria for structural components have to be established.

2. The results of existing analysis methods are not consistent.

Although the *UFC* and *GSA* guidelines permit four analysis procedures, these procedures may lead to different results even for the same structure under the same initial damage scenario (Marjanishvili and Agnew 2006). It is not reasonable to predict the

highly nonlinear response of structures during collapse using linear analysis procedures. On the other hand, taking into account current design practices, time-domain nonlinear dynamic analysis seldom is practical in design of new buildings, although it may be feasible in certain renovation/rehabilitation situations. Hence, a new static nonlinear analysis procedure consistent with finite element models built for design should be developed. Energy-based nonlinear static analysis methods have received little attention but appear quite promising in this regard. In one such method proposed by Dusenberry and Hamburger (2006), the strain energy is calculated directly from the internal forces and the corresponding displacements of structural elements. For a complex structure with various connections, beams and columns, their method loses some of its attractiveness. In another method presented by Izzuddin et al.(2008), the interactions among the components comprising a high level model may be over-or underestimated through separate analysis of each low level component, and the accurate deformation compatibility factors cannot be established easily without analysis because of the nonlinear response that follows local damage. Perhaps most importantly, instability of the building frame, which is likely to be a consideration in assessment of flexible multi-story frames, has not been considered in either of these energy-based methods.

3. The relationship between the deterministic and probabilistic assessment frameworks has not been properly examined.

In the deterministic assessment, a structure is considered to be safe if it can sustain the stipulated local damage, sudden column loss. In the probabilistic assessment framework, the structure is judged to be safe if the annual probability of structural collapse, which is obtained through considering uncertainties in extreme events and

structural capacities, is below the target risk level. If the structure is considered safe in the deterministic assessment frameworks, which safety level can it achieve when assessed probabilistically and with what level of confidence? There has been no examination of the level of safety implied in the GSA or DOD criteria. A linkage between the levels of safety in the deterministic and probabilistic assessment frameworks is required.

2.5 CLOSURE

This review has identified some of the pressing research issues in disproportionate collapse, which are addressed subsequently in the following chapters of this dissertation. The behavior of damaged structures, especially beam-column connections, which are usually most vulnerable components during collapse, is studied in Chapter 3. An energy-based static analysis method, which can provide consistent results with dynamic analysis, will be developed as an alternative assessment tool. Risks of disproportionate collapse of typical steel building structures will be assessed with developed structural models. Finally, the effects of uncertainties in the collapse-resisting capacities of structures and gravity loads are also investigated through analysis on the prototype pre-Northridge moment-resisting frames, leading to insights and perspectives on the development of practical collapse-resistant design tools.

CHAPTER 3 MODELING CONNECTION BEHAVIOR

Beam-column connections are among the most vulnerable components during disproportionate collapse and the most difficult to model accurately. Unfortunately, the experimental data on the performance of connections during collapse are quite limited. Therefore, analytical connection modeling approaches are utilized in this research. Generally, three modeling approaches can be used. The first approach is to investigate the connection behaviors through detailed finite element modeling (micro-modeling). The second is to obtain a connection macro-model by assembling the corresponding models of each separate element in a connection. The third method is to adapt the records of seismic tests to develop a model for the analysis of general structural integrity under gravity loads.

Three connection models for use in robustness assessment are developed in this chapter according to these different modeling methods summarized above. We begin by developing probabilistic model of a pre-Northridge moment-resisting connection through finite element simulations, in which the connection fracture strength is defined using a J-integral formulation of fracture demand. Next, a macro-model for bolted T-stub connections is developed by modeling the connection components (i.e. T-stub, shear tab and panel zone) with a series of rigid elements and connecting springs, in which the element properties are developed by analysis and subsequently are calibrated to experimental data. Finally, for modeling riveted connections in older buildings (such models might be important for assessing the vulnerability of older buildings), an improved analytical method is proposed to take advantage of available experimental data

from tests of seismic connections and to model unequal compressive and tensile stiffnesses and catenary effects.

3.1 MOMENT-RESISTING CONNECTIONS

The pre-Northridge moment-resisting frames studied in the SAC Project (FEMA 2000a) were fabricated with welded flange-bolted web (WFBW) connections, which were typical of construction in seismic regions in the Western United States prior to the 1994 Northridge earthquake. One representative pre-Northridge moment-resisting connection is illustrated in Figure 3.1. Beam flanges were welded to column flanges using full-penetration groove welds. Shear tabs were welded to the column flange and bolted to the beam web. A self-shielded flux cored electrode, E70T-4, which has a very low toughness, was commonly used at that time in fabricating such connections. Typical field welding practice left the weld-backing bar in place, which resulted in an initial flaw. The dominant failure mode in these connections, observed in inspections following the Northridge earthquake and verified in subsequent tests, involved fracture of the E70T-4 weld metal connecting the beam bottom flange and column flange (FEMA 2000b), with the crack propagating rapidly into the beam or column webs through flanges.

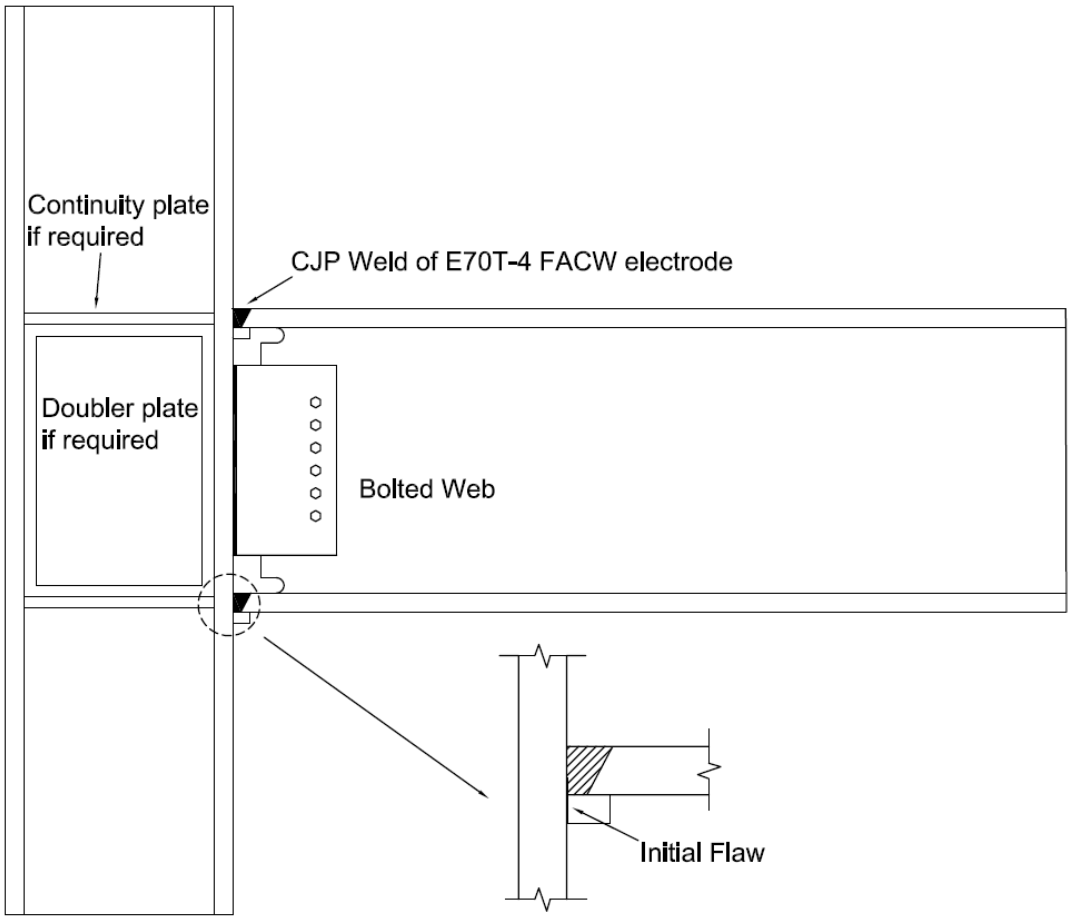

Figure 3.1 Pre-Northridge steel moment-resisting connection (after FEMA 1997b)

A large number of tests and analytical studies of welded connection behavior were performed after the Northridge earthquake. A summary of test results applicable to the frames considered herein, presented in Table 3.1, indicates that the variability in connection capacity (normalized by the fully plastic moment capacity of the beam) is quite large (FEMA 1997b; SAC Connections Database <http://www.sacsteel.org/connections/>). In Table 3.1, the mean yield strengths (FEMA 1995) are utilized if the corresponding data are not available (N/A). Joh and Chen (1999) examined the fracture strength of the pre-Northridge moment-resisting connections with

linear elastic fracture mechanics and 3-D finite element simulations to reflect the uncertainties in initial flaw size and beam yielding strength. In Chi et al. (2000), the effects of various factors on the fracture demand in the elastic-plastic range were investigated with 2-D and 3-D finite element analyses (FEA). Matos and Dodds (2001) modeled the connection fracture probabilistically, and developed a Weibull stress model for cleavage through a 3-D FEA which incorporated major geometric factors characterizing connections (e.g. access holes, shear tabs, etc.). The probability distribution of fracture for the same connections in the elastic range was derived theoretically based on a simplified 2-D crack model by Righiniotis and Imam (2004).

3.1.1 Model Development

To simulate the behavior of pre-Northridge moment-resisting connections in a frame following sudden column loss, a subassembly with W14x257 columns and W36x150 beams representing two bays of a frame, each spanning 30 ft (9.1 m), with a damaged center column (no damage to the center connections) was modeled, as shown in Figure 3.2. The columns extended half of the story height (i.e. 6.5 ft (2 m)) above and below the floor and were pinned at their ends, under the assumption that inflection points are located approximately at the middle of each story. Due to the symmetry of the subassembly, only half of the subassembly was modeled explicitly, as shown in Figure 3.2(a). Strain rates in members in the immediate vicinity of the damaged column were sufficiently small that dynamic effects on weld fracture toughness, beam and column yielding strength could be ignored in the analysis. Static analyses were performed by pushing down on the subassembly at the top of the center column under displacement

control. Eight-node brick elements with reduced integration were used except that the area around the weld access holes were modeled by six-node wedge elements. The fillet weld between the shear tab and beam web as well as the bolts were modeled with the assumption that the fillet weld does not fail and the deformation of bolts is negligible prior to the initiation of fracture of the weld metal connecting the beam bottom flange and column flange. The relatively small vertical displacement makes this assumption reasonable. The steel in the column, beam and connection and the E70T-4 weld between beam and column flanges were modeled as isotropic elastic-plastic materials characterized by a von Mises yield surface.

To simulate the fracture demand from the initial flaw in the weld metal connecting the beam bottom flange and column flange accurately and to reduce the time required for the computation, a refined sub-model of the subassembly, including the backing bar and a portion of beam and column flanges, was developed, as illustrated in Figure 3.2(b). The boundary conditions for the sub-model were determined from the global model results (e.g. displacements). The fracture demand was quantified in terms of a J-integral (Rice 1968) for the elastic-plastic analysis conducted in this investigation. The J-integral, which is path-independent, represents the rate of change of net potential energy of a crack front of unit thickness with respect to crack advance in the elastic range, and the singularity strength at the crack tip in the inelastic range (Barsom and Rolfe 1999). The numerical value of the J-integral was calculated by evaluating a contour integral, in which the contour is defined as a ring of elements surrounding the crack tip.

Table 3.1 Summary of pre-Northridge connection tests from SAC project

Test ID	Beam Steel	Beam Section	Yielding Strength (ksi)	Maximum deflection (in)	Load at Failure (kip)	Normalized Failure Moment
AD1	A36	W21x68	N/A	1.5	108	1.11
AD11	A36	W21x68	N/A	2	120	1.26
AD12	A36	W21x68	N/A	2	95	1
AD2	A36	W21x68	N/A	2.25	105	1.08
EERCPN1	A36	W30x99	50	2.8	105	0.95
EERCPN2	A36	W30x99	49	2.8	112	1.04
EERCPN3	A36	W30x99	47	4.2	122	1.18
LA1	A36	W36x150	38	1	130	0.71
LA2	A36	W36x150	38	1	160	0.87
UCBPN3	A36	W36x150	41	2.7	198	1.19
UCSD1	A36	W30x99	47	1.4	93	0.9
UCSD2	A36	W30x99	47	2.8	115	1.11
UCSD3	A36	W30x99	47	2.8	115	1.11
UCSD4	A36	W30x99	47	1.2	80	0.77
UCSD5	A36	W30x99	47	1.2	80	0.77
USC5	A36	W24x76	N/A	1.5	115	0.95
USC7	A36	W24x76	N/A	2.2	120	0.99
UTA1	A36	W36x150	42	1	130	0.76
UTA2	A36	W36x150	42	2	175	1.02
UTA3	A36	W36x150	42	1	120	0.7
UTAISC1A	A36	W36x150	40	1	170	0.96
UTAISC1B	A36	W36x150	40	1.5	200	1.13
UTAISC2A	A36	W36x150	40	0.8	150	0.85
UTAISC2B	A36	W36x150	40	1.8	220	1.24
UCBPN1	A572Gr50	W36x150	61	2.5	223	0.9
UCBPN2	A572Gr50	W36x150	61	1.6	195	0.79
UMSP1.1	DualA36	W24x68	N/A	1.42	47	0.68
UMSP1.2	DualA36	W24x68	N/A	1.42	50	0.72

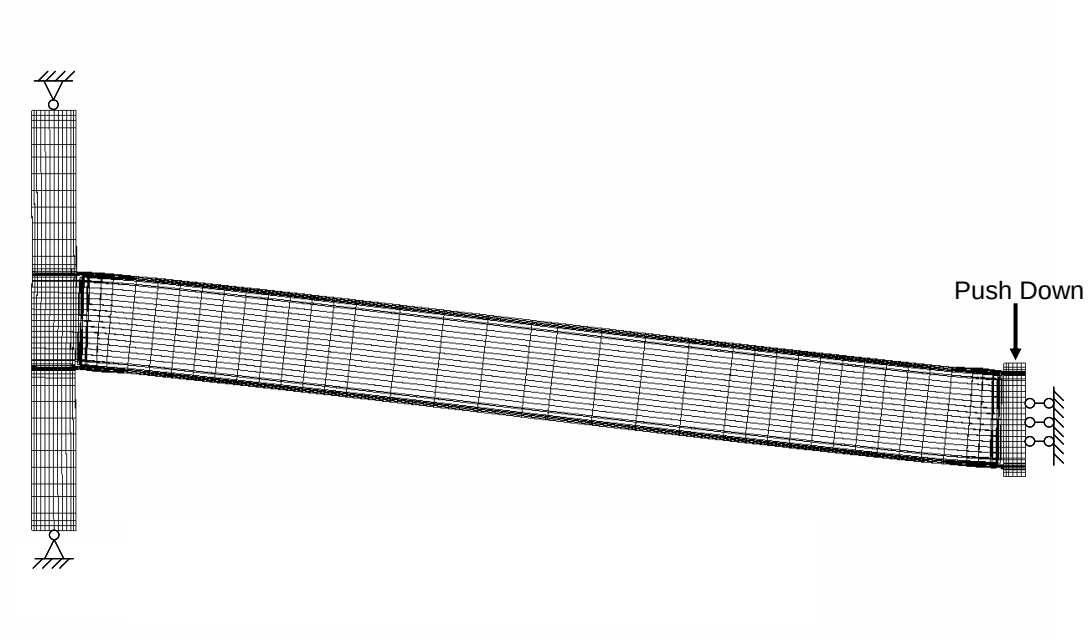

(a) Finite element model of the subassembly and boundary conditions

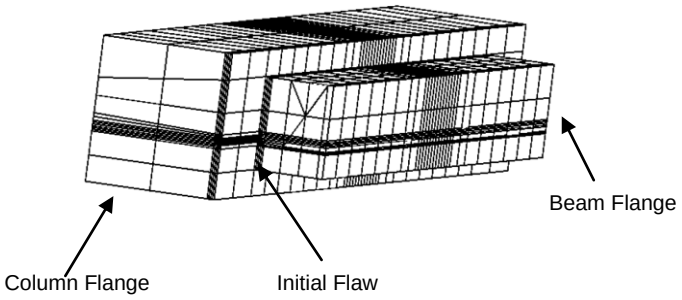

(b) Submodel including backing bar and a portion of beam and column flanges

Figure 3.2 Finite element model of subassembly

3.1.2 Model Validation

The finite element predictions of behavior of the pre-Northridge moment-resisting connections under gravity load following instantaneous column loss cannot be validated

directly due to the unavailability of test data for this load condition. In this investigation, therefore, they were validated indirectly through a comparison with test results for specimen UCBPN2 (cf Table 3.1), a typical pre-Northridge moment-resisting moment connection that was tested by Popov et al. (1998) for seismic response. Figure 3.3 depicts the test setup and connection details. Specimen UCBPN2 consisted of a W36x150 beam welded to a W14x257 column with an E70T-4 electrode. Both the beam and column were ASTM A572 Grade 50 steel. The material properties (i.e. yielding and ultimate strength) were based on the Popov et al. (1998) study. A shear tab was welded to the column flange and bolted to the beam web. A fillet weld was added to the corner of the shear tab where it connected to the beam web. The initial flaw size at the bottom flange of the beam was assumed to be 0.5 in (12.7 mm), which includes the depth of the backing bar (Kaufmann and Fisher 1997). Cyclic displacements were applied following the standard SAC/ATC-24 loading history (ATC 1992) at the end of the beam quasi-statically until the connection failed at the displacement of 1.94 in (0.05 m).

The finite element model (Figure 3.4) utilized the same eight-node brick elements and mesh density as used in Figure 3.2. The results of the FEA of specimen UCBPN2 are shown in Figure 3.5. The predicted results are very close to the test results reported previously (Table 2 of Popov et al. 1998); the yield forces are 159 kip (707 kN) and 153 kip (681 kN) for the analysis and test, respectively, while the maximum forces at a total displacement of 1.94 in (0.05 m) is 197 kip (876 kN) in the analysis and 201 kip (894 kN) in the test. Therefore, the finite element modeling process described in the previous section appears to be sufficiently accurate to capture the behavior of similar pre-Northridge moment-resisting connections.

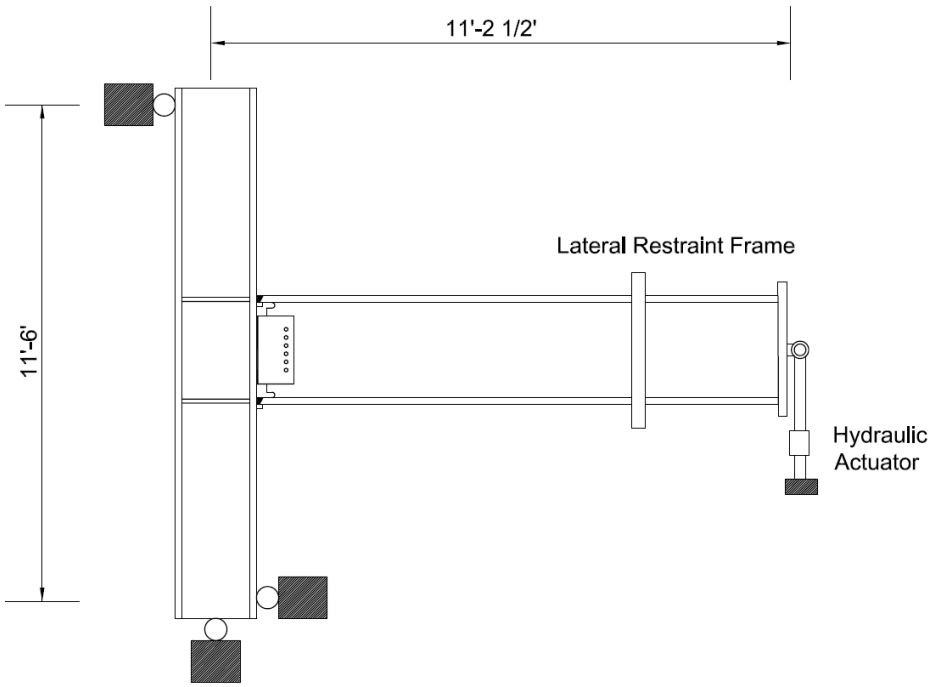

(a) Test setup

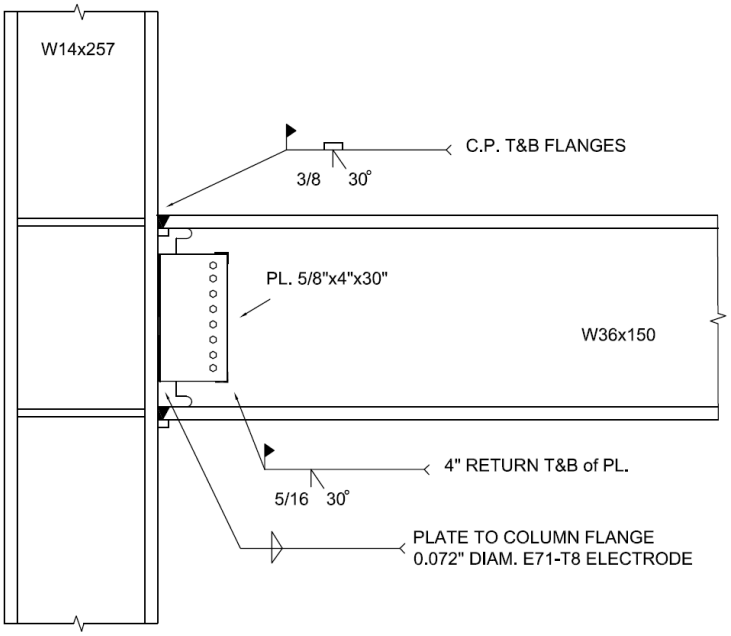

(b) Connection detail

Figure 3.3 Test setup for specimen UCBPN2

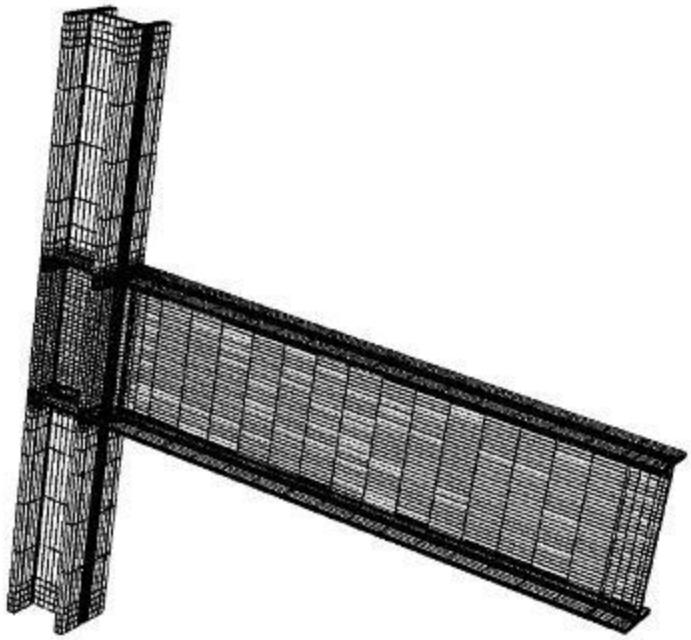

Figure 3.4 Full-scale finite element model of test UCBPN2

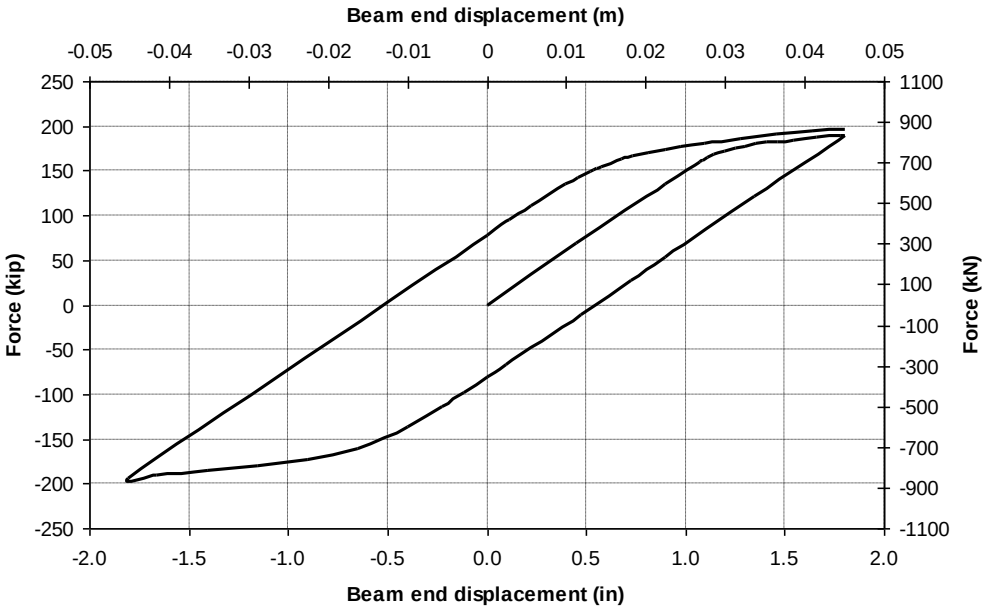

Figure 3.5 Finite element analysis results of test UCBPN2

3.1.3 Probabilistic Modeling of Main Parameters Affecting Fracture

Investigations performed following the pre-Northridge earthquake (Kaufmann and Fisher 1997) showed that the initial flaw size, beam yield strength and fracture toughness of the weld were highly variable. Subsequent research confirmed that these highly variable parameters were critical factors in the behavior of pre-Northridge moment-resisting connections (Joh and Chen 1999; Chi et al. 2000; Matos and Dodds 2001). Accordingly, a probabilistic model is required to deal properly with uncertainty in connection strength.

The investigation by Kaufmann and Fisher (1997) showed that the depth of the weld flaw was not uniform along the beam web. However, since no data are available to describe this non-uniformity, a uniform edge crack was assumed to represent the flaw. The (random) depth of this assumed flaw was taken as the depth at the middle of the beam flange, the point at which the depth usually was greatest due to lack of weld penetration. The initial flaw size in sixteen connections taken from inspection of five buildings after the Northridge earthquake was reported by Kaufmann and Fisher (1997). According to the shape of the histogram of initial flaw size and its physical characteristics (i.e. physical limits exist for minimum and maximum depth), a simple triangular distribution (Figure 3.6) was adopted to describe the uncertainty of initial flaw size. The lower limit of the flaw size is the thickness of the backing bar (9.5 mm), since the backing bar was not removed in the pre-Northridge connections, while the upper limit is set to be the maximum recorded flaw size (19.6 mm).

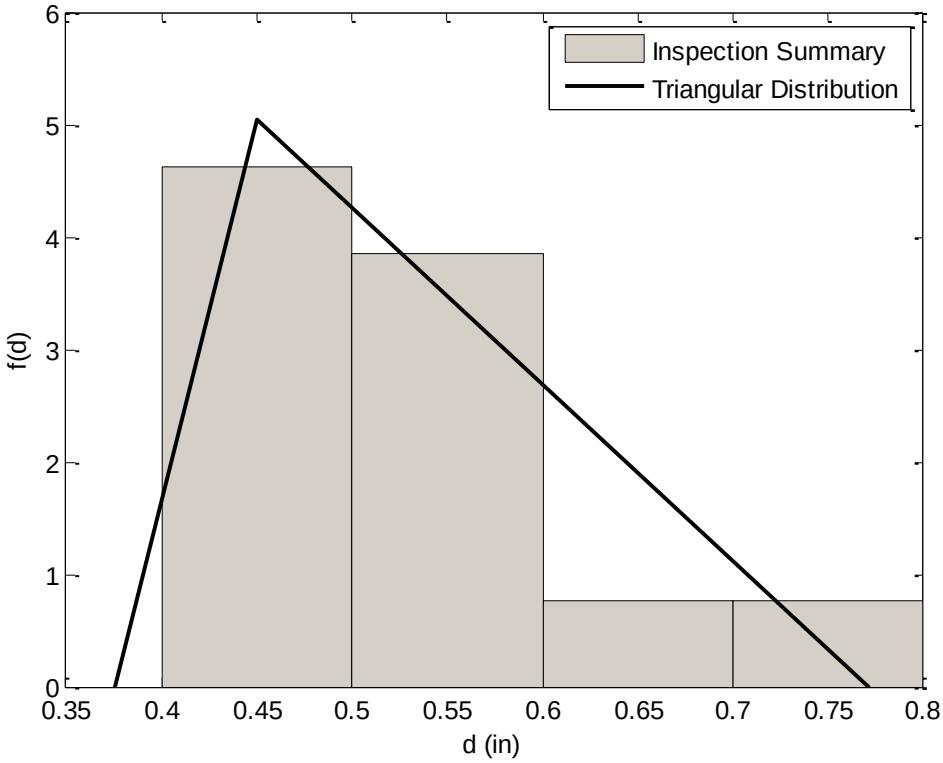

Figure 3.6 Inspection summary by Kaufmann and Fisher (1997) and probability distribution of initial flaw size (1 in=2.54 cm)

The mean fracture toughness of the E70T-4 weld metal, expressed in terms of J-integral, J_{IC}, was assumed conservatively to be 0.11 in-kip/in^2 (19.26 kJ/m^2). The plane strain fracture toughness, K_{IC}, reported by Kaufmann and Fisher (1997) ranged from 40 ksi-√in to 60 ksi-√in, which corresponds to a range in J_{IC} of 0.05 to 0.11 in-kip/in^2 (8.76 to 19.26 kJ/m^2). The coefficient of variation (COV) of J_{IC} is assumed to be 0.3, based on the correlation between J_{IC} and Charpy V-Notch (CVN) test data (Barsom and Rolfe 1999), as reported in Kaufmann and Fisher (1997). A two-parameter Weibull distribution, which is based on the weakest link principle (Beremin et al. 1983; Mudry

1987), was utilized to model the fracture toughness and fracture demand. This distribution has the form,

$$F(x) = 1 - \exp\left[-(\frac{x}{\lambda})^k \right] \tag{3-1}$$

where λ, $k > 0$ are distribution parameters. With the mean and COV above, $\lambda = 0.125$ and $k = 3.715$.

A probabilistic model for fracture of connections involving ASTM A36 steel beams is developed first because such beams were used in most of the test specimens that subsequently were compared with the analysis results. A model for connections involving A572 steel beams will be developed subsequently. The yield strength of A36 steel beams varies over a wide range (Bartlett et al. 2003), which was confirmed in the summary of pre-Northridge connection tests from the SAC Project (FEMA 1997b). The mean and COV of the yield strength of the beams can be derived from the data provided in Table 3.1, assuming that data to be representative of typical construction. The mean value and COV are 46.7 ksi (322 MPa) and 0.074, which are comparable to 49.2 ksi (339 MPa) and 0.10 reported in FEMA 267 (1995). The statistical data for strength of A572 steel is taken from FEMA 267 (1995), in which it was reported that the mean yield strength and COV are 57.6 ksi (397 MPa) and 0.089, respectively. The yield strength is modeled by a lognormal distribution in both cases.

3.1.4 Analysis of Uncertainty in Connection Behavior

The uncertainties in connection behavior were determined using Latin hypercube sampling (McKay et al. 1979) due to the heavy computational demand of each run of the

FEA. Ten samples of yield strength and initial flaw size were taken from the corresponding distributions, grouped randomly into ten pairs, and incorporated in a FE model that determined the fracture demands at representative displacements during the static pushdown analysis. At each representative displacement, a lognormal distribution was fitted to the set of fracture demands determined from the FEA. Figure 3.7 shows the fitted lognormal distribution of fracture demand when the vertical displacement of the center column is 6 in (0.15 m) at the top of the center column.

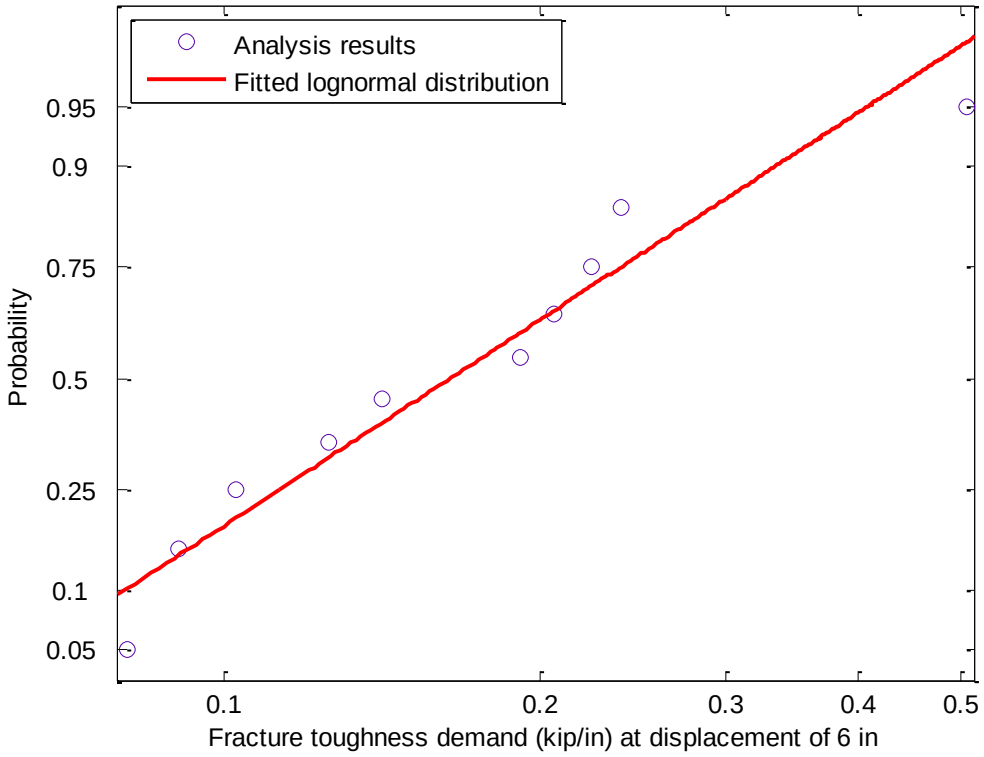

Figure 3.7 Lognormal CDF of fracture demand at vertical displacement of 6 inches

Once the distribution of fracture demand was obtained at each representative location, the probability of fracture P_f was calculated according to

$$P_f = \iint_{f>t} f_F(f) f_T(t) df dt \tag{3-2}$$

where $f_F(f)$ is the probability density function (PDF) of fracture demand (derivative of the distribution in Figure 3.7) and $f_T(t)$ is the PDF of fracture toughness. A comparison of probability densities of fracture demand and fracture toughness at a displacement of 6 in (0.15 m) is presented in Figure 3.8 for the A36 beams. The fracture toughness is concentrated around the mean value, while the fracture demand varies over a wider range due to the various uncertainties in connection behavior alluded to above. Figure 3.9 shows that the probability of fracture increases rapidly as the vertical displacement increases, reaching nearly 1.0 at a vertical displacement in the center column of 10 in (0.25 m). At that point, the connection rotation (i.e. vertical displacement / beam span) is less than 0.03, which is substantially less than the rotation demand expected under a severe earthquake. Conversely, P_f is almost zero when the column vertical displacement is less than 2 in (51 mm).

In this investigation, a general index of connection failure is sought in order to extend the model of uncertainty in connection strength to beams with different depths, spans and grades of steel. The vertical displacement of the center column and the connection rotation are not appropriate indices of connection failure, in that their critical values depend on beam depth, beam span and frame configuration. The internal forces at beam ends should be better measures, since the connection fails in a brittle manner. Accordingly, the index of connection failure is chosen to be the beam end moment adjacent to the connection when the connection failure occurs, denoted M_f, normalized by the full plastic moment M_p of the beam section. The moment at the beam end can be

related to the vertical displacement, allowing the cumulative distribution function (CDF) of failure moment illustrated in Figure 3.10 to be determined from the CDF in Figure 3.9. To validate this CDF, the relationship directly obtained from the available test data of the specimens with A36 beams is also presented in Figure 3.10, where it is shown to match the available test data reasonably well.

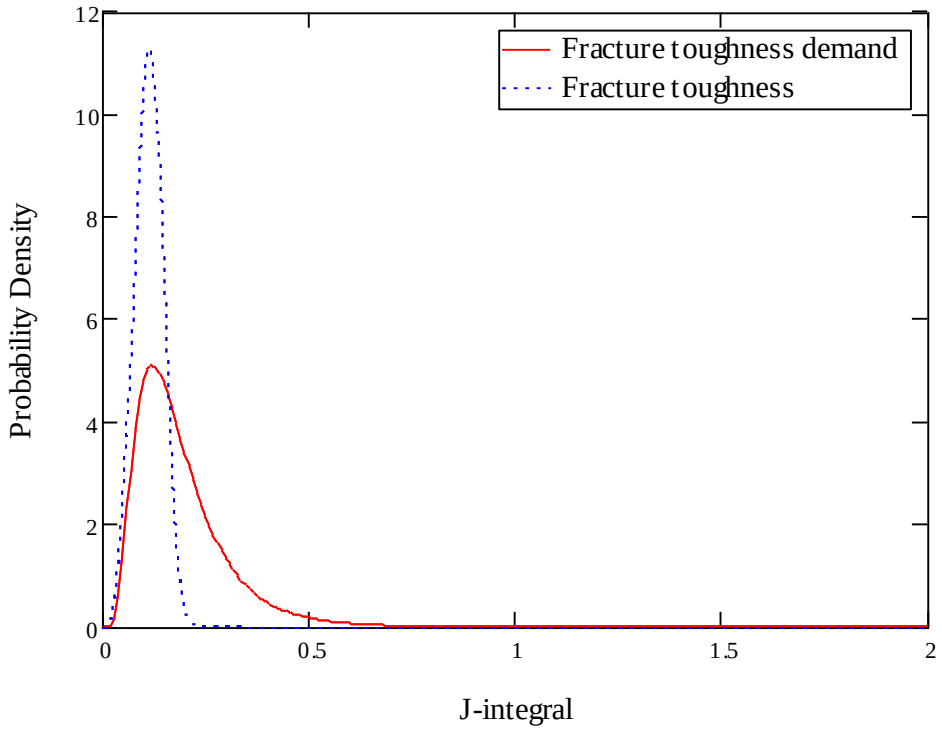

Figure 3.8 Comparison of fracture demand and fracture toughness at displacement of 6 in (0.15 m)

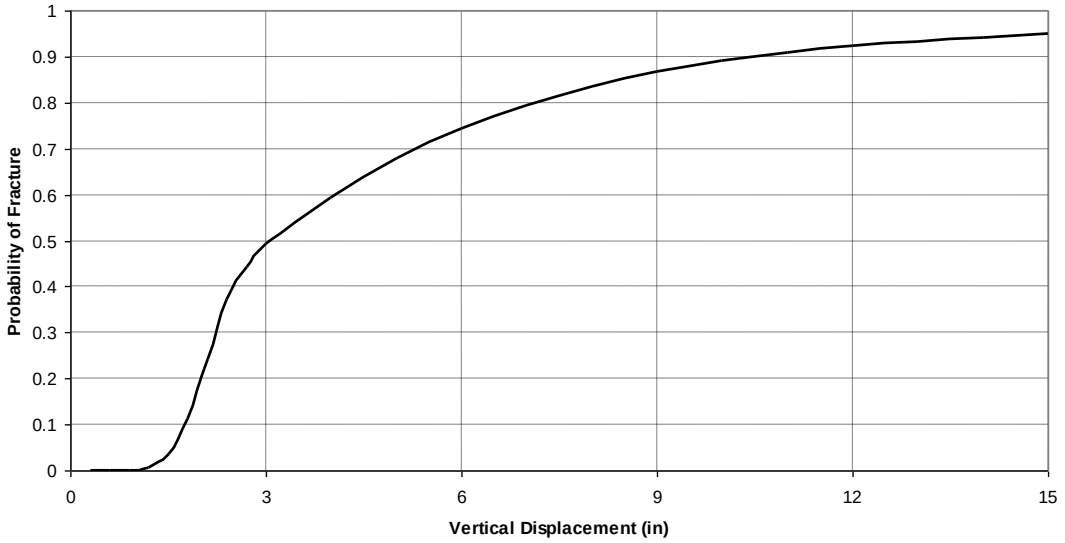

Figure 3.9 Relationship between vertical displacement and probability of fracture (1 in = 2.54 cm)

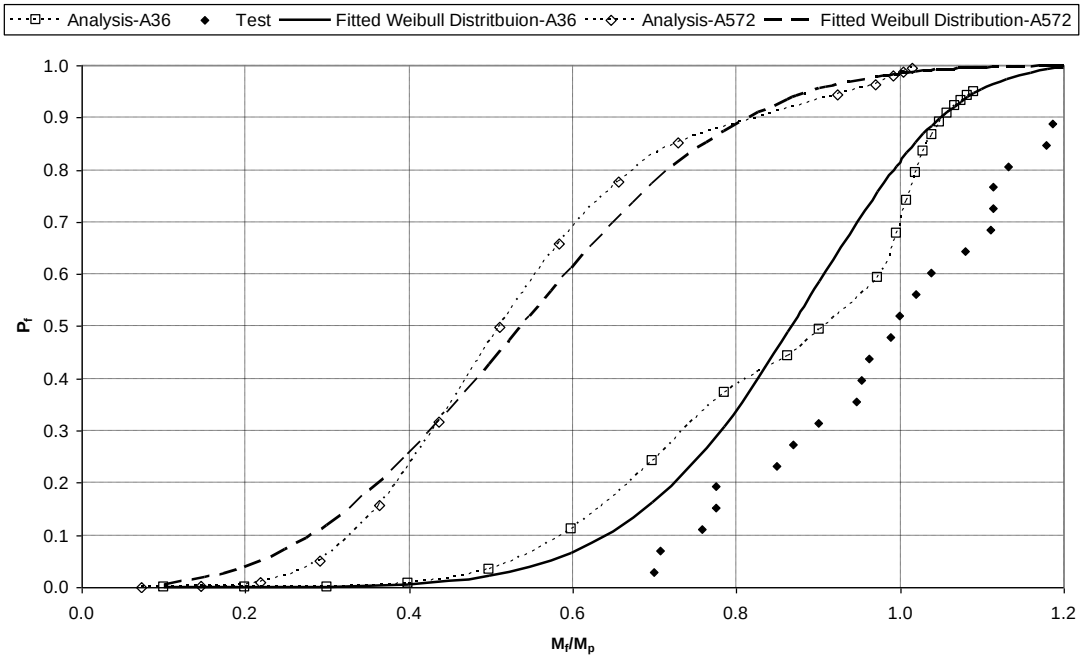

Figure 3.10 Probability distribution of failure moment

The shear force was found to have little effect on the connection failure, which also has been verified by the tests in the SAC project. The axial force developed in the beam during the pushdown analysis is presented in Figure 3.11. The axial force is quite small and has little effect on the connection failure. The displacements are insufficient to develop catenary action, which would require a plastic rotation of 0.07 or more (Hamburger and Whittaker 2004), suggesting that catenary effects need not be considered in assessing robustness assessment of steel moment frames with similar geometries and such connections.

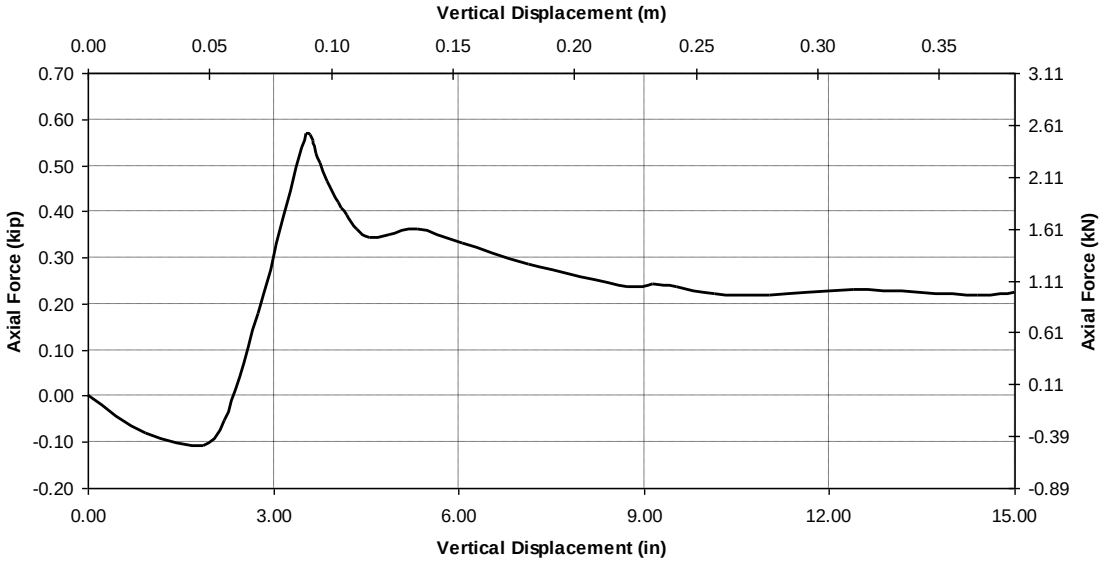

Figure 3.11 Beam axial force history during analysis (1 in=2.54 cm)

Figure 3.10 shows that the probability of connection fracture is quite small when the normalized beam end moment is less than 0.6, but increases rapidly beyond that point and approaches unity when M_f/M_p exceeds 1. The CDF is fitted with a two-parameter

Weibull distribution (Equation (3-1)) denoted as F_{Frac}, where λ = 0.92 and k = 6.30. Accordingly, the mean normalized failure moment is 0.86, a result that is consistent with that found by other investigators (Gross 1998).

The probability distribution of failure moment for connections involving A572 beams is also presented in Figure 3.10. These connections apparently are more vulnerable than those consisting of A36 beams if the same *normalized* moment is applied. The parameters of the fitted Weibull distribution are λ = 0.61 and k = 2.90. The mean normalized failure moment is 0.54, which is quite small compared to the mean normalized failure moment of 0.86 for the A36 beam connections.

3.1.5 Applicability and Limitations of Model

The connection failure mode addressed by the connection model developed above involves cracking initiated from the weld defect between the column flange and the bottom beam flange, which is under tension. This model is applicable to failure of the connections directly adjacent to a notionally removed column, in that the bottom beam flanges of those connections are in tension after column removal. The possibility of failure of connections to the undamaged columns at the far ends of the affected spans cannot be predicted with the proposed failure criteria, however, since the top beam flanges at those connections are in tension, and the internal forces are distributed differently. However, the analyses conducted in this study revealed that failure of the connections adjacent to the notionally removed column invariably occurs prior to failure of the connections to the side (far-end) columns.

The tests conducted in the SAC program revealed that the crack propagated rapidly into the beam or column web after the initiation of connection fracture and that the residual capacity of the connection was negligible. However, the SAC tests involved cyclic loads; monotonic load tests would be more appropriate for investigating the behavior of the connection in mitigating vulnerability to disproportionate collapse (Powell 2005). If the crack does not propagate into the beam or column web under monotonic loads, the residual capacity of the connection in shear may be a relatively large fraction of the undamaged connection shear capacity. This behavior was verified by a finite element analysis, in which the bottom flange of the beam was "detached" from the column flange at a vertical displacement of 4 in (0.10 m) to simulate the brittle fracture of the connection without crack propagation.

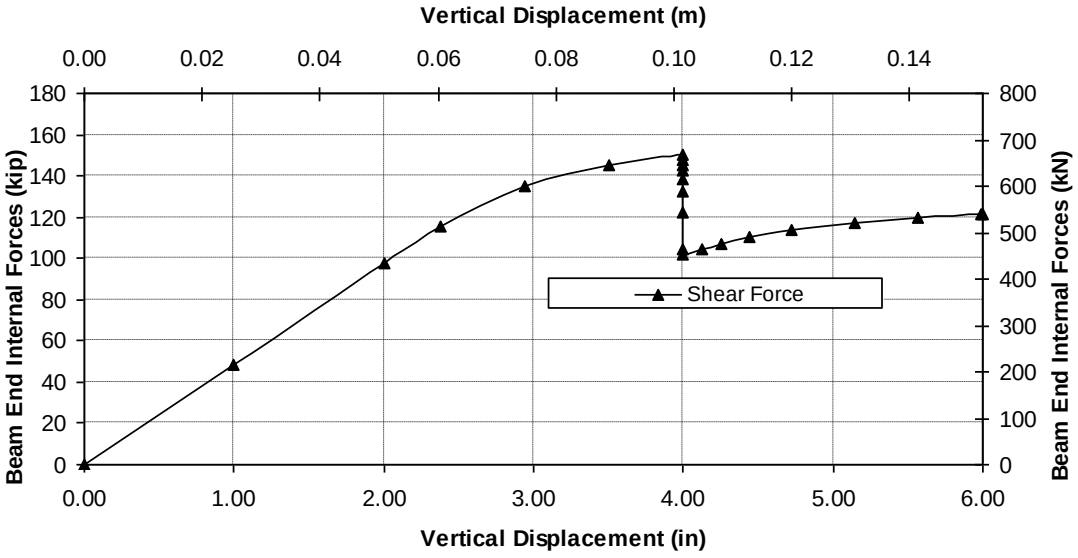

Figure 3.12 Beam end internal force of connection failure at vertical displacement of 4 in (0.10 m)

The resulting beam end internal forces are presented in Figure 3.12; the shear force transferred (equal to the pushdown force on the subassembly), retains approximately 70% of its capacity after fracture. Further research and test verification on this issue are needed.

3.2 T-STUB CONNECTIONS

A typical T-stub connection is illustrated in Figure 3.13. The shear from the beam is transferred to the column with a web plate or web angle, while the moment is transferred by the T-stubs attaching the beam flange to the column flange. The moment transfer is determined by the axial stiffness of the stem and the flexural rigidity of the flanges of the T. Rather than developing the macro-model of the connection from high-fidelity finite element analysis as in the previous section, the macro-model in this study was developed by modeling the connection components (i.e. T-stub, shear tab and panel zone) with a series of rigid elements and connecting springs (Figure 3.14), with element properties developed by analysis and the connection properties as a whole subsequently calibrated to experimental data. In particular, the shear tab model was derived based on the relationship of a bolt bearing on a single plate developed by Rex and Easterling (2003), while the macro-models of T-stub and panel zone were based on proposals of Swanson and Leon (2001) and Krawinkler (1978) respectively. Finally, the proposed macro-model was verified by comparing to the data obtained from a bolted T-stub connection test.

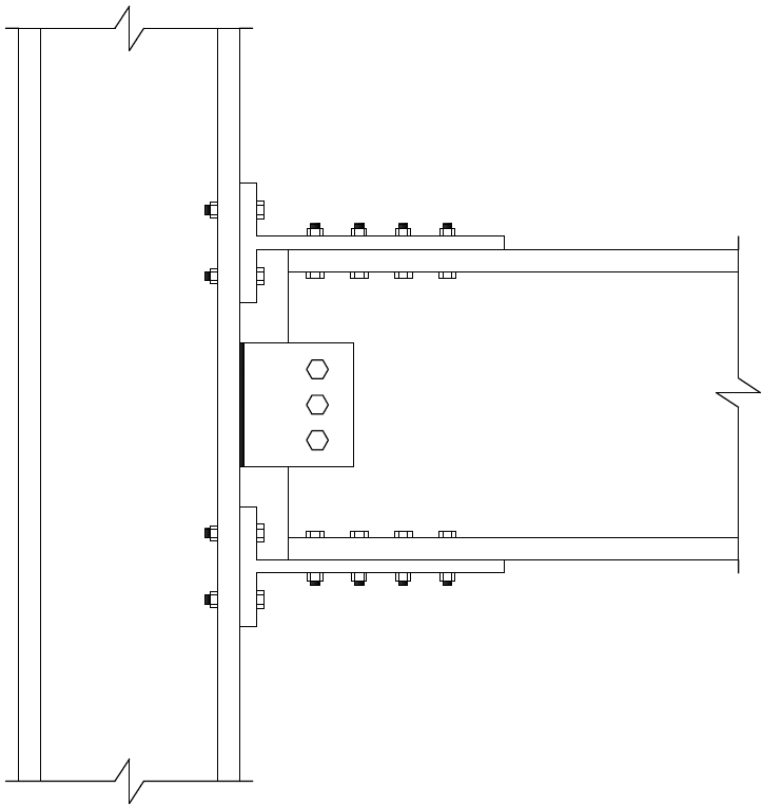

Figure 3.13 Typical bolted T-stub connection

3.2.1 Component Modeling

Following notional column removal, the main resistance of bolted T-stub connections is provided by the T-stubs undergoing tension or compression. As shown in Figure 3.14, the top and bottom T-stubs are modeled by translational springs. The shear tab and web angle, which may contribute to connection stiffness, are also modeled by translational springs. The number of springs depends on how the resistance mechanisms of the shear tab and web angle are modeled. For the shear tab, the behavior of each bolt bearing against the shear tab and beam web is usually modeled by one spring. The

resistance capacity of the web angle is provided by a combination of bearing and bending behavior. Here, the number of springs depends on how the web angle is discretized (Azizinamini et al. 1987; Astaneh-Asl et al. 2001). The panel zone is modeled by rigid beam-column elements with a rotational spring. The connection failure modes considered are the failure of the T-stub under tension and the failure of beam due to excessive rotational deformation; the possibility of shear failure in bolted T-stub connections is quite small due to current design practice (AISC 2005), and that failure mode is neglected. A rigid constraint is applied in the vertical direction, under the assumption that the shear deformation in such connections is usually negligible and need not be considered. The length of the undeformed spring for the T-stub is set equal to the length of the T-stub stem, and the length of the undeformed spring modeling the bearing between a bolt and shear tab is set equal to the distance from the column flange to the center to the bolt.

The model of T-stub adopted in this study was based on the model developed by Swanson and Leon (2001) for seismic response, in which the contributions (stiffness and deformation limit) from the T-stub flange, the T-stub stem, the bearing deformations and the slip between the T-stub stem and the beam flange were considered. The T-stub flange bending and tension bolt elongation were modeled together because they deform together and it is difficult to distinguish their individual contributions from the available test data. The T-stub flange stiffness and corresponding prying gradient, which were derived using the direct stiffness method, were used in an incremental solution procedure to calculate the response of the T-stub flange up to the point where the tensile force limit was reached. For the stem of the T-stub, a bilinear model was developed to predict the initial

stiffness, yielding force, plastic stiffness and the ultimate displacement based on research conducted by Whitmore (1952). The bearing stiffness of the stem and the beam flange was modeled using the nonlinear relationship of a bolt bearing on a single plate developed by Rex and Easterling (2003):

$$\frac{R}{R_n} = \frac{1.74\overline{\Delta}}{(1+\overline{\Delta}^{0.5})^2} - 0.009\overline{\Delta} \tag{3-3}$$

in which R is the plate load; R_n is the nominal plate strength; $\overline{\Delta}$ is the normalized deformation = $\Delta\beta K_i / R_n$ (Δ = hole elongation, β = steel correction factor and K_i = initial stiffness). The slip between the stem and the beam flange was modeled using the modified slip model proposed by Rex and Easterling (1996). After calculating the stiffness of each component, the total analytical response of the connection was obtained by assembling the bearing and slip stiffnesses in parallel and the remaining stiffnesses in series. From the shapes of the experimental and analytical force-deformation responses, it was observed that slip between T-stub stem and beam flange occurred following initial elastic deformation as load increased. Once slip occurred, the dominant deformations occurred in the T-stub stem (yielding) and flange (bending) until either the stem or flange failed. Hence, the nonlinear responses of the T-stub can be represented by a tri-linear force-deformation relationship, as illustrated in Figure 3.15 for one of the connections considered subsequently in more detail. The first line segment of this relationship fits the initial stiffness; the second line segment models slip and bearing and the third segment represents the stem yielding and flange bending.

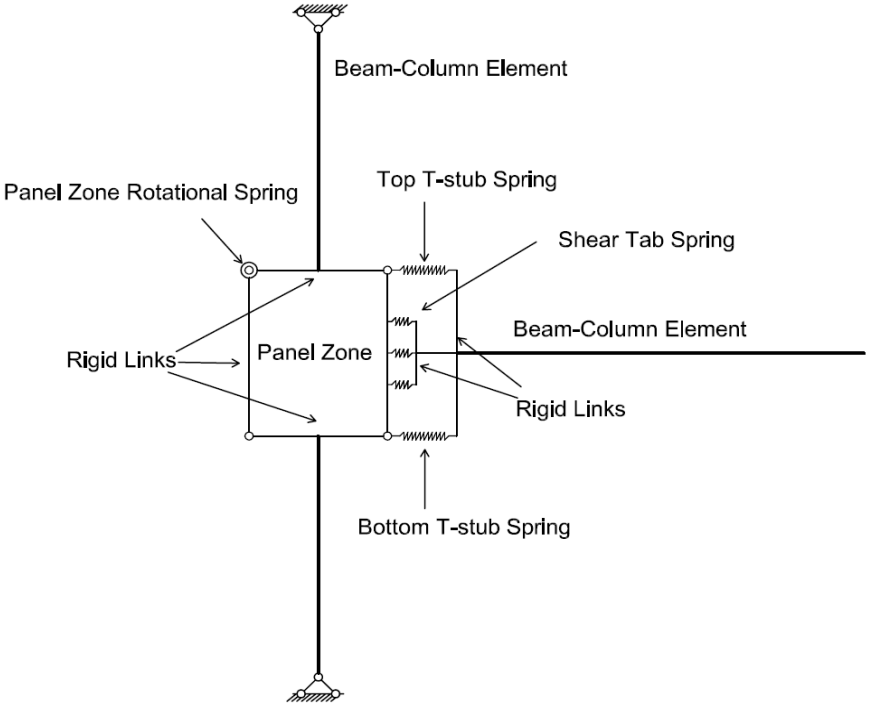

Figure 3.14 Macro-model of bolted T-stub connections

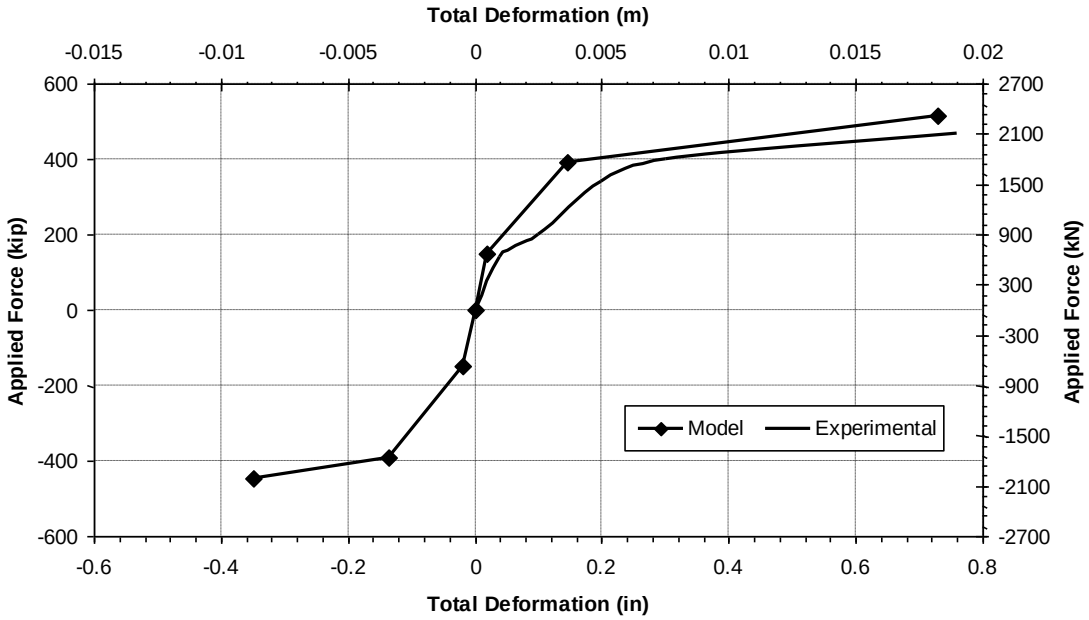

Figure 3.15 Monotonic analytical and experimental force-deformation relationship of T-stub TA-05

The bearing stiffness of the shear tab was modeled using the nonlinear relationship suggested by Rex and Easterling (2003) as well. First, the force-deformation relationships for a bolt bearing on a shear tab and on a beam web was calculated according to Equation (3-3), as illustrated in Figure 3.16. The total force-deformation relationship then was obtained by combining these two relationships, modeling the stiffness of their combined action by two springs in series. For the sake of simplicity, the total nonlinear relationship was approximated by the tri-linear model shown in Figure 3.16, in which the model has the same initial stiffness as the total force-deformation relationship. The ultimate strength (i.e. maximum bearing force denoted F_u in Figure 3.16) was defined as the minimum value of the forces defined by the points at which the slopes of the relationships for the bolt bearing on the shear tab and the bolt bearing on the beam web equal zero. The yield strength (denoted as F_y) was set equal to 70% of F_u. Rex and Easterling (2003) did not provide the force-deformation relationship of the shear tab beyond the point of ultimate strength. Although the contribution of the bolt bearing on the shear tab and the beam web to the resistance is relatively small compared to the contribution of the T-stub, sudden bearing failure at the ultimate strength may lead to numerical problems, causing the nonlinear structural analysis to terminate. Hence, the deformation limit was simply set to the bolt end distance being considered and the residual capacity was decreased linearly to zero from that deformation limit (denoted as D_t in Figure 3.16).

The stiffness of the panel zone was modeled by a tri-linear rotational spring; this model was discussed in detail in Gupta and Krawinkler (1999) and is based on a prior formulation by Krawinkler (1978).

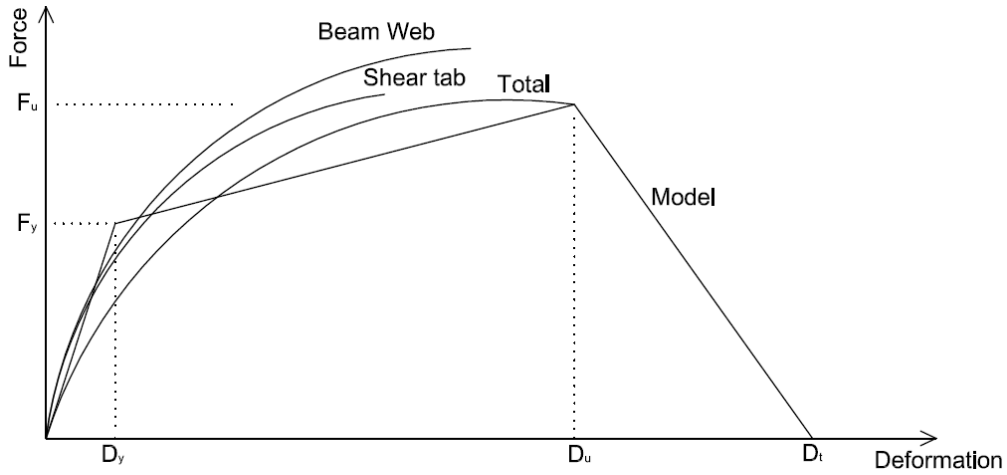

Figure 3.16 Tri-linear model of bearing stiffness of a single bolt bearing on shear tab and beam web

3.2.2 Model Validation

The proposed macro-model of the T-stub connection was validated by comparing the analytical predictions with the result of a connection test conducted by Smallidge (1999) of a specimen designated as FS-05. In this test, as illustrated in Figure 3.17, a W14x155 column 3.8 m (12 ft-4 in) long and pinned at both ends was bolted to a 4.6 m (15 ft) long W24x55 beam with two T-stubs (Figure 3.18), which were cut from a W16x100 section, and a L12x5x3/8 shear tab. The column flange and each T-stub were fastened with ten 22 mm (7/8 in) diameter A490 bolts 64 mm (2-1/2 in) in length, while the beam flange was fastened with each T-stub stem by eight 22 mm (7/8 in) diameter A490 bolts 89 mm (3-1/2 in) in length. The panel zone was reinforced with a 13 mm (1/2 in) thick doubler plate on each side and four stiffeners with the thickness of 13 mm (1/2 in). All components of the specimen were manufactured with A572 Grade 50 steel, with

material properties as listed in Table 3.2; the material properties of the T-stub in this table were adopted from Swanson (1999) since no corresponding material properties were listed in Smallidge (1999).

Table 3.2 Material properties of specimen FS-05 (1 ksi = 6.9 MPa)

Component	Grade	Yield Strength (ksi)	Ultimate Strength (ksi)
Beam	A572 Gr50	61.0	76.0
Column	A572 Gr50	56.0	74.0
T-stub	A572 Gr50	53.0	70.0
Shear Tab	A572 Gr50	57.9	77.4

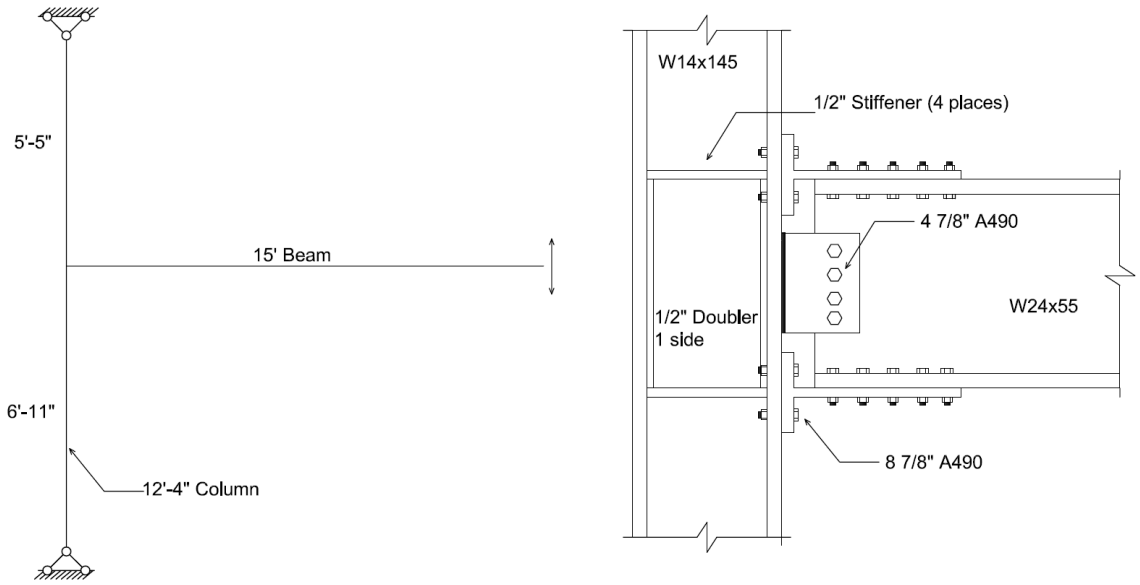

Figure 3.17 FS-05 connection test setup (1 in = 25.4 mm; 1 ft = 0.3048 m)

The T-stubs used in specimen FS-05 were identical to T-stubs designated as TA-01 and TA-05, which were tested by Swanson and Leon (2000); accordingly, the results of these later tests and the analytical model in Figure 3.15 were used to define the spring

properties needed for the connection model in Figure 3.14. T-stubs TA-01 and TA-05 were identical, except that TA-01 was tested cyclically while TA-05 was tested monotonically under tension. Figure 3.15 compares the behavior of T-stub TA-05 predicted by the model in Figure 3.14 with its experimental behavior. The stiffnesses of the panel zone and shear tab were also calculated according to the proposed models. All analyses in this portion of the connection study were performed using the computer program OpenSees (Mazzoni et al. 2009).

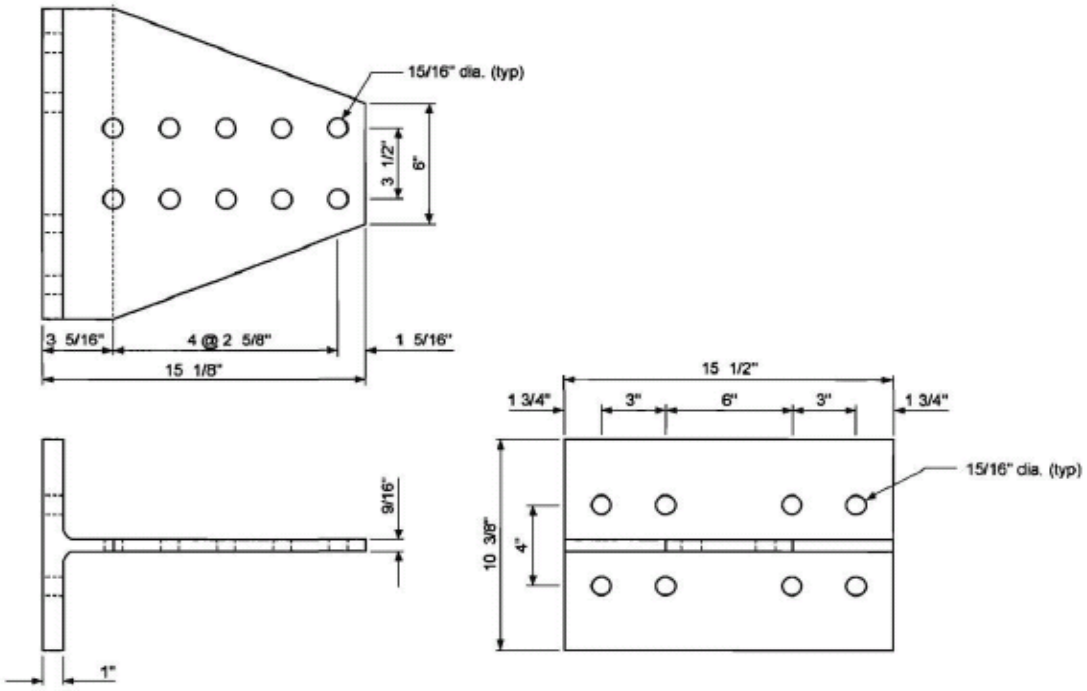

Figure 3.18 Detail of T-stubs TA-01 and TA-05 (1 in = 25.4 mm) (Swanson 1999)

The comparison of analytical and experimental force-displacement relationship for connection FS-05 is illustrated in Figure 3.19. The maximum force observed in the test was 236 kN (53 kip) at a displacement of 241 mm (9.5 in), while the corresponding

maximum force estimated from the connection model was 274 kN (61.5 kip), a difference of nearly 16.0%. One reason for the difference is that the proposed analytical model is based on the monotonic stiffness which, as shown in Figure 3.19, is larger than the cyclic stiffness. For this reason, it is reasonable that the model, which incorporates the monotonic stiffness of the T-stub, predicts a larger load than the cyclic test result. Note that monotonic stiffness is a more appropriate parameter for connection modeling during collapse than cyclic stiffness in that the maximum displacement usually is reached in the first half-cycle of vibration following the initial damage event (Powell 2005). In the circumstances, this connection model is believed to be sufficiently accurate to capture the behavior of typical frames with such connections following damage due to sudden notional column removal.

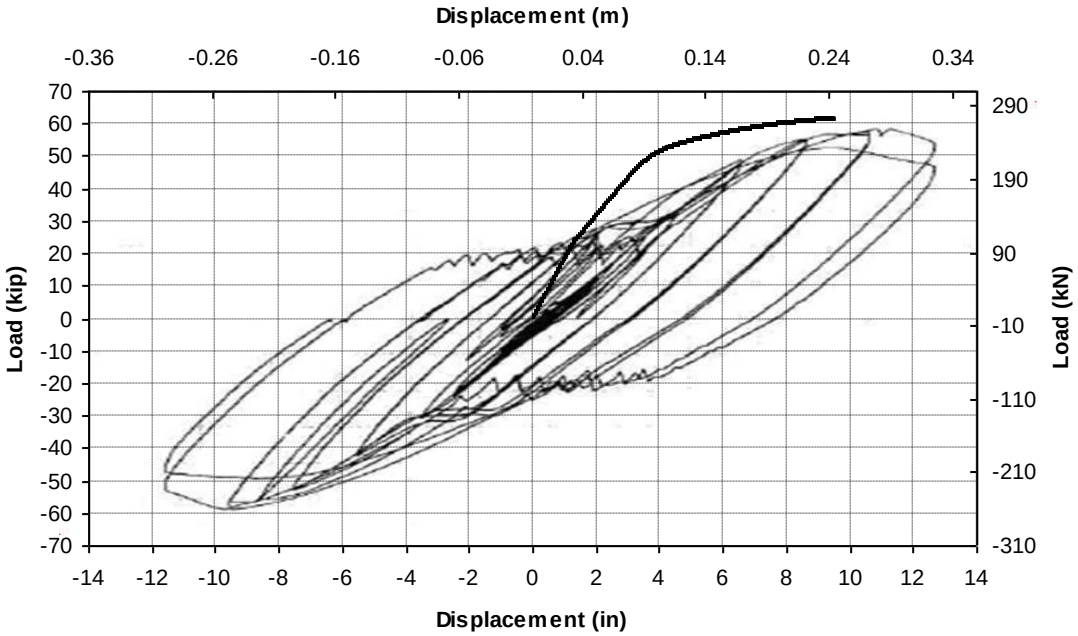

Figure 3.19 Model and experimental force-displacement relationship of FS-05 (Smallidge 1999)

3.3 RIVETED CONNECTIONS

The seismic behavior of PR connections is commonly modeled with rotational springs (e.g. Kinali and Ellingwood 2007), with which the contribution of the axial forces in beams during earthquake is neglected. Although the seismic behavior of PR connections has been extensively investigated and the corresponding simplified models are available for use, these models may not be suitable or directly integrated with the structural models for analysis of disproportionate collapse performance. To compare the influences of different connection modeling approaches on evaluating collapse-resisting capacity, a simplified model of two spans of a frame of one story directly above the instantaneously damaged column is illustrated in Figure 3.20. It is assumed that the two spans have the same beam section and the model is symmetric. For the sake of simplicity, the deformation of the column on the left side is neglected and the left end of the beam model is fixed. While the right end of the span is modeled with roller boundary conditions. With the connection model with the rotational spring at the end of the beam, both the top and bottom of the corresponding connection have the same (absolute) displacements. This model may be inappropriate for modeling collapse behavior of connections since the top and bottom displacements of a connection following instantaneous column removal are usually unequal due to the difference in the compressive and tensile stiffnesses of the components (e.g. T-stub) in PR connections. Even if the stiffnesses are same, the top and bottom displacements still are not equal since the tensile forces in the beams are transferred to the columns through connections. Therefore, the rotational spring model will lead to an axial deformation of the beam that is larger than the actual value, as shown in Figure 3.20.

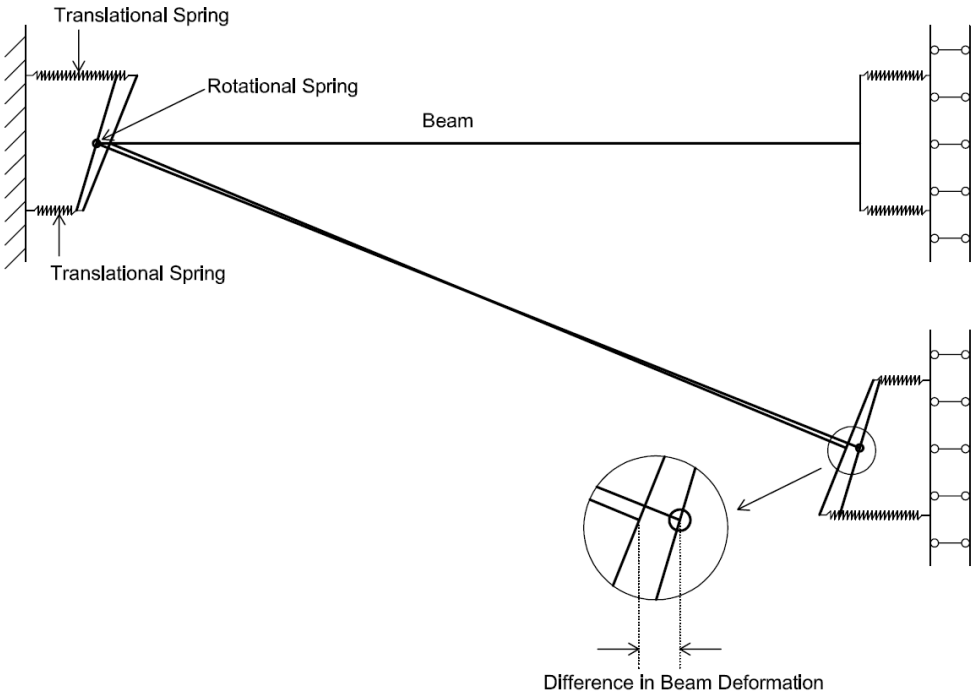

Figure 3.20 Comparison of connection models

3.3.1 Proposed Connection Modeling Methodology

To overcome the problems associated with the use of rotational spring models, translational spring models in which axial forces (catenary effects) and unequal compressive and tensile stiffnesses can be taken into account, are more appropriate for modeling behavior of connections during collapse. In such models, the behavior (stiffness and strength) of each main component (e.g. top and bottom T-stubs, web angles) of a connection is modeled individually with one translational spring and these translational springs are assembled in parallel or series according to the arrangement of the components in the connection to form the total response. This method has been applied to

model behavior of connections during collapse, e.g. by Sadek et al.(2008) for simple shear connections and by Xu and Ellingwood (2011) for bolted T-stub connections.

Although this approach is effective, for some connections, it is very difficult to investigate the behaviors of the components of a connection separately and assemble them to obtain a global model because no experimental data for the response of individual components is available. If the effects of connection encasement or slab are considered, the mechanism will become even more complicated. Moreover, experimental data of seismic behavior of connections are often available; in contrast, experimental data of connection behavior during collapse is very limited. Therefore, an improved method for modeling connection is proposed in the following to take advantage of available experimental data of seismic connections and to reflect the unequal compressive and tensile stiffnesses and catenery effects. Rather than investigating and modeling each connection component individually, in the proposed method, only two translational springs are utilized to model the global behavior of a connection as shown in Figure 3.21. The distance between the springs is set to the depth of the connected beam (denoted as d). The responses of connections in seismic tests, which often are recorded as the relationship between connection moment M and rotation θ, are transformed into the stiffnesses of the two springs through the equation $T = M / d$, as illustrated in Figure 3.22, where T is the force in the two springs.

Since the compressive and tensile stiffnesses are different, the corresponding displacement Δ cannot be simply obtained through the equation $\Delta = \theta d / 2$ under the assumption that the center of rotation of the connection is located in the middle of beam end. Several methods can be used to determine the center of rotation. One way is to

directly utilize the test record of center of rotation if available. Another way is to determine the center of rotation analytically through the characteristics of the connection components. For example, for riveted connections without encasement and slab, the main deformation of the connection is due to the shear deformation of the rivets. Therefore, the center of rotation can be assumed to be approximately located in the middle of beam section, which was confirmed by tests (Roeder et al. 1994). In Kishi and Chen (1990), the center of rotation for the top- and seat-angle connection (with or with double web angle) was assumed to be located at the leg adjacent to the compression-beam flange at the end of beam, which implies that the compressive stiffness of angles can be assumed to be quite large and modeled as rigid.

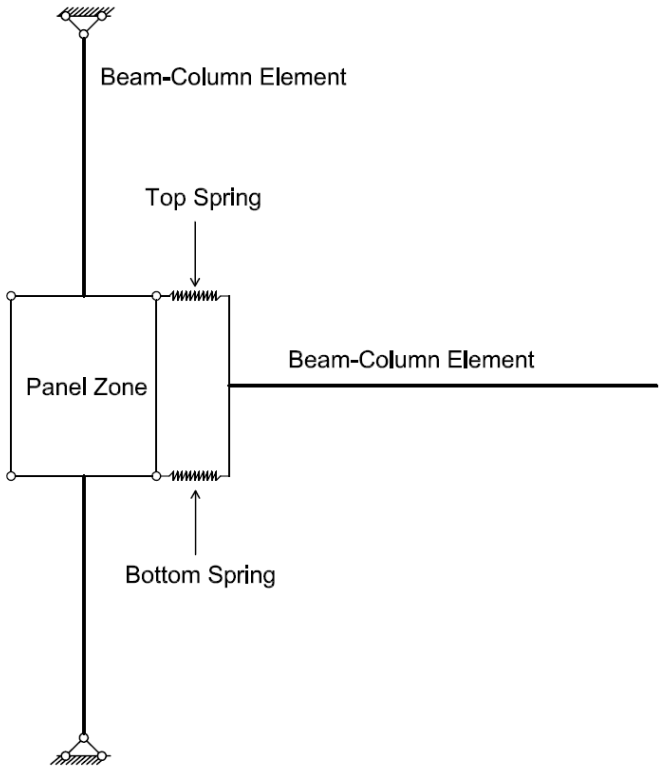

Figure 3.21 Proposed simplified model

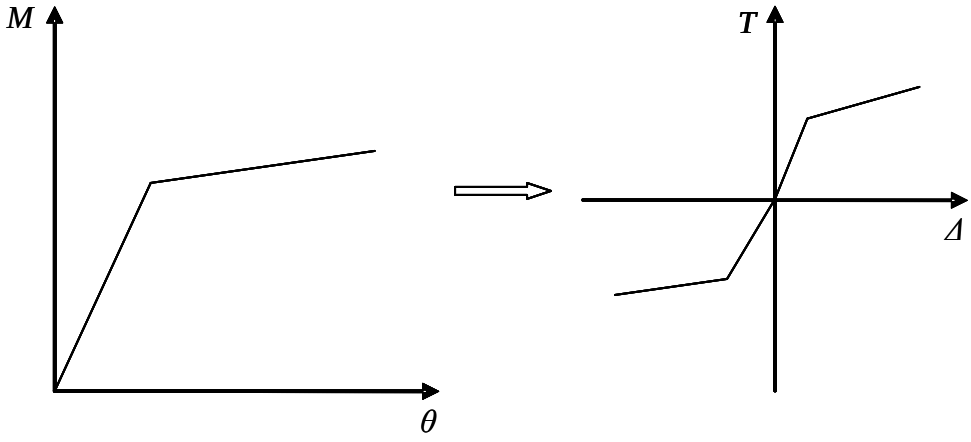

Figure 3.22 Transformation of stiffness

3.3.2 Applicability of Seismic Connection Model in Collapse Analysis

The applicability of seismic connection models to collapse analysis depends on many factors (e.g., initial stiffness, rotational limit, beam depth, beam span and etc.) and no criteria have yet been developed to determine whether these factors will permit large catenary effect. Accordingly, the applicability of seismic model for the analysis of riveted connections was checked through a comparison of the results of pushdown analysis of assemblies with seismic and collapse connection models, which are similar to the assembly shown in Figure 3.20. The connection B4RC7 tested by Forcier et al. (2002) as illustrated in Figure 3.23, was selected for this purpose because it was typical of construction of older steel frames (Hamburger 1993; Roeder et al. 1996) and had the same beam section as the frame which will be analyzed subsequently.

Connection B4RC7 had 19 mm A502 hot-driven rivets installed and was encased with 3 in (7.62 cm) of concrete cover to all steel in the column and 2 in (5.08 cm) of

cover to all steel in the beam and had a reinforced concrete slab with width of 60 in (1.52 m) and thickness of 5 in (12.7 cm). The yield strengths of steel in the column and beam are 44.1 and 45.5 ksi (304 and 312 MPa) respectively.

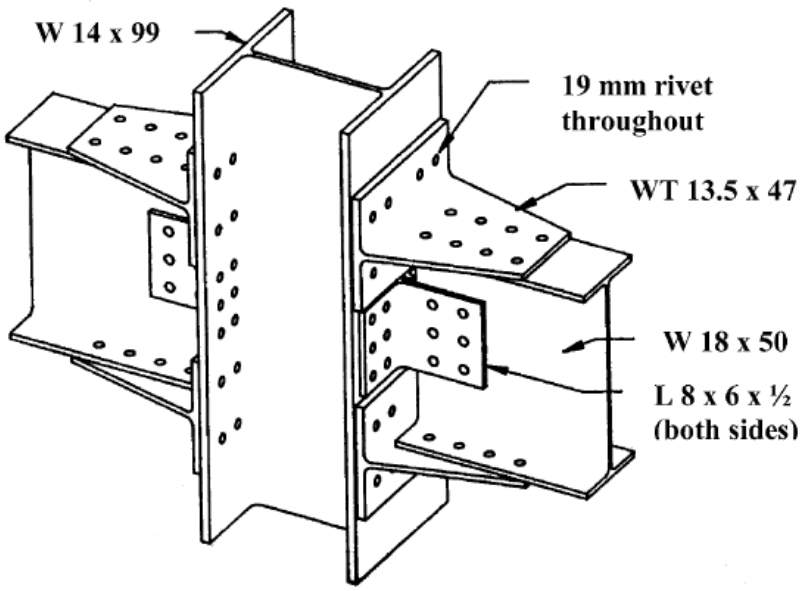

Figure 3.23 Typical riveted connection (Forcier et al. 2002)

The specimen was tested under cyclic loading and the corresponding envelope of the test results is shown in Figure 3.24. For the rotational spring (seismic) model, a bilinear model was used to approximate the envelope (stiffness and deformation), while for the translational spring model, the center of rotation needs to be determined first. The center of rotation of specimen B4RC7 during positive bending (beam bottom under tension) can be reasonably approximated as 15 in (38.1 cm) relative to the bottom of the beam, which was recorded in Roeder et al. (1994) as shown in Figure 3.25, while the center of rotation during negative bending was not reported. However, it can be estimated

through the record of specimen B4RC6 in the same test program, which was nearly the same as B4RC7 except that it had no slab. Due to the symmetric configuration of B4RC6, the location of the center of rotation during negative bending can be assumed to be the same as in the case of positive bending, which is located at 12 in (30.48 cm) relative to the T-stub (beam flange) under tension as presented in Figure 3.25. Since the slab provides more constraints than the concrete cover alone during negative bending, the center of rotation should be less than 12 in (30.48 cm) relative to the T-stub under tension (the top of the beam). However, to investigate the effect of the location of center of rotation, the center of rotation of B4RC7 during negative bending has been conservatively assumed to be 12 in (30.48 cm) relative to the top.

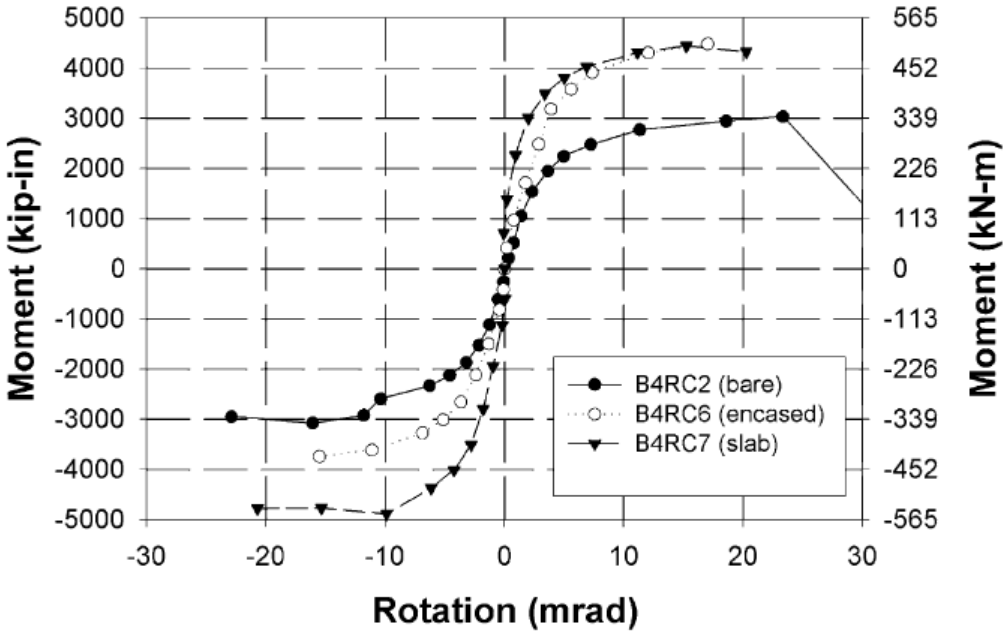

Figure 3.24 Envelope curves for specimen B4RC7 (Forcier et al. 2002)

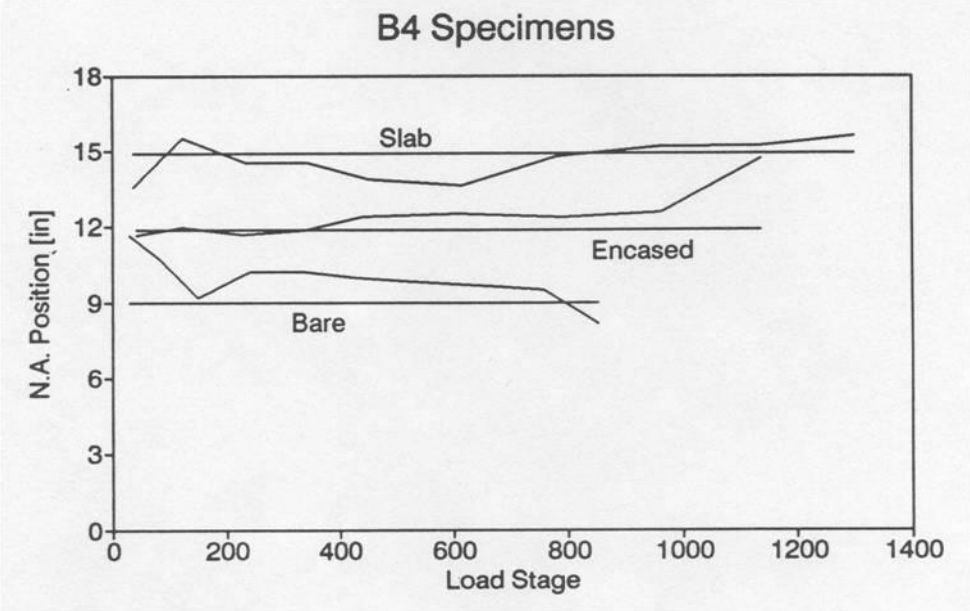

Figure 3.25 Neutral axis during positive bending (Roeder et al. 1994)

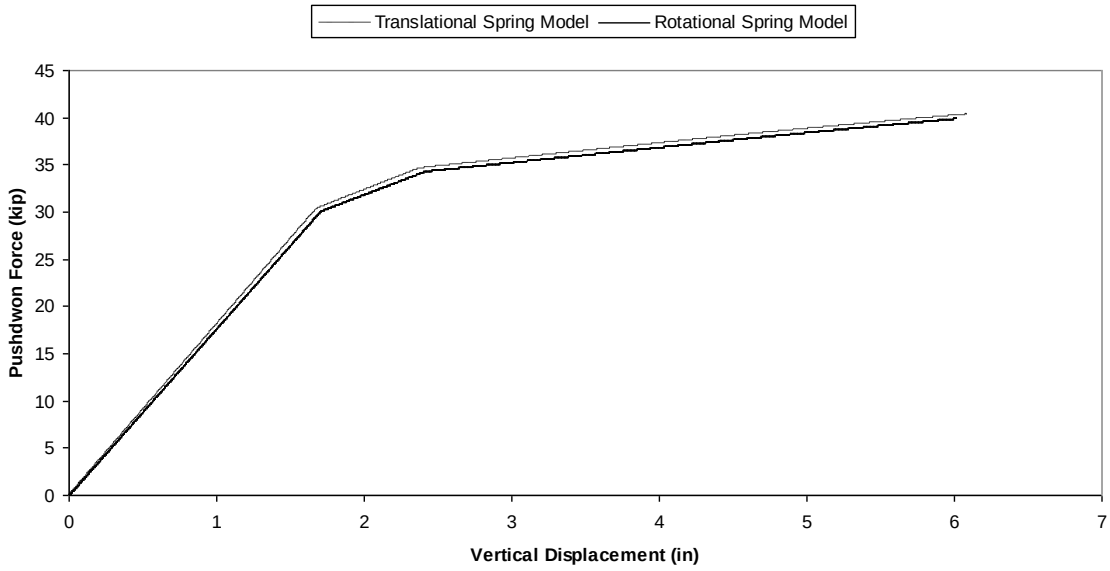

Figure 3.26 Comparison of pushdown results

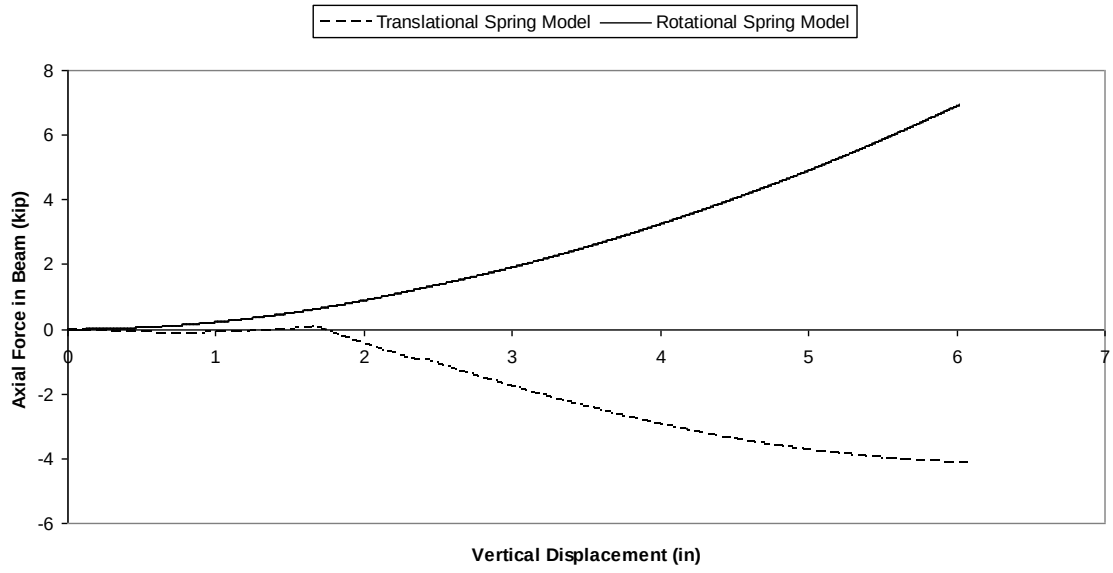

Figure 3.27 Predicted axial forces in beams in two models

The comparison of pushdown results is presented in Figure 3.26, which shows that the relationships between vertical displacement and pushdown force (collapse-resisting capacity) for the two assemblies are nearly the same. However, the aforementioned effect of the location of center of rotation and unequal stiffnesses on axial forces in beams has been confirmed in Figure 3.27, which shows that, during pushdown, the beam of the assembly with seismic connection is under tension, while the assembly with connection model for collapse analysis is under compression. Since the rotational limit is relatively small, the discrepancy in axial forces in beams does not lead to large differences in the collapse-resisting capacity of the frames with riveted connections, as illustrated in Figure 3.26. Therefore, the seismic model of riveted connections can be directly applied for collapse analysis in this paper. Hereafter, the

seismic connection model will be used in the analysis of older steel frames during collapse.

3.4 CLOSURE

The behaviors of three typical connections during collapse of structures were modeled with different methods in this chapter. The behaviors of pre-Northridge moment-resisting connections were investigated through detailed finite element simulation. The macro-model of the bolted T-stub connections was obtained by assembling the corresponding models of each separate element in a connection. The model of the riveted connections was developed through adapting the records of seismic tests. These models will be integrated into nonlinear structural models of steel buildings to perform robustness assessment in next chapter.

CHAPTER 4 ROBUSTNESS ASSESSMENT OF TYPICAL STEEL BUILDINGS

With the connection models developed in Chapter 3, the robustness of several typical steel structures in the United States (pre-Northridge moment-resisting frames, partially-restrained frames) is assessed. For the pre-Northridge moment-resisting frames, the significance of uncertainties in collapse assessment is examined by comparing the results from mean-centered deterministic and probabilistic assessments of the frames. A deterministic assessment of frames with bolted T-stub connections is conducted with consideration of three typical beam spans in both directions. For the older steel buildings with riveted connections, the contribution from unreinforced masonry infill and slab are taken into account.

4.1 ROBUSTNESS OF STEEL MOMENT FRAMES

The robustness of two steel moment frames designed in the SAC project is evaluated using (a) the deterministic method found in the new *Unified Facilities Criteria* (2009) and (b) a system reliability analysis method to investigate the role of uncertainties in connection behavior. Both evaluations are performed with nonlinear dynamic analysis. In the system reliability analysis method, the uncertainties in gravity loads and resisting capacities described by the probabilistic connection model are considered, while the mean failure moment of the connections is used as a "best estimate" of connection capacity in the deterministic method.

4.1.1 Description of the Steel Moment Frames Considered

The Seattle and Boston three-story steel moment frames, denoted as SE3 and BO3, were designed using the *1994 Uniform Building Code* (UBC 1994) and the *1993 National Building Code* (BOCA 1993) respectively. Both frames have the same plan view and elevation, as shown in Figure 4.1; the perimeter moment-resisting frames are illustrated by the bold lines in the plan view. All columns and beams in the perimeter frames are ASTM A572 Gr. 50 steel and are oriented to bend about their strong axes. The member sections for the north-south (NS) moment-resisting frames are provided in SAC Project Report 355D (FEMA 2000b). Frame SE3, which was designed for a highly seismic area, would be considered a strong column-weak beam frame, while frame BO3, which was designed for only moderate seismicity, has columns that are relatively weaker with respect to the beams. The gravity load distributions for both structures calculated from details provided in SAC Project Report 355C (2000a) are floor dead load of 96 psf (4.60 kPa), roof dead load 83 psf (3.97 kPa), and reduced live load 20 psf (0.96 kPa). Further details on the design and detailing of these frames are available in that report.

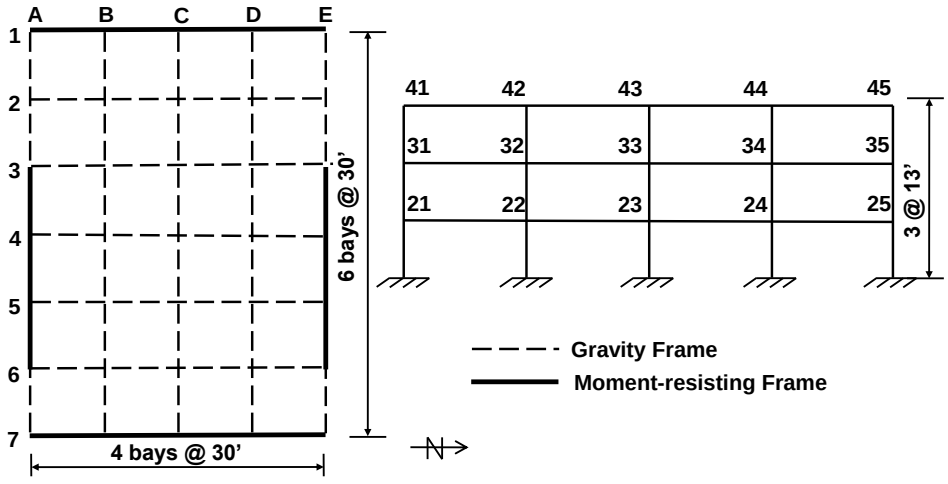

Figure 4.1 Floor plan and elevation for the frames SE3 and BO3 (FEMA 2000a)

The NS moment-resisting frames are used for the robustness assessment. In the finite element model of the frames, each beam is divided into 4 elements while each column is modeled by one element. Columns and beams both are modeled using nonlinear beam-column elements with fiber sections to account for the interaction of moment and axial force. Masses are calculated based on the gravity loads. The material model is bilinear elastic-plastic, with a 3% strain hardening ratio. The mean yield strength is used in the structural analysis. The nonlinear analysis allows for the development of P-Δ effects in the frame, if required. The catenary action in beam elements can be captured through a co-rotational transformation of geometry.

Two column removal scenarios are considered. The first scenario involves the removal of a quarter-point column at the first floor level (column D7-1, see Figure 4.1), while in the second scenario, a column is removed at the corner of the first floor (E7-1). Prior to initiating the dynamic analysis, the gravity load is preloaded on the frames; once static equilibrium is achieved, the dynamic analysis is initiated by sudden removal of one column. All analyses of the moment frames are performed using the computer program OpenSees (Mazzoni et al. 2009). In Scenario 1 involving sudden removal of column D7-1, the connections adjacent to the nodes 24, 34 and 44 (Figure 4.1) are most vulnerable to the dominant failure mode, which is fracture at the bottom of the connections. The two connections adjacent to node 24 are designated as 24-L and 24-R, where the number 24 denotes the number of the adjacent node and L and R denote left and right side of the node. The same naming rule is also applied to the other connections. In Scenario 2 involving sudden removal of column E7-1, connections 24-R, 34-R, 44-R, 25-L, 35-L and 45-L are susceptible to failure. However, only the possibility of failure of

connections 25-L, 35-L and 45-L is considered. In all analyses, the absolute values of the connection moments are normalized with the full plastic moment of the connected beam section to obtain the corresponding normalized moment.

4.1.2 Deterministic Assessment

The nonlinear dynamic procedure in the *Unified Facilities Criteria* (DoD 2009) stipulates that the following gravity load combination is to be applied to each frame:

$$GL = 1.2DL + 0.5LL \tag{4-1}$$

where DL = nominal dead load and LL = nominal live load (ASCE 2006). The analysis of the scenario involving sudden removal of column D7-1 shows that the moments in the two connections adjacent to a node are very close; hence, only the moment history at the left connection is presented. The dynamic response at that connection is illustrated inFigure 4.2. Following the instantaneous removal of column D7-1 in BO3, the normalized moment in connection 24-L reaches the maximum value 1.08 after 0.38 s, which is larger than the mean failure moment 0.54 determined in Section 3.1. Therefore, connection 24-L of BO3 is susceptible to fracture under this damage scenario. The maximum normalized moments of connections in BO3 and SE3 following sudden removal of one column are summarized in Figure 4.3. Since the maximum normalized connection moment following sudden removal of column E7-1 also exceeds the mean failure moment, the *UFC* requirements for robustness are not satisfied for Frame BO3.

The maximum normalized connection moments in Frame SE3 following sudden removal of columns D7-1 and E7-1 are also larger than the mean failure moment.

Therefore, the requirements of robustness are not satisfied for Frame SE3, even though the Seattle frame has stronger beam and column sections than the Boston frame.

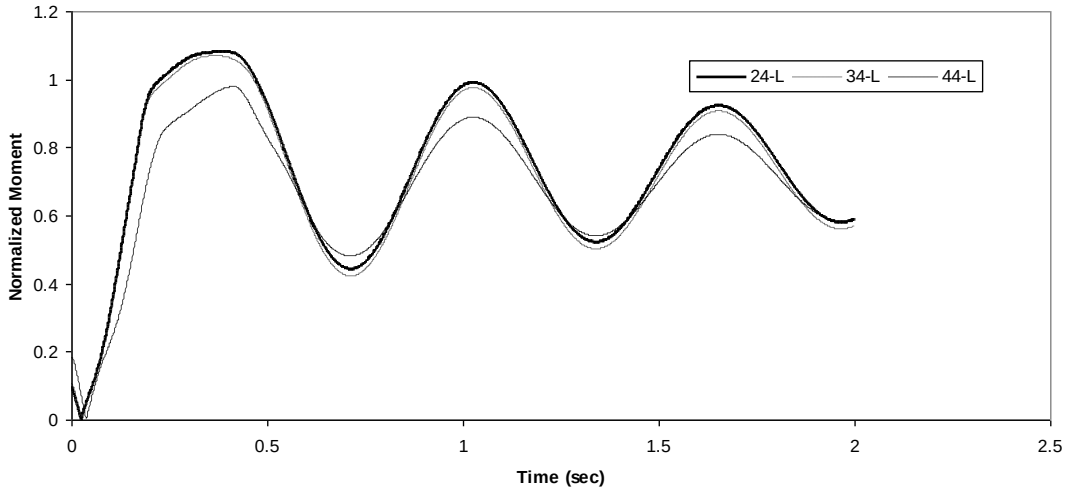

Figure 4.2 Normalized connection moment history following removal of column D7-1 in BO3

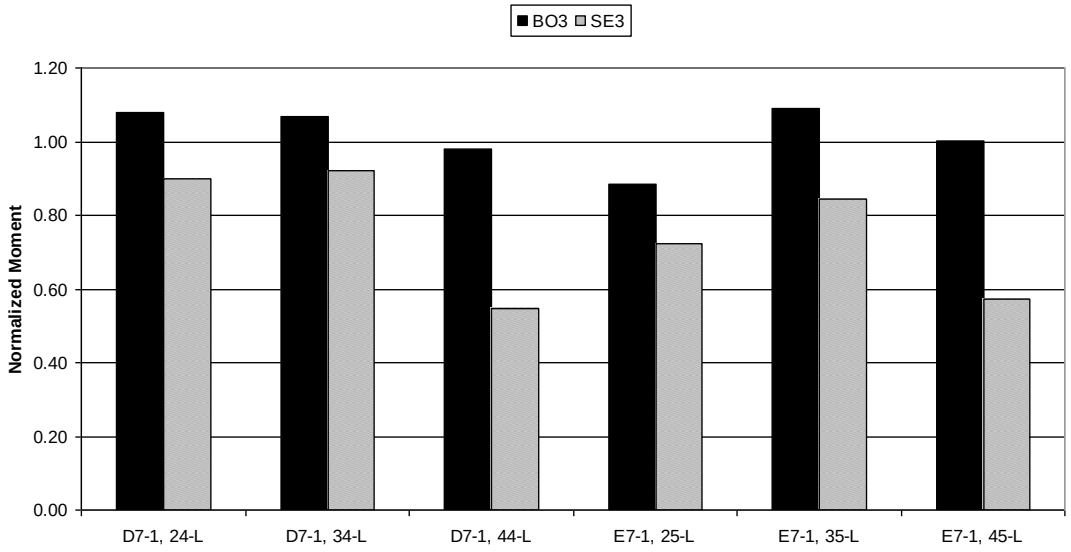

Figure 4.3 Maximum normalized moments of connections in BO3 and SE 3 following sudden removal of one column

4.1.3 Probabilistic Assessment

In the probabilistic assessment, the randomness of the dead and live loads and fracture moment are considered explicitly. The dead and live load distributions are consistent with those used by Ellingwood et al. (1982) to develop the load combinations in *ASCE Standard 7-05* (ASCE 2006). The dead load was modeled with a normal distribution with a mean value of 1.05*DL* and a COV of 0.10. The live load was modeled with an extreme value type I distribution, with a mean value of 0.3*LL* (approximately the average load on the floor at any point in time) and a COV of 0.6. The uncertainties in loads and fracture moments were propagated through the nonlinear FE analysis using Latin Hypercube sampling with 100 samples, and the maximum connection moments were recorded for each sample. An example of the distribution for maximum moment in connection 24-L in Frame BO3 following sudden removal of the column D7-1 is shown in Figure 4.4, where the data have been fitted by a lognormal distribution.

The probability of connection failure following notional column removal is

$$P_f = \int_0^\infty F_{Frac}(m)\, f_M(m) dm \tag{4-2}$$

where f_M is the fitted PDF of the maximum normalized moment of a connection in a scenario of sudden column removal. The probabilities of connection failures in Frames BO3 and SE3 for comparable column damage scenarios are compared in Figure 4.5. Following sudden removal of column D7-1, connection 24-L in BO3 has a probability of failure of 0.98; the probability of failure of connection 34-L is approximately 0.98. In contrast, for SE3, in the failure scenario of the column D7-1, connection 34-L is most likely to fail, with probability of failure 0.85. After sudden removal of column E7-1, the

maximum probability of failure of the connections in BO3 is still very close to 1.0, while the maximum probability of failure in SE3 is 0.78.

4.1.4 Summary

This section has presented a probabilistic robustness assessment of two typical seismically designed pre-Northridge steel moment-resisting frames. A probabilistic model of fracture of the connections, which was developed in Section 3.1, was integrated into the structural model of the frames. An alternative path analysis of the frames incorporating the connection model was performed using nonlinear dynamic finite element analysis. The FE analysis revealed that catenary action was not developed on these particular frames due to the small vertical displacement. On the other hand the flexural demands on the connections were found to be much larger than the mean failure moment derived from the probabilistic model, indicating that the probability of connection failure is quite high. Therefore, SMRF with connections similar to those found in pre-Northridge building construction may not satisfy the *UFC* robustness requirements. Uncertainties in connection behavior had little impact on collapse behavior, suggesting that a mean-centered deterministic analysis should be sufficient for a general structural integrity assessment in accordance with the *UFC* requirements. While the residual capacity of the connections following fracture was non-negligible for these frames and connections, further research is needed to properly model the behavior of connections after the occurrence of fracture. Accordingly, the connection behaviors in the following two sections are modeled as deterministic.

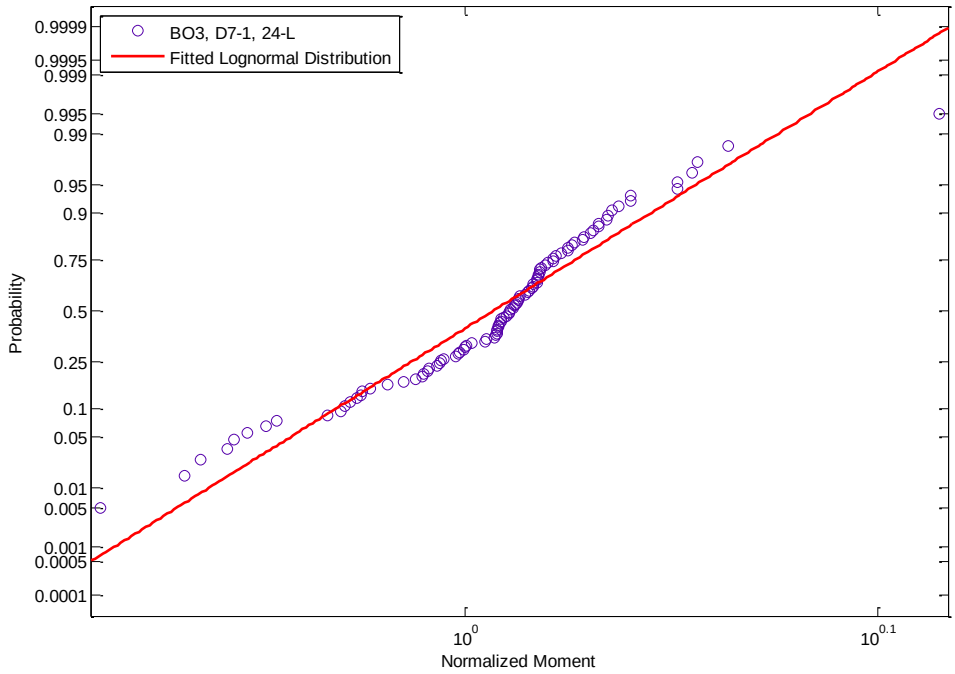

Figure 4.4 CDF of the maximum moments of the connection 24-L in BO3 following sudden removal of the column D7-1

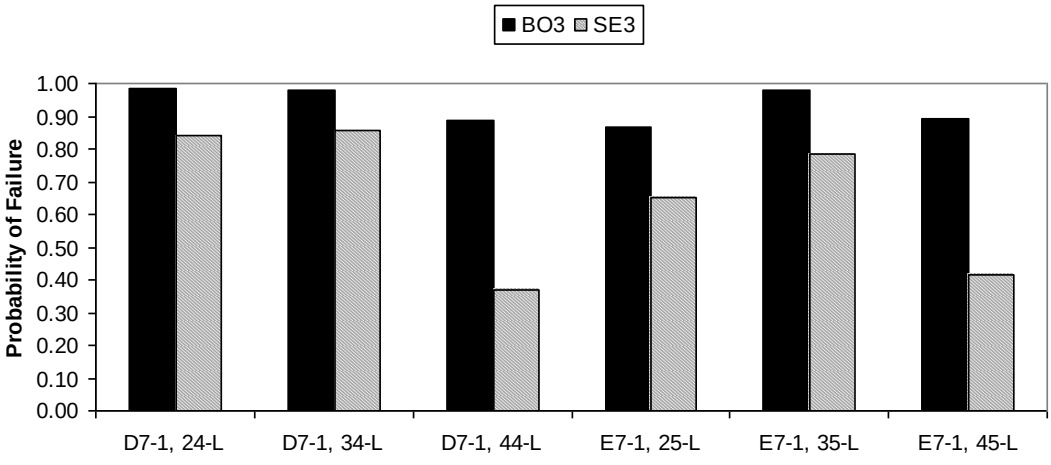

Figure 4.5 Probability of failure of connections in BO3 and SE 3 following sudden removal of one column

4.2 ROBUSTNESS OF STEEL FRAMES WITH PARTIALLY RESTRAINED (PR) T-STUB CONNECTIONS

The robustness of generic steel frames with PR T-stub connections is examined using a method proposed by Izzuddin et al. (2008), in which the vulnerability of a steel frame to collapse following notional column removal is checked by means of an energy-based static pushdown analysis. It is assumed that a column in a frame shown in Figure 4.6(a) is notionally severed immediately below the T-stub connecting the bottom beam flange to the column. Here, the method is applied to a subassembly consisting of two stories and one beam of a frame spanning two bays in which the center column at the lower story has been damaged, as demonstrated in Figure 4.6(b).

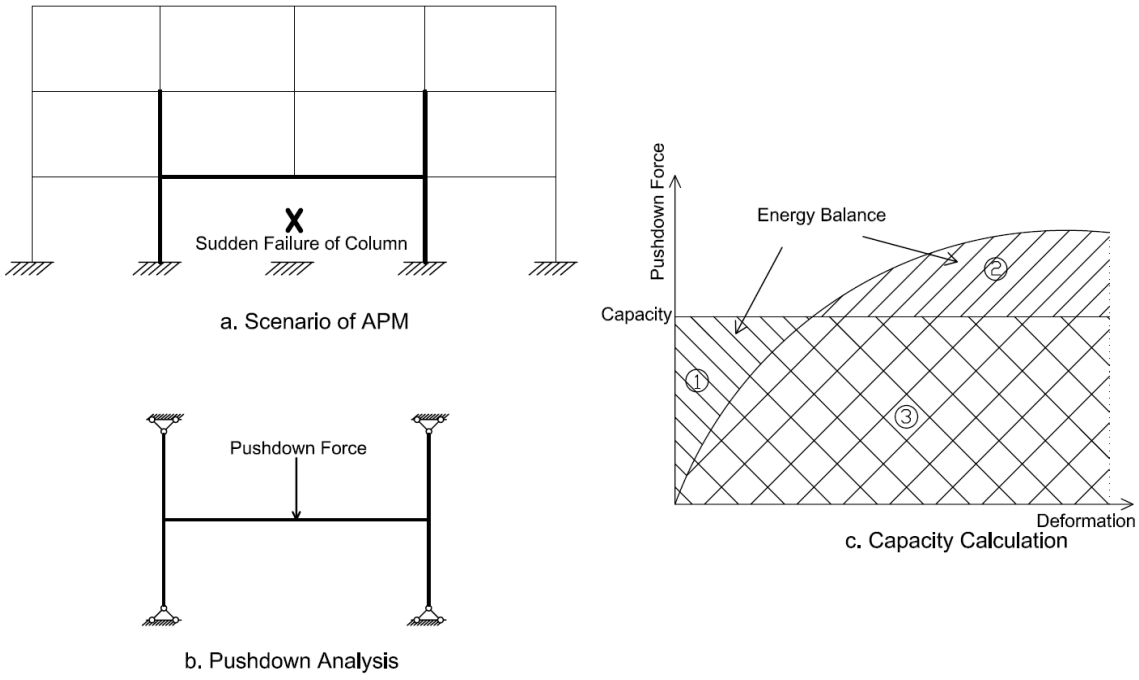

Figure 4.6 Illustration of assessment methodology

The pushdown analysis is conducted by applying a concentrated vertical force at the top of the center column of the upper story. This vertical force is increased under displacement control until the point is reached at which failure of the connections adjacent to the center column occurs. As the vertical load is increased, the energy balance between the work done by the external loads (i.e. gravity loads) and the strain energy stored in structural members is checked. The strain energy can be calculated indirectly from the work done by the incremental external pushdown forces acting through the corresponding displacements, which is equal to the sum of hatched areas 2 and 3 shown in Figure 4.6(c). If the energy balance can be maintained between the work done by a specific gravity force (the sum of hatched areas 1 and 3) on the frame subassembly and the strain energy of deformation before the occurrence of connection failure, the subassembly can resist the gravity force. The capacity of a subassembly is defined by the maximum concentrated gravity force that it can resist. For the frame subassembly in Figure 4.6, when either the failure of the bottom T-stub of a connection connected to the center column or the rotational failure of the beam framing into that connection occurs, the capacity of the connection is assumed to be completely lost (i.e., the connection has no residual capacity). With this assumption, the displacement versus pushdown force curve is monotonically increasing, and the frame capacity can be simply obtained through dividing the strain energy at the point of connection failure by the corresponding displacement (i.e. the maximum vertical displacement). The boundary conditions for the frame subassembly are shown in Figure 4.6(b). It is assumed that the bracing of the undamaged frame is sufficient to preclude instability of these two side columns following the removal of the center column. On the other hand, the rotational

restraint provided by the beams in the outer two spans connecting the subassembly to the exterior columns is not considered as part of the boundary conditions. Studies have shown that including these beams in the analysis does not affect the conclusions.

There are two limitations of the simplified assessment method. First, the stability of the columns adjacent to the removed column following its removal is not checked. Second, the method only assesses the performance of the stories and bays that are immediately adjacent to the damaged (removed) column rather than the whole frame. Accordingly, while the simplified model provides a basis for assessing the integrity of the framing system adjacent to the bays in which damage occurs, it may not provide sufficient information about frame robustness if the structural frame configurations differ significantly from story to story. In other words, the method of assessment is limited to framing systems which are regular in plan and in elevation.

4.2.1 Pushdown Analysis

Subassemblies with connections fabricated using two representative T-stubs TA-01 and TD-01 from test series A and D, respectively, reported by Swanson and Leon (2000) were evaluated. Both T-stub connections are prequalified (Leon, private communication); one (designated as "full-strength") is intended to develop the full plastic moment capacity of the connecting beam while the second (designated as "partial strength") transfers only a portion of the plastic moment capacity. All T-stubs were fabricated from ASTM A572 Grade 50 Steel, which was also used for all columns and beams. The series A T-stubs cut from W16x100 shapes are representative of relatively stiff PR connections, while the series D T-stubs cut from W16x45 shapes represent

relatively flexible PR connections. The nominal yield strength for ASTM A572 Gr. 50 steel is 50 ksi (345 MPa). The mean yield strength for this grade of steel is 57.6 ksi (397 MPa) and the mean ultimate tensile strength is 75.6 ksi (521 MPa) (FEMA 1995). All analyses performed in this study utilized the mean values of material properties. Two failure modes were considered. For full-strength connections, both the tensile failure of T-stubs and the rotational failure of beams must be taken into account due to the possible development of catenary action in the beams. For the partial-strength connections, only failure of the T-stubs needs to be considered. Due to the lack of experimental data to establish the beam rotation limit of full-strength bolted T-stub connections, that limit cannot be determined directly. However, the rotation limit of connections in steel special moment-resisting frames, which are full-strength connections and have the same failure mode (i.e. ductile fracture of bottom beam flange), should be comparable to the rotation limit for full-strength bolted T-stub connections. Khandelwal and El-Tawil (2007) found that the rotation limit of connections in steel special moment-resisting frames increases as the depth of the beam decreases. Hence, it was assumed in this study that the plastic rotation limit for the beams is 0.05, which is the lower limit in Khandelwal and El-Tawil (2007). This value is believed to be conservative. A similar limit (i.e. 0.054) was proposed in FEMA (2000b) for seismic design.

The subassemblies first are simplified by neglecting components with negligible contributions to frame behavior. Subassemblies with T-stub TA-01 connections and representing three typical beam spans are analyzed. To study the effect of different bolt configurations (i.e. size, grade, number, gauge and spacing of bolts), subassemblies with T-stub TA-07 connections, which have a different gage of tension bolts, are also

evaluated. Finally, subassemblies with T-stub TD-01 connections are analyzed to assess the capacity of partial strength T-stub connections.

4.2.2 Model Simplification

The panel zone must be considered in the connection model if the shear deformation is large. The beam-column connections of a structure subjected to large lateral forces undergo high shears due to the significant imbalance of beam moments during an earthquake. In contrast, the imbalance of beam moments following column removal due to gravity loads alone is usually small. Sadek, et al. (2008) noted that even though the strength of shear connections is not negligible, they cannot resist collapse alone following sudden failure of one column. Figure 4.7 shows the comparison of pushdown results of models of a subassembly with a span of 30 ft (9.14 m) and a story height of 13 ft (3.96 m) with three different connection modeling assumptions. The subassembly has the same beam, column and connection configuration as specimen FS-05, except that the panel zone is not reinforced. The subassemblies were loaded at the top of the center column of the upper floor until the failure of bottom T-stubs connected to the center column occurred. Figure 4.7 shows that the shear tab makes a substantial contribution to the strength and ductility of the connection; this contribution may become even more important for connections with weak T-stubs (e.g. T-stub TD-01 in this study). In contrast, the deformation of the panel zone has little effect. Hence, in the following subassembly analyses, shear tabs will be included in the connection models but the effect of panel zone deformations will be neglected. Due to the symmetry of the subassembly

considered, only half of the subassembly is modeled and the center column need not be modeled explicitly.

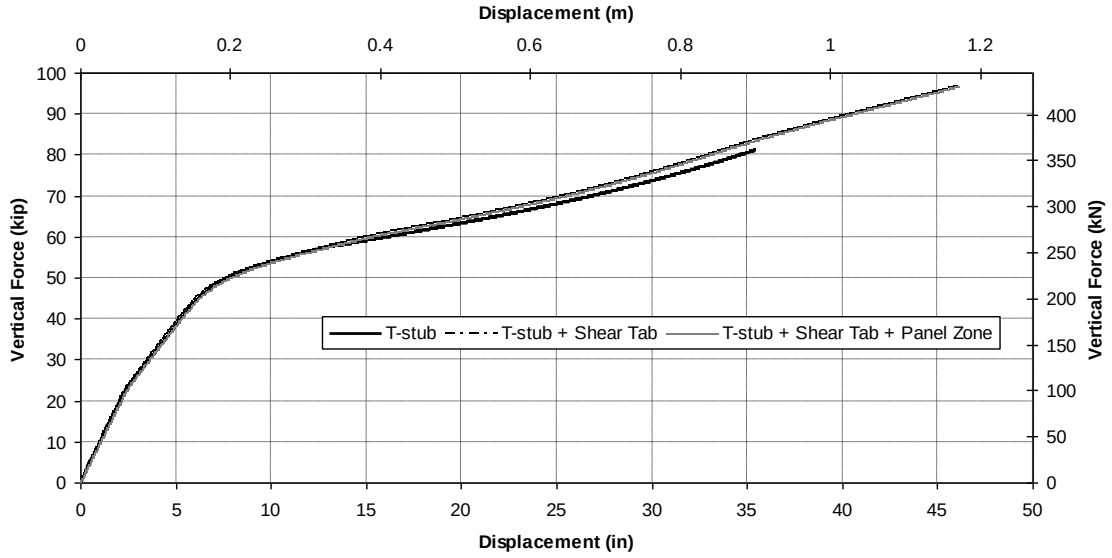

Figure 4.7 Comparison of component contributions to T-stub connection performance

4.2.3 PR Connections with T-stub TA-01

To assess the capacity of frames with PR T-stub connections, three subassemblies as illustrated in Figure 4.6(b) with different bay sizes - 20, 25 and 30 ft (6.10, 7.62 and 9.14 m) - but the same story height 13 ft (3.96 m) are pushed down at the center column until failure occurs in the bottom T-stub adjacent to the center column. The three subassemblies have the same W14x155 columns and W24x55 beams, PR connections with T-stub TA-01 and shear tab, as shown in specimen FS-05 (see Figure 3.17 and Figure 3.18). The connections are full-strength, in the sense that the fully plastic moment

of the beam is less than the maximum moment that can be transferred by a pair of TA-01 T-stubs. The assumption that failure of the bottom T-stub determines the subassembly capacity is confirmed by Figure 4.8, which shows that the maximum beam end plastic rotations during pushdown in all three cases are less than the stipulated beam end rotation limit of 0.05. The comparison of pushdown results presented in Figure 4.9 shows that the maximum vertical pushdown force decreases as the beam span increases, while the maximum displacement increases at the same time. For the subassembly containing beams with spans of 6.10 m, the maximum vertical pushdown force is 135.7 kip (604 kN) and the vertical displacement reaches 24.8 in (0.63 m). In contrast, the subassembly with span of 9.14 m has the maximum displacement of 46.1 in (1.17 m) and the maximum pushdown force of 96.1 kip (428 kN). The capacities of each subassembly calculated from the pushdown force-displacement curves are also shown in Figure 4.9 with dashed lines, showing that the collapse resistance capacity decreases as the span increases. The subassembly with the span of 6.10 m can resist 100.5 kip (447 kN) concentrated gravity force at the center column, while the subassembly with the span of 9.14 m can only resist 65.9 kip (293 kN) concentrated gravity force.

Figure 4.10 shows the internal forces developed in the T-stubs connecting the beam flanges to the damaged center column during pushdown following notional column removal. The top T-stubs undergo compression (i.e. negative force), while the bottom T-stubs undergo tension (i.e. positive force). Were this frame subjected to lateral forces due to an earthquake, the axial forces in the beams would be small and the internal forces in the top and bottom T-stubs would be nearly balanced. In contrast, following column removal, a substantial imbalance of the internal forces in the top and bottom T-stubs

develops under gravity loads as a result of catenary action, leading to high tensile axial force in the beams. Due to this catenary effect, the failure of the T-stub may control the connection strength even in connections with full-moment strength, which seldom occurs as a result of an earthquake. Moreover, the maximum imbalance increases as the span increases, behavior that is consistent with the increasing significance of catenary action as the span increases. The imbalance reaches 66.2 kip (295 kN) at the point of bottom T-stub failure in the subassembly with the span of 9.14 m, while the imbalance is 32.9 kip (147 kN) in the subassembly with the span of 6.10 m. Accordingly, the catenary effect should be included when modeling the behavior of a frame with PR connections following column removal.

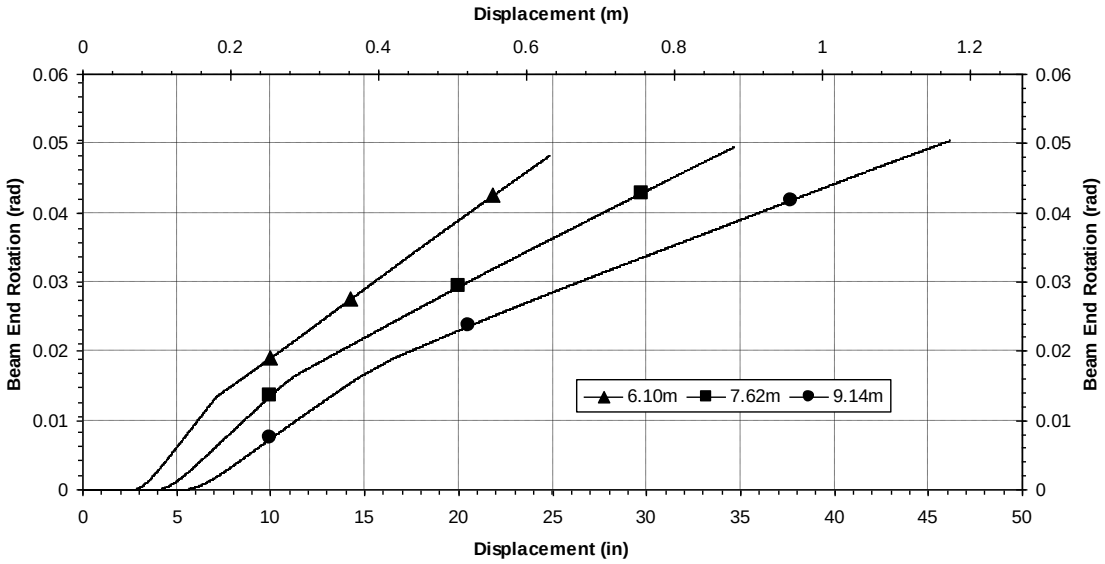

Figure 4.8 Subassembly pushdown analysis - beam end plastic rotations

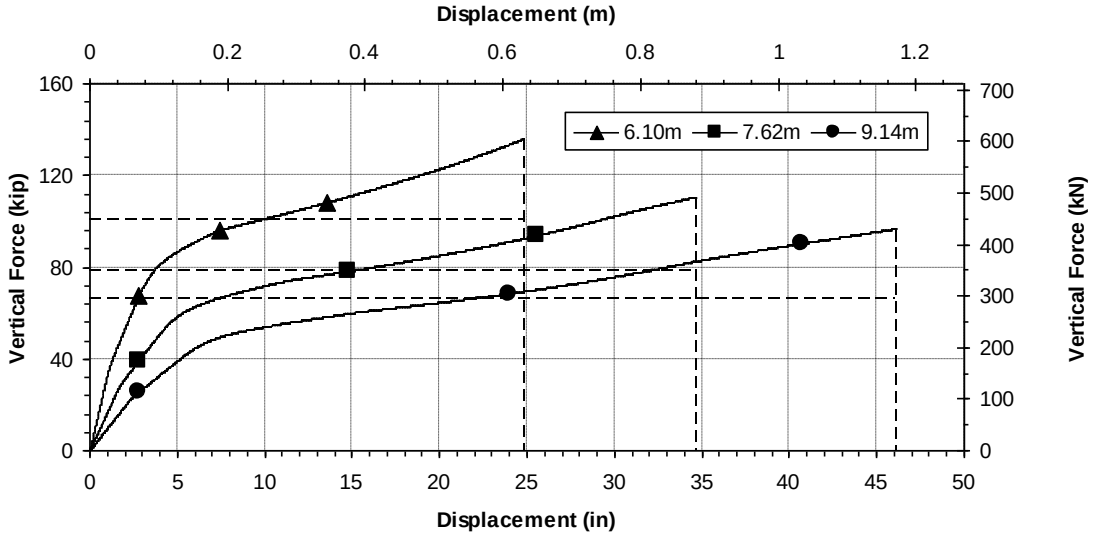

Figure 4.9 Subassembly pushdown analysis – force-displacement for different spans

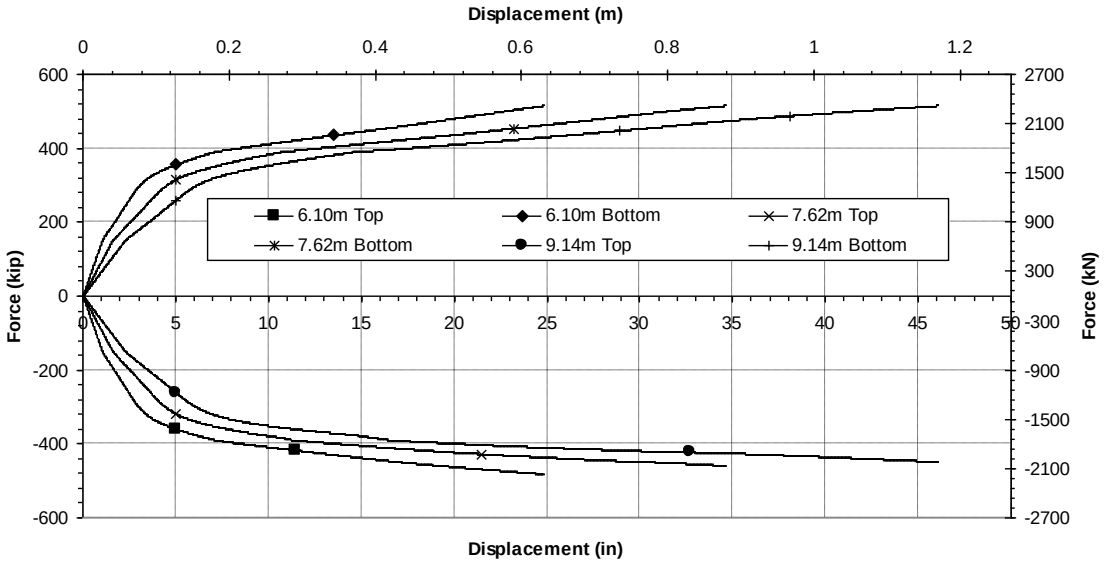

Figure 4.10 Internal forces developed in connection T-stubs TA-01 during pushdown

4.2.4 PR Connections with T-stub TA-07

T-stub TA-07 is nearly identical to T-stub TA-01 except that the gage between the two rows of tension bolts is 6 in (152 mm) rather than 4 in (102 mm) as in T-stub TA-01. The static force-displacement relation for T-stub TA-07 is shown in Figure 4.11; both the ultimate strength and deformation are slightly less than the ultimate strength and deformation of T-stub TA-01 that was presented in Figure 3.15.

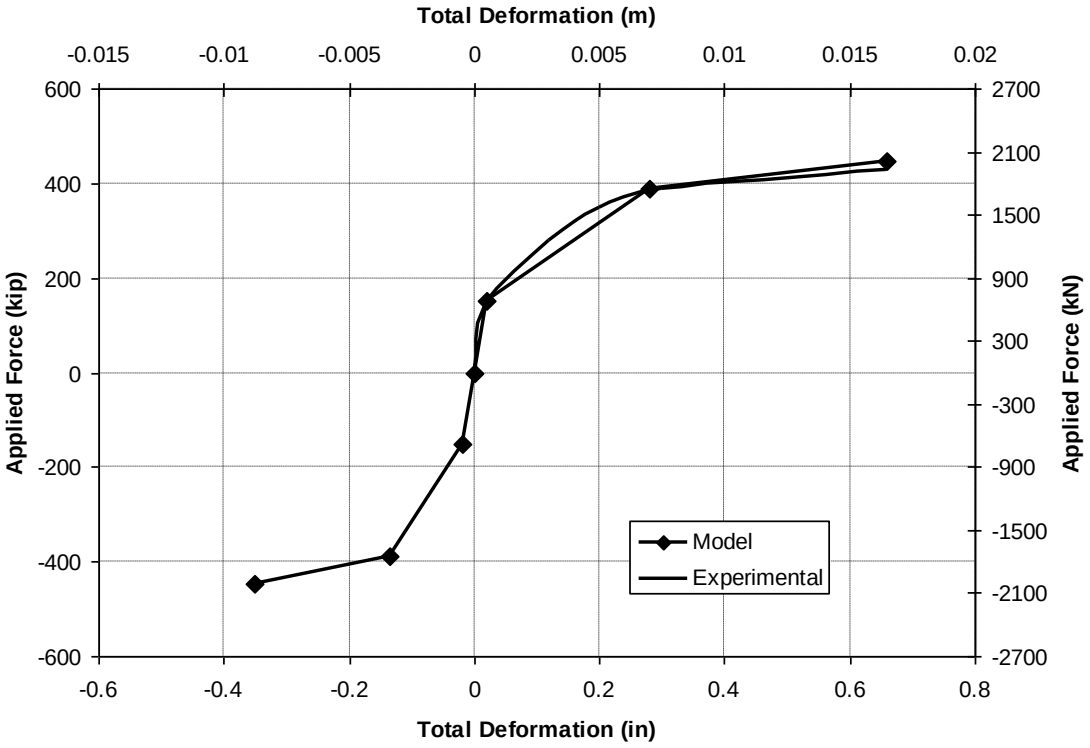

Figure 4.11 Model and experimental force-deformation relationship of T-stub TA-07

The pushdown analysis of the subassembly with this PR connection is presented in Figure 4.12. Subassemblies with spans of 20, 25 and 30 ft (6.10, 7.62 and 9.14 m) have capacities of 88.8, 68.1 and 55.4 kip (395, 303 and 246 kN), respectively, which are

slightly smaller than, but comparable to, the corresponding capacities of the subassemblies with T-stub TA-01 as well. Accordingly, it may be inferred that the use of PR connections with T-stubs having the same dimensions but slightly different bolt configurations does not change the collapse resistance capacity of the frames significantly.

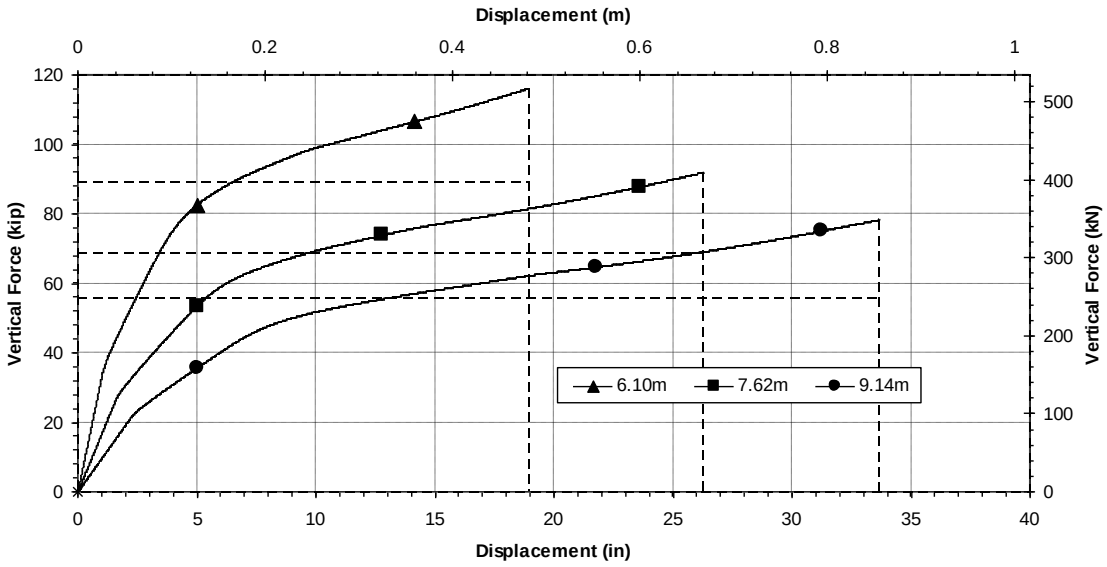

Figure 4.12 Pushdown analyses for subassemblies with PR connections of TA-07

4.2.5 PR Connections with T-stub TD-01

Pushdown analyses were conducted on a second set of subassemblies compromised of W21x44 beams bolted to W14x145 columns by L9x5x3/8 shear tabs and T-stubs cut from W16x45 sections. The T-stubs for these frames are designated as TD-01, details of which are shown in Figure 4.13. The shear tab and beam web were

fastened by three 7/8 in (22 mm) diameter A490 bolts 2-1/4 in (57 mm) in length. The panel zones were unreinforced. The Swanson and Leon (2001) model overestimated the ultimate deformation of T-stub TD-01, although the prediction of its ultimate strength was quite accurate. Accordingly, the tri-linear connection model was fit to the experimental data directly, as shown in Figure 4.14. Only the failure of the T-stub is considered since the connections are partial strength and cannot transfer the full plastic moment of beam W21x44. T-stub TD-01 was incorporated in PR connections in subassemblies with three typical spans - 20, 25 and 30 ft (6.10, 7.62 and 9.14 m) - and story heights of 13 ft (3.96 m) as before. The results of the pushdown analyses of these assemblies are summarized in Figure 4.15. Due to the limited capacity in tension of T-stub TD-01, the maximum vertical pushdown forces and the maximum vertical displacement are less than half the maximum forces developed by the PR connections with T-stub TA-01 with the same span. Furthermore, the subassemblies with T-stub TD-01 fail in a brittle rather than the ductile manner observed previously for subassemblies fabricated with T-stub TA-01.

The imbalance between top and bottom T-stub developed during collapse is quite small, as confirmed in Figure 4.16, indicating that the resultant axial force in the beam is small. One reason is that the maximum vertical displacement is small, meaning that the catenary effect cannot be fully developed. In addition, the bolts bearing on shear tab and beam web transfer a portion of axial force in beam, which reduces the imbalance in the T-stub forces as well.

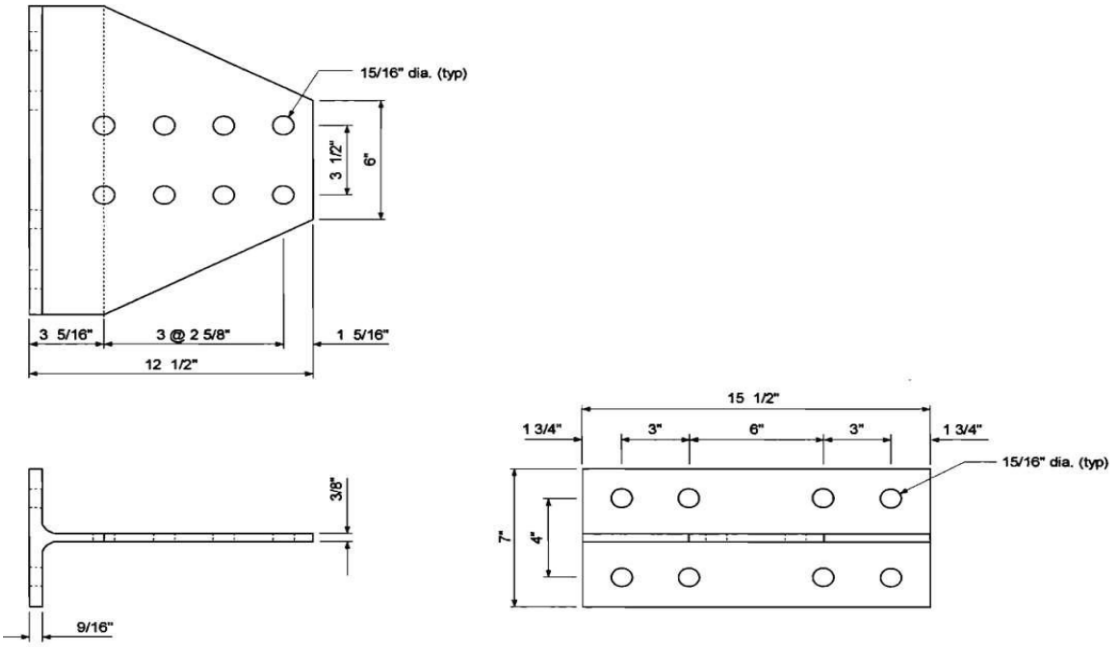

Figure 4.13 Details of T-stub TD-01 (1 in = 25.4 mm) (Swanson 1999)

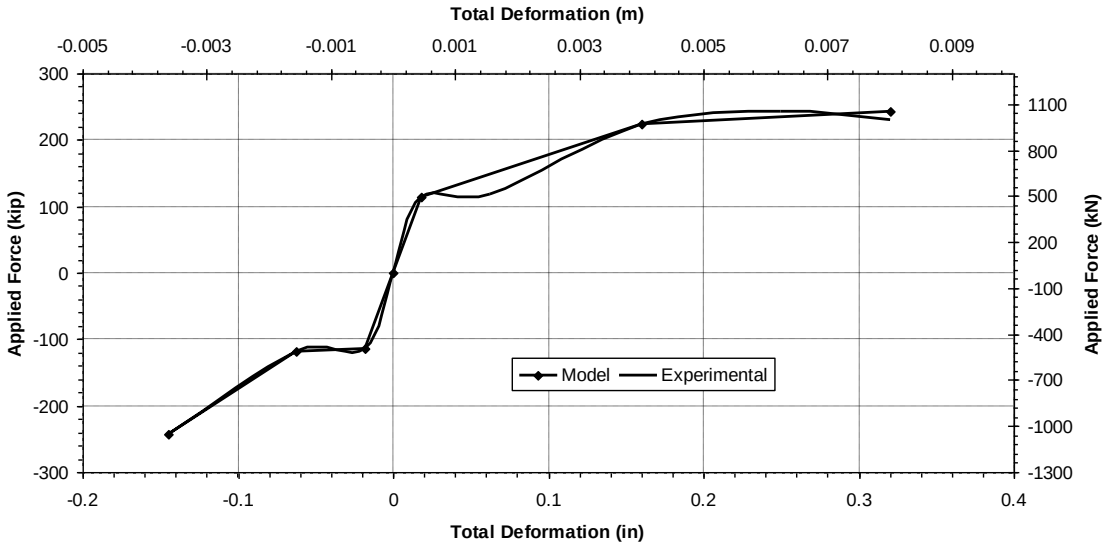

Figure 4.14 Model and experimental force-deformation relationship of T-stub TD-01

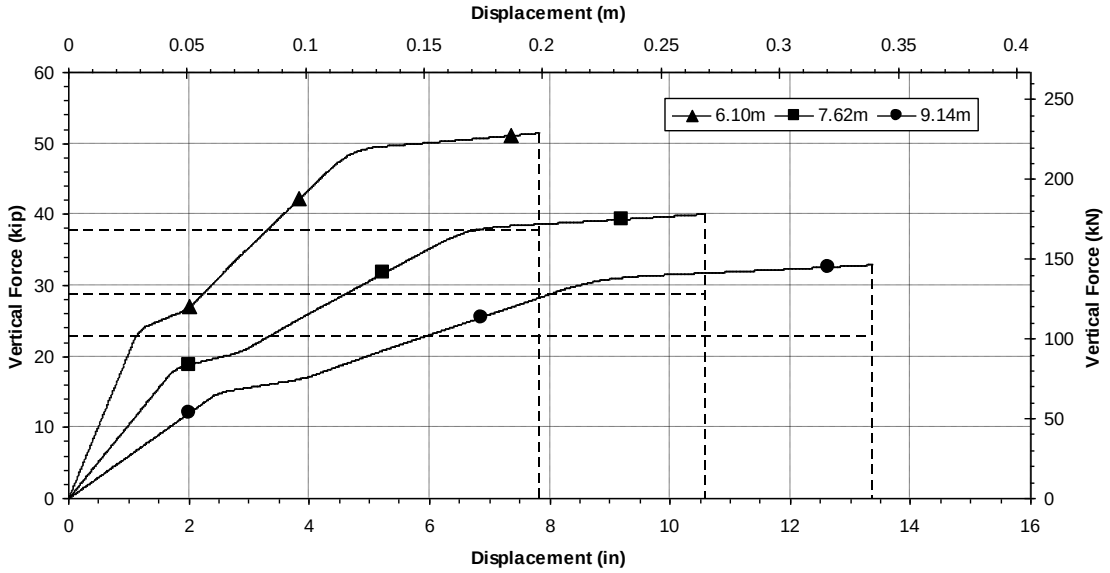

Figure 4.15 Comparison of pushdown results with different spans

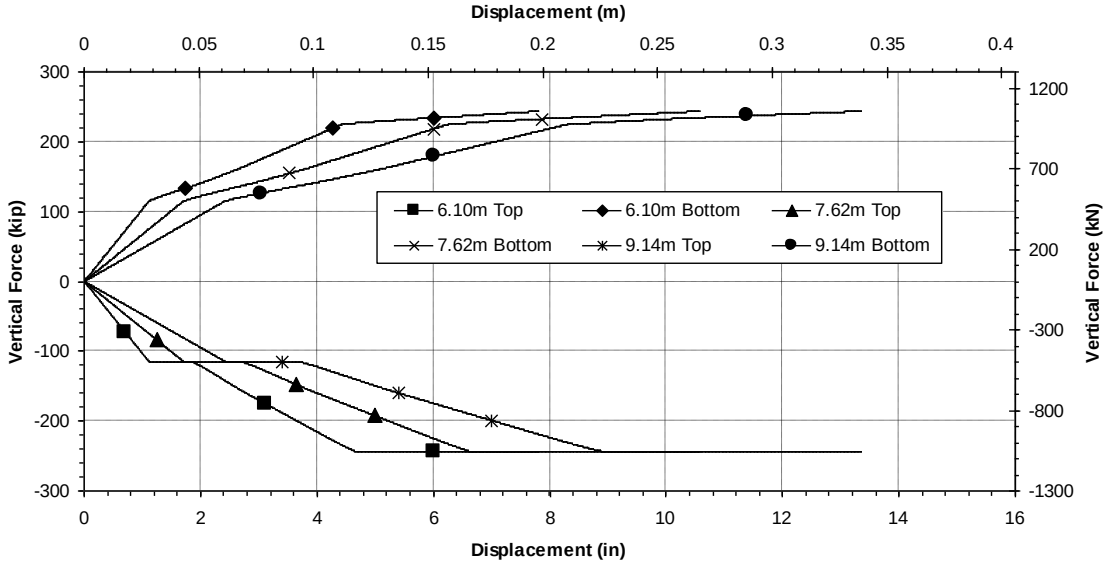

Figure 4.16 Internal forces in T-stubs TD-01 during pushdown

4.2.6 Assessment of Frame Robustness

Current design and construction practices usually place moment-resisting frames at the building perimeter. Perimeter frames also are most likely to sustain damage from vehicular collision or explosive detonations. Accordingly, the frames with PR T-stub connections used to illustrate the assessment of robustness are assumed to be perimeter frames of standard office buildings. For such buildings, the dead load typically is on the order of 100 psf (4.79 kN/m^2), while the fully reduced nominal live load according to *ASCE Standard 7-05* (ASCE, 2006) is 20 psf (0.96 kN/m^2). For plan layout, three typical bay sizes, 20, 25 and 30 ft (6.10, 7.62 and 9.14 m), in both directions are considered. For the case of 2D frame evaluation, gravity loads acting on the hatched area in Figure 4.17 are assumed to act uniformly on the exterior beams. The deflected shape of the beams of a double-span subassembly once the column is notionally removed is assumed to be linear for simplicity. Hence the equivalent concentrated gravity force on the center column of half of a subassembly can be calculated as

$$GL = 0.25L_1L_2(1.2DL + 0.5LL) \tag{4-3}$$

where L_1 = the span at the direction evaluated (i.e. in-plane direction); L_2 = the span at the perpendicular direction (i.e. out-of-plane direction); DL = uniformly distributed dead load on floor; and LL = uniformly distributed reduced live load on floor. The gravity load is defined by the load combination in the *Unified Facilities Criteria* (DoD 2009).

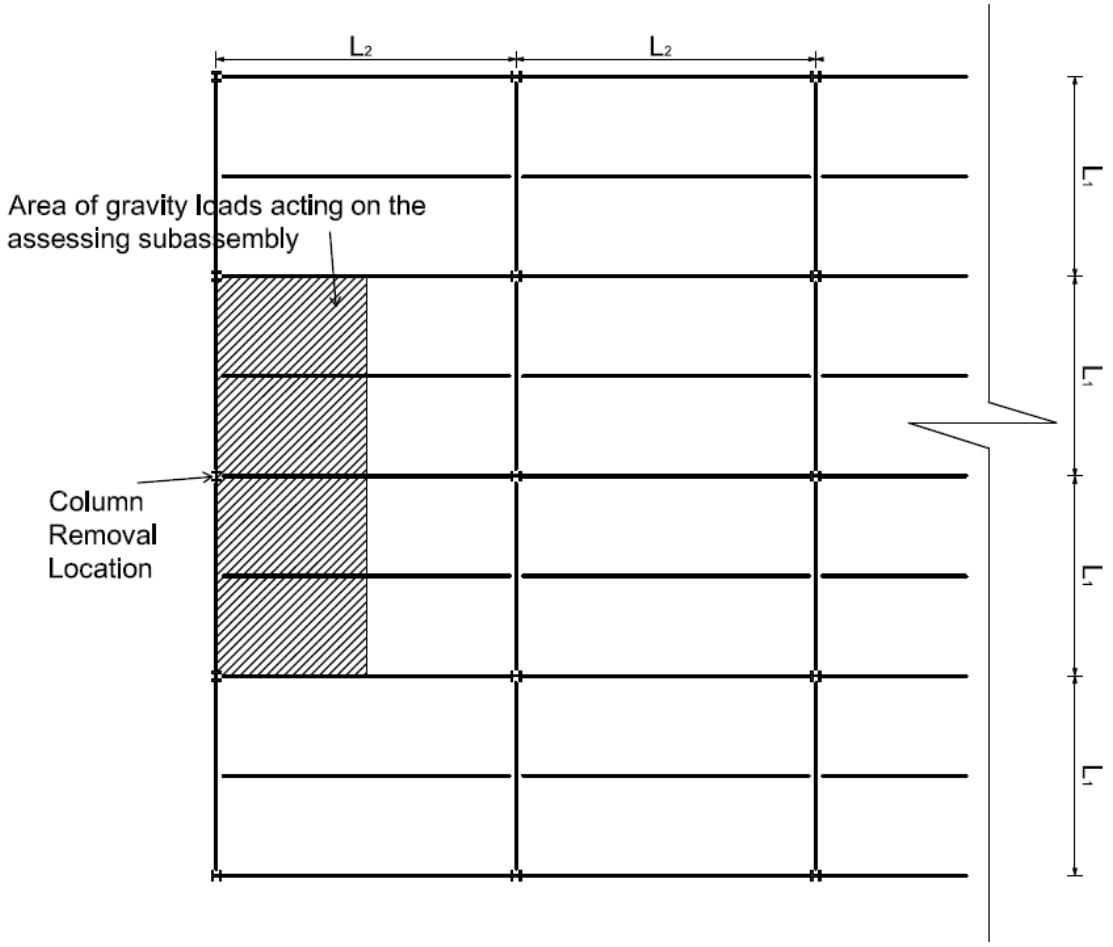

Figure 4.17 Gravity loads on an assessing subassembly

The equivalent concentrated gravity force computed from Equation (4-3**)** acting on the center column for the different structural bay sizes (beam spans) are given in Figure 4.18. The largest force is 29.3 kip (130 kN) for the case in which spans in both directions are 30 ft (9.14 m). Figure 4.18 also summaries the capacities of subassemblies with PR connections fabricated using T-stubs TA-01 and TD-01. The capacities of subassemblies with T-stub TA-01 (fully moment-resistant) are far larger than the demand following sudden failure of one column in frames with all three bay sizes, indicating that

frames with PR connections having comparable stiffness and strength to that provided by T-stub TA-01 should be robust if subjected to an alternative path analysis in accordance with the requirements of the *UFC* (DoD 2009). The capacities of subassemblies with T-stub TD-01 are close to the demands imposed by column removal; indeed, the capacity is smaller than the demand if the span of the in-plane direction is 30 ft, 25 ft and 30 ft (9.14 m, and 7.62 m or 9.14 m) of the out-of-plane direction. Hence, uncertainties in strength and stiffness of such T-stubs and gravity loading should not be ignored, as they may have a substantial effect on the robustness of structural frames with PR connections.

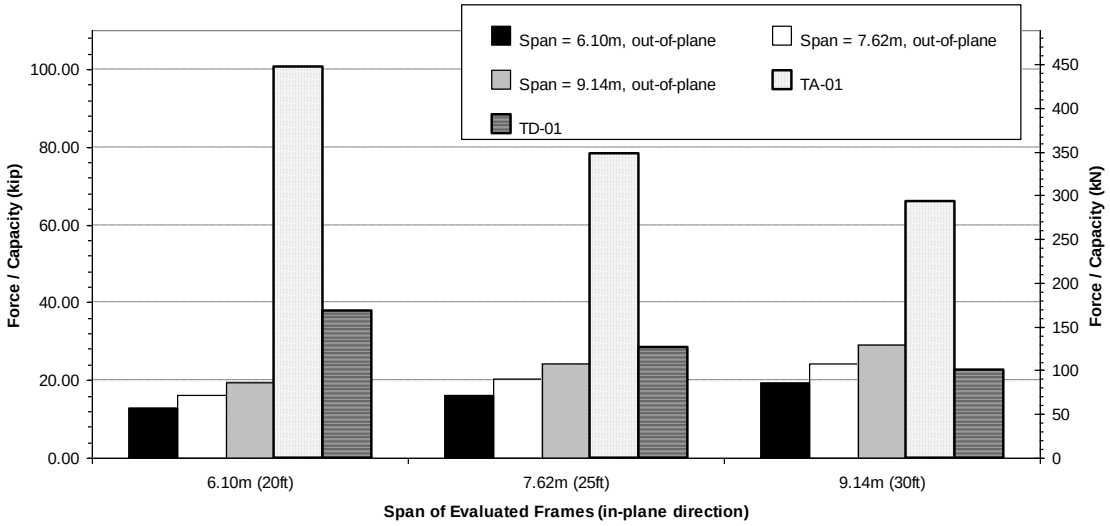

Figure 4.18 Assessment of robustness of frames with PR T-stub connections

4.2.7 Summary

The robustness of typical steel frames with PR connections fabricated from bolted T-stubs has been examined in this section. A macro-model of bolted T-stub connections,

which captures the nonlinear behavior of the connections during collapse, was assembled from individual connection elements. This macro-model was verified by comparing its predictions to test results from a specific T-stub connection. The capability of two steel frames with PR connections representing typical prequalified full-strength and partial-strength connections to withstand sudden column removal was evaluated. The robustness of these frames was assessed by comparing the structural capacities with collapse demands derived from various typical floor plans of standard office buildings. Frames with full-strength bolted T-stub connections can be considered to be robust if evaluated by APM, while the frames with partial-strength connections may not sustain the initial damage from loss of a perimeter column.

4.3 Robustness of Older Steel Structures

4.3.1 Prototype Structure

An eight-story frame presented in Boe (1952) (denoted as frame Boe) was selected for vulnerability as a prototype structure to represent typical older steel structures constructed between the 1920s and 1960s. The elevation of the frame is shown in Figure 4.19, in which the beam and column section properties are also listed. The left and right spans were 20 ft (6.1 m), while the central span was narrower and only 10 ft (3.05 m). The frame is similar to that of the 450 Sutter Building (Roeder et al. 1994), a 26-story steel structure constructed around 1923 in San Francisco, California. The design dead load and live load are assumed to be 80 and 40 psf respectively.

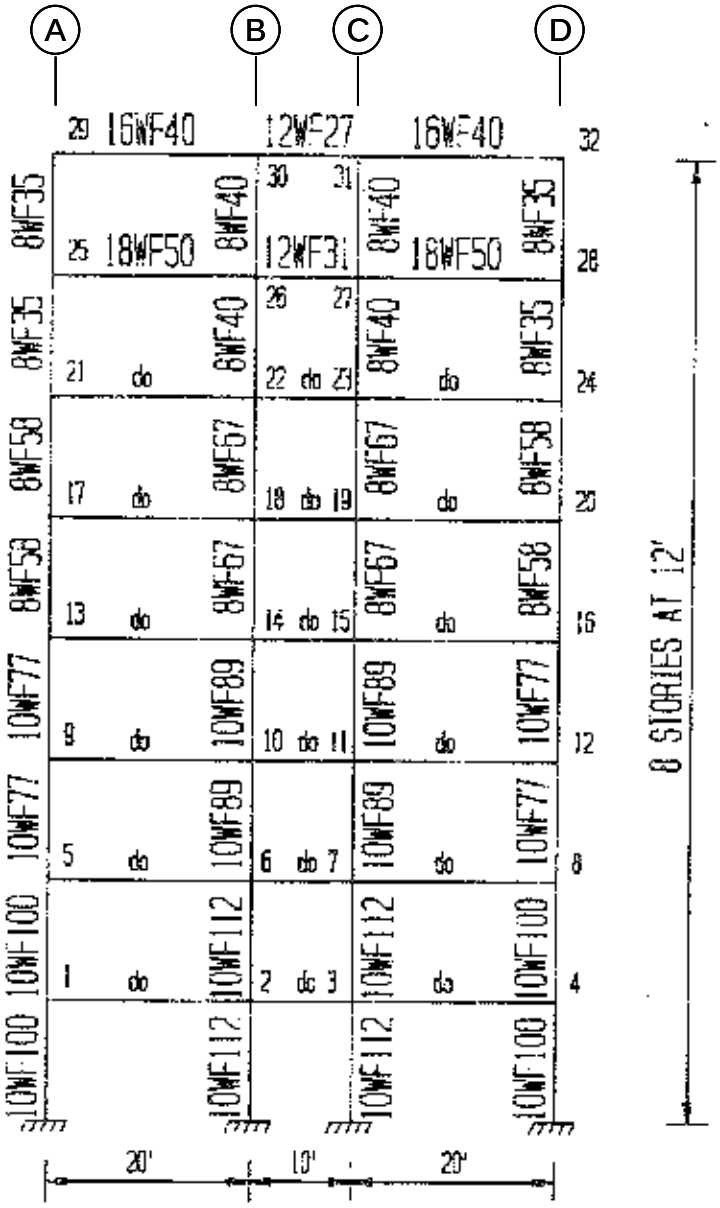

Figure 4.19 Elevation view of frame Boe (Boe 1952)

The frame was filled with unreinforced structural clay tile masonry with a thickness of 6 in, the weight of the infill is assumed to be 22 psf (Hool and Johnson 1920). The frames were spaced 20 ft (6.1 m) out-of-plane. As illustrated by this frame, older steel structures have characteristics that are different from modern steel structures.

Compared to modern steel structures, older steel structures have narrower frame spans and smaller story heights. The spacing between the frames is also less than in modern frames. The spans of old steel frame are uneven, while modern steel frames have more uniform bay size. Moreover, many older steel structures have unreinforced masonry infill walls, which are seldom found in modern steel structures. Since the historical data about the compressive strength of structural clay tile (f'_m) is quite limited and the minimum requirements of f'_m were usually substantially exceeded (Beall 1984), the recommended value (735 psi) from Fricke and Flanagan(1995) was utilized. According to the recommendation in Ghosh and Amde (1987), the elastic modulus of brick masonry (E_m) can be estimated to be $650 f'_m$. All analyses in this section were performed using the computer program OpenSees (Mazzoni et al. 2009).

4.3.2 Modeling Behavior of Unreinforced Masonry Infills

The masonry infill is usually modeled with a pair of equivalent compressive masonry struts (Stafford Smith 1966; Mainstone and Weeks 1970). The width of the equivalent masonry strut can be calculated according to the properties of the masonry and the infilled frame, with the same net thickness and material properties (e.g. elastic modulus) as the masonry infill. Since no research on the capacity of infill panels resisting vertical forces could be located, the existing methods to evaluate the lateral capacity of infill panels are utilized here, based on the analogy between the deformed shape of a structure after column removal and when withstanding lateral forces. From the comparison between the deformed shapes under gravity loads vs under lateral forces, it can be reasonably assumed that the beams in a confining frame after column removal act

as the columns when withstanding lateral forces, while the behavior of the columns after sudden column failure is similar as the behavior of the beams when sustaining lateral forces. Therefore, the properties from beams and columns in the original equations for lateral capacity of infill panels have been interchanged hereafter.

The force-deformation relationship of the unreinforced masonry infill panels has been idealized in Figure 4.20, as described in FEMA 273(1997a), which assumes that the behavior of an infill panel is perfectly plastic after reaching the elastic limit, and then drops to a certain level (residual capacity) as the deformation increases. The method proposed by Flanagan and Bennett (1999) is utilized to determine the area of the equivalent diagonal strut

$$A = \frac{\pi t}{C\lambda \cos\theta} \tag{4-4}$$

in which C is an empirical constant varying with the in-plane (drift) displacement of the confining frame, t is the thickness of the infill, θ is the angle of the infill diagonal with respect to the vertical and λ is determined according to Stafford-Smith and Carter(1990)

$$\lambda h = h\sqrt[4]{\frac{E_m t \sin(2\theta)}{4EIh'}} \tag{4-5}$$

in which h is the length of the confining frame, EI is the flexural rigidity of the beams, and h' is the length of the infill panel

Existing methods (e.g. FEMA 1997a) to evaluate the shear strength of an infill panel are usually based on the net cross sectional mortar/grouted area of infill panel along its length when a structure undergoes lateral forces. In this study, the concept of net cross sectional mortar/grouted area along the height of the infill panel is not applicable

when the structure is subjected to the gravity rather than lateral forces. Moreover, shear failure is usually more prevalent in concrete frames than steel frames (Flanagan and Bennett 2001). Therefore, the shear strength of the infill panel is not considered. Flanagan and Bennett (1999) found that frame properties and geometry do not appear to have a significant effect on the corner crushing strength of structural clay tile infilled frames and proposed an equation to estimate the corner crushing strength as follows

$$H_{ult} = tK_{ult} f'_m \tag{4-6}$$

where K_{ult} is an empirical constant with the value of 246 mm, which is independent of frame properties and geometry, and f'_m is the prism compressive strength of the structural clay tile masonry.

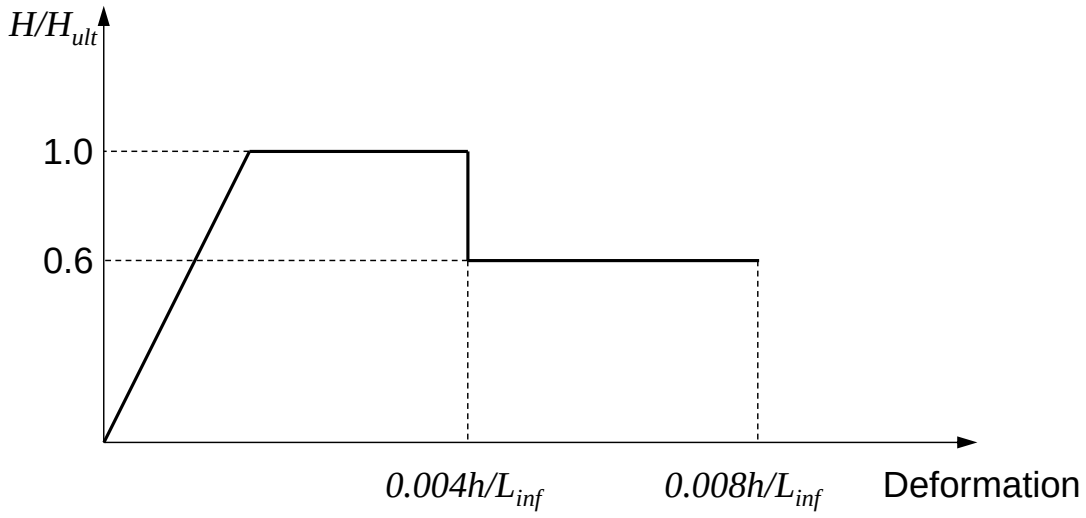

Figure 4.20 Force-deformation relationship for infill panels

The deformation limit and residual capacity of the struts are determined (transformed according to the geometric relationship) from the recommendation of

FEMA 273(1997a), in which the residual capacity is 60% of peak strength, and the plastic deformation and ultimate limit of infill panels are $0.004h/L_{\inf}$ and $0.008h/L_{\inf}$ respectively ($L_{\inf}$ is the height of infill panels).

4.3.3 Assessment of Frame Boe following Notional Column Removal

Frame Boe is evaluated for two extreme cases; as a bare frame and as a fully infilled (infilled with structural clay tile partitions except the first floor and the central span of all other floors) frame. In each case, two column removal scenarios are considered. The first scenario involves the removal of one interior column of the first floor (column B-1), while in the second scenario, a column is removed at the corner at the first floor level (column A-1). The finite element models are preloaded with gravity loads first through nonlinear static analysis; nonlinear dynamic analyses then are performed after sudden removal of one column. In the finite element models of the frame, each beam is divided into 4 elements while each column is modeled by one element. Columns and beams both are modeled using nonlinear beam-column elements with fiber sections to account for the interaction of moment and axial force. As discussed previously, the behavior of the riveted connections is modeled with rotational springs. For the connections to the 18WF50 beam, the moment-rotation relationship is obtained from fitting the test result of specimen B4RC7, while the moment-rotation relationships for other connections are scaled according to Batho and Lash (1936) as follows

$$\theta' = \frac{d}{d'}\theta \tag{4-7}$$

$$M' = \frac{d'}{d}M \tag{4-8}$$

$$k' = \left(\frac{d'}{d}\right)^2 k \tag{4-9}$$

in which d, θ, M, k are the depth of the beam, rotation, moment and stiffness of the connection, the moment-rotation relationship of which is known, while d', θ', M', k' are the corresponding unknown values of a connection before scaling. Masses are calculated based on the gravity loads. The material model is bilinear elastic-plastic, with a 3% strain hardening ratio. The mean yield strength is used in the structural analysis. The nonlinear analysis allows for the development of *P-Δ* effects in the frame, if required. The catenary action in the beam elements can be captured through a co-rotational transformation of geometry. The nonlinear dynamic procedure in the *Unified Facilities Criteria* (2009) stipulates that the following gravity load combination is to be applied to each frame according to Equation (4-1).

Damage Scenario I

After sudden removal of column B-1, the two spans directly above and adjacent to the removed column deflect vertically. The time histories of the vertical displacement of the nodes directly above column B-1 are shown in Figure 4.21. For the bare frame, the maximum displacement, 1.8 in (4.57 cm), is reached at 0.17 s, while the fully infilled frame deflects to the maximum, 0.82 in (2.08 cm), at 0.11 s, which indicates that the maximum displacement has been substantially decreased with the introduction of the

structural clay tile partition, which stiffens the frame. Figure 4.21 also shows that frame Boe gradually reaches its static equilibrium position after 3 s and no subsequent failure in the structural members of the frame occurs for either case. The amplified deformed shapes of both frames at their peak responses are illustrated in Figure 4.22. The masonry partitions affect the force redistribution as well, which is illustrated in Figure 4.23 and Figure 4.24. Figure 4.23 presents the comparison of the axial forces in the columns adjacent to the removed column B-1 at the first floor (A-1 and C-1), which shows that, with masonry infill, both columns A-1 and C-1 undergo larger axial forces. In contrast, the moment demands at the beam ends have been decreased due to the effect of masonry infill (Figure 4.24).

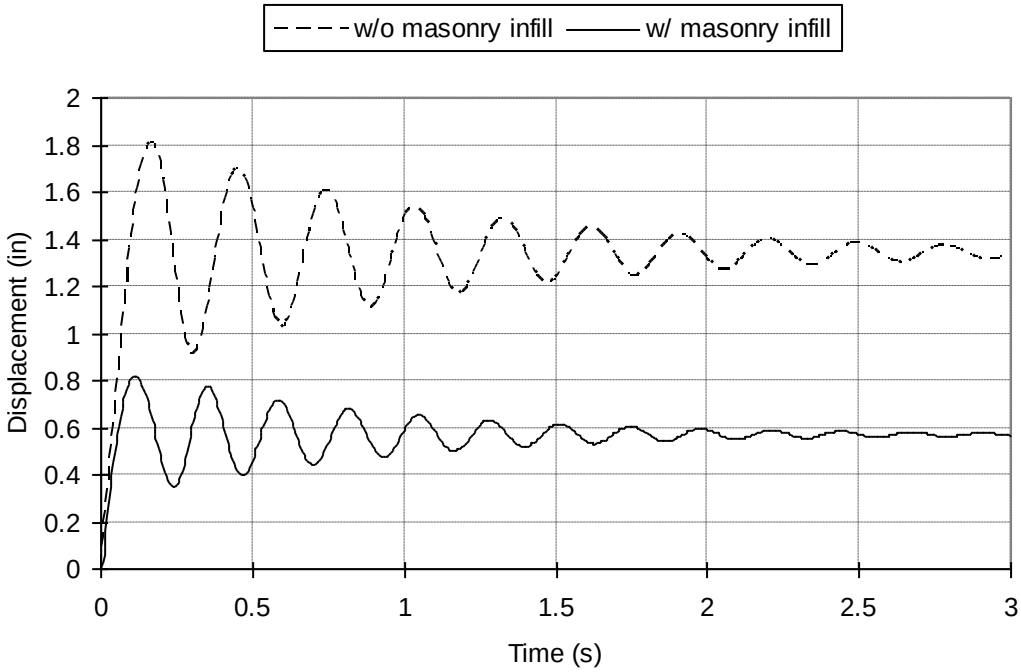

Figure 4.21 Dynamic response of the nodes above the removed column after removal of column B-1

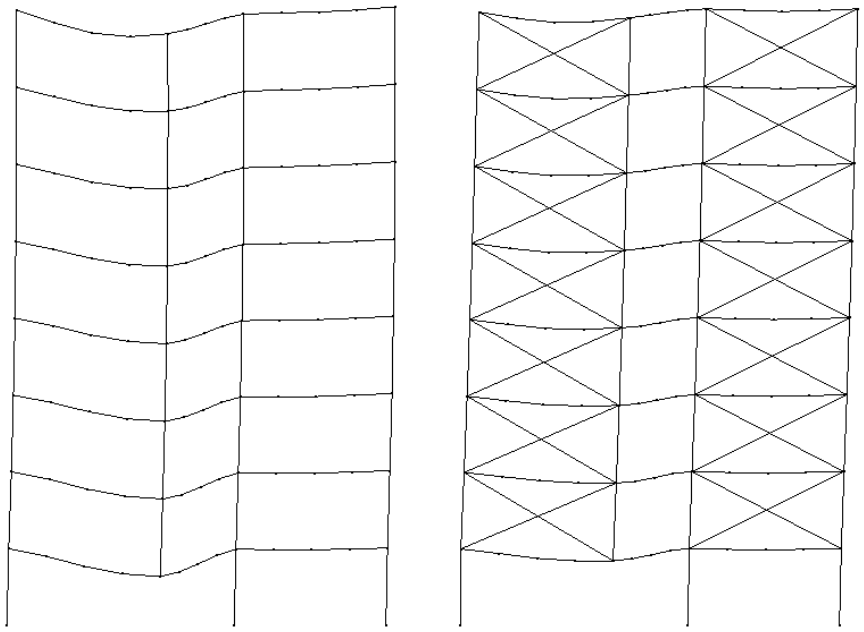

Figure 4.22 Deformed shapes of frame Boe after removal of column B-1 at peak responses (Amplification factor = 30)

From Figure 4.23, it is observed that the axial force in column C-1 is larger than the force in column A-1 in the case without masonry infill, because column C-1 sustains gravity loads from two spans, while column A-1 only resists gravity loads only from one span. However, in the frame with masonry infill panels, the axial force in column A-1 becomes larger as a result of the masonry infills in the side spans. In this case, the stiffness of the side span is much higher than that of the central span, causing most of the gravity loads on the side span to be resisted by column A-1.

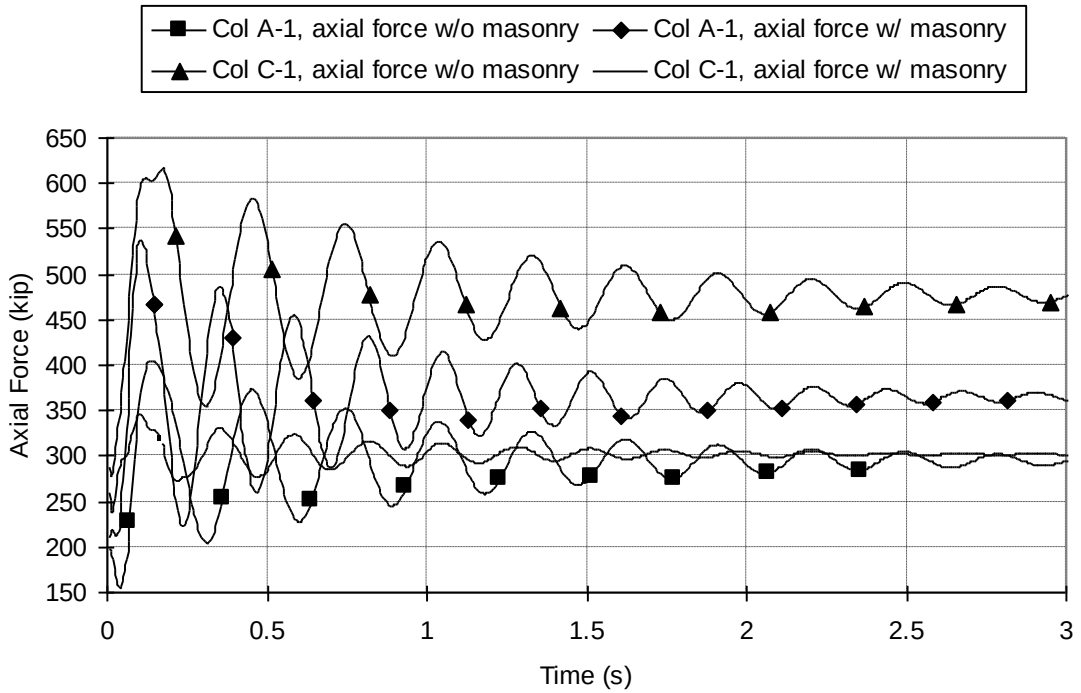

Figure 4.23 Axial forces in adjacent columns after removal of column B-1

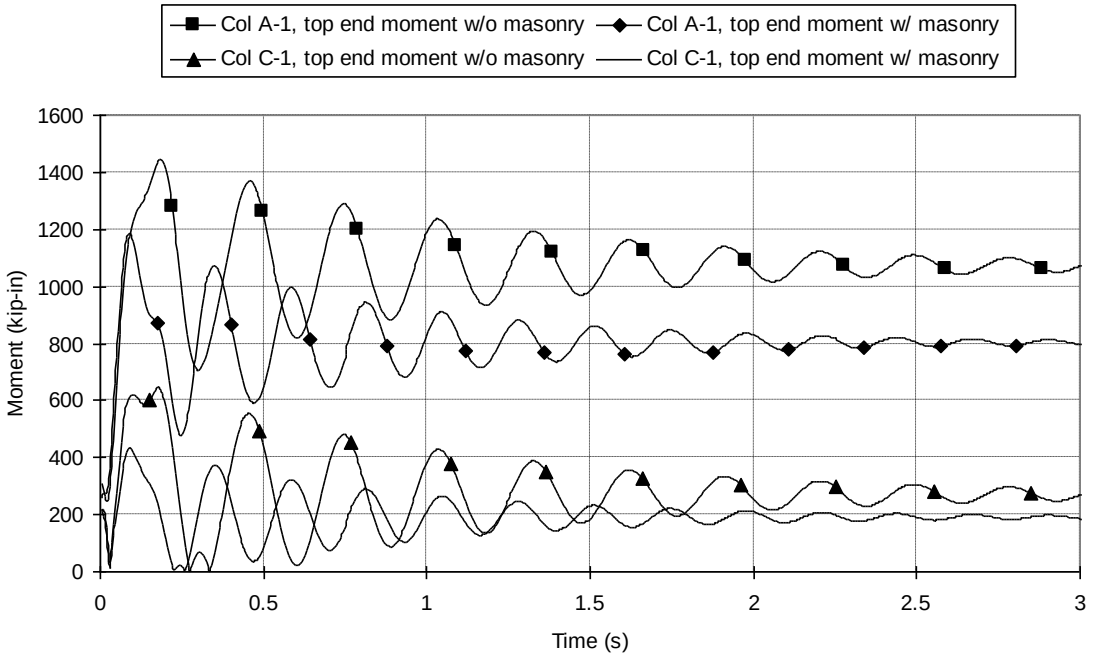

Figure 4.24 Moment in adjacent columns after removal of column B-1

Damage Scenario II

In damage scenario I, after failure of column B-1, the new span is 30 ft (9.14 m). Damage scenario II is analogous to damage scenario I, but the new span is 40 ft (12.19 m). Therefore, damage scenario II results in higher demands on the structural members and connections. The comparison of the histories of vertical displacements for the two cases following immediate failure of column A-1 is presented in Figure 4.25. The vertical displacement of the node above column A-1 in the frame without masonry infills increases dramatically with no rebound after removal of column A-1, indicating that the frame cannot withstand the assumed initial damage. The failure of the structural members in the frame first occurs at 0.24 s, at which time the rotational limits of the right beam-column connections at the left side span of the first three floors are exceeded as shown in Figure 4.26. Subsequently, the right connections of the other floors fail rapidly, which leads to complete failure of the left side span. Since the riveted connections are quite vulnerable and may not provide sufficient anchorage, the left span may separate from the rest of the frame and the rest of the structure may not collapse. The robustness of frame Boe has been improved in the frame that utilizes masonry infill panels. As illustrated in Figure 4.25, the maximum displacement of the frame with structural clay tile partition is only 1.68 in (4.27 cm) at 0.16 s and the system arrives at a steady displacement of 1.1 in (2.79 cm) after 3 s, showing that the initial failure has been contained. The force redistributions following column failure in adjacent column B-1 are compared in Figure 4.27 and Figure 4.28. Figure 4.27 shows that the difference in axial forces in column B-1 in both fames is not large, while the moment at the top end of column B-1 in the bare frame increases dramatically until failure of connections occurs. The maximum moment

demand is far larger in the bare frame than the corresponding maximum moment in the fully infilled frame, as presented in Figure 4.28.

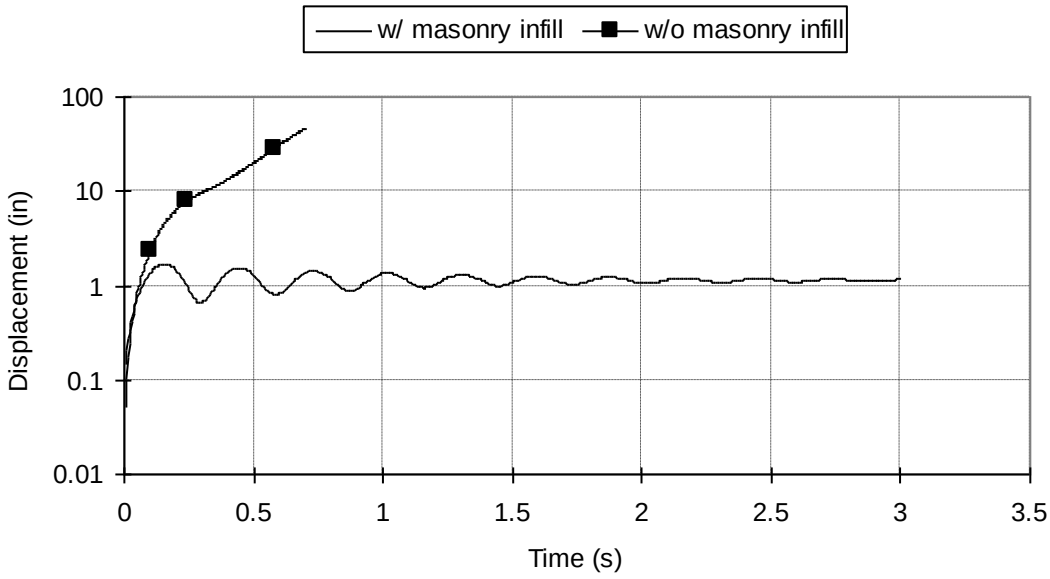

Figure 4.25 Dynamic response of nodes after removal of column A-1

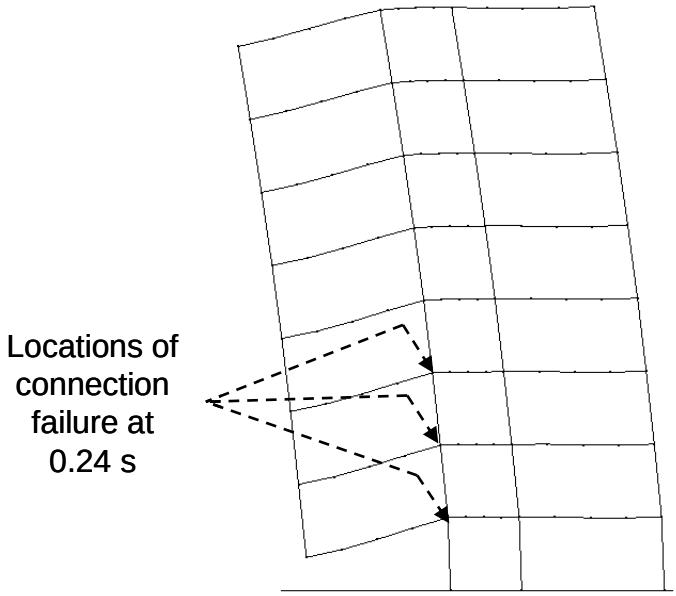

Figure 4.26 Deformed shape of frame Boe after removal of column A-1 at time = 0.24 s (Amplification factor = 10)

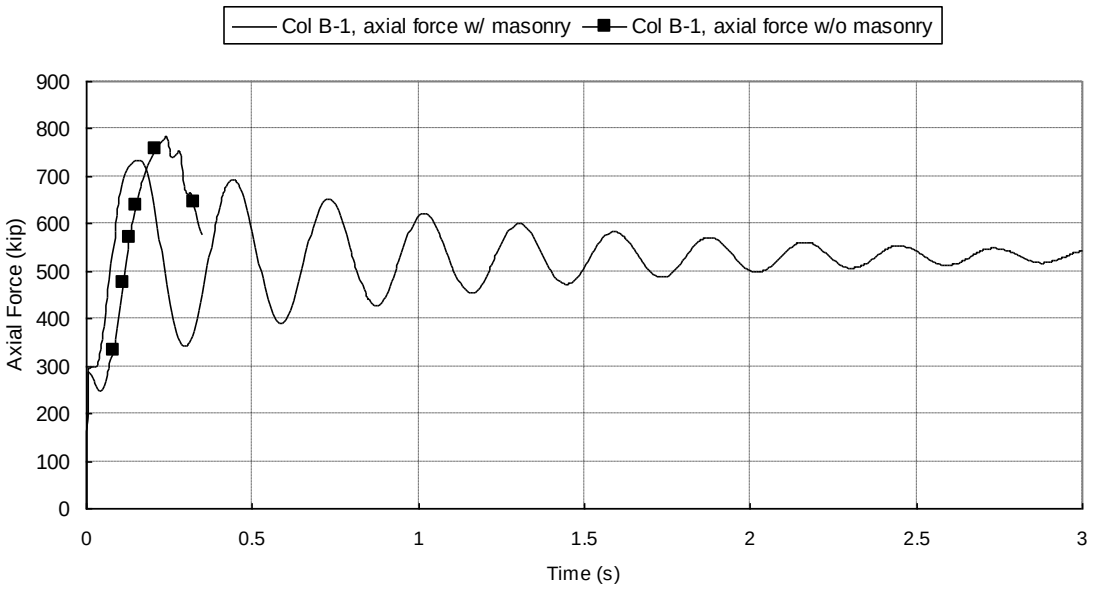

Figure 4.27 Axial forces in adjacent column B-1 after removal of column A-1

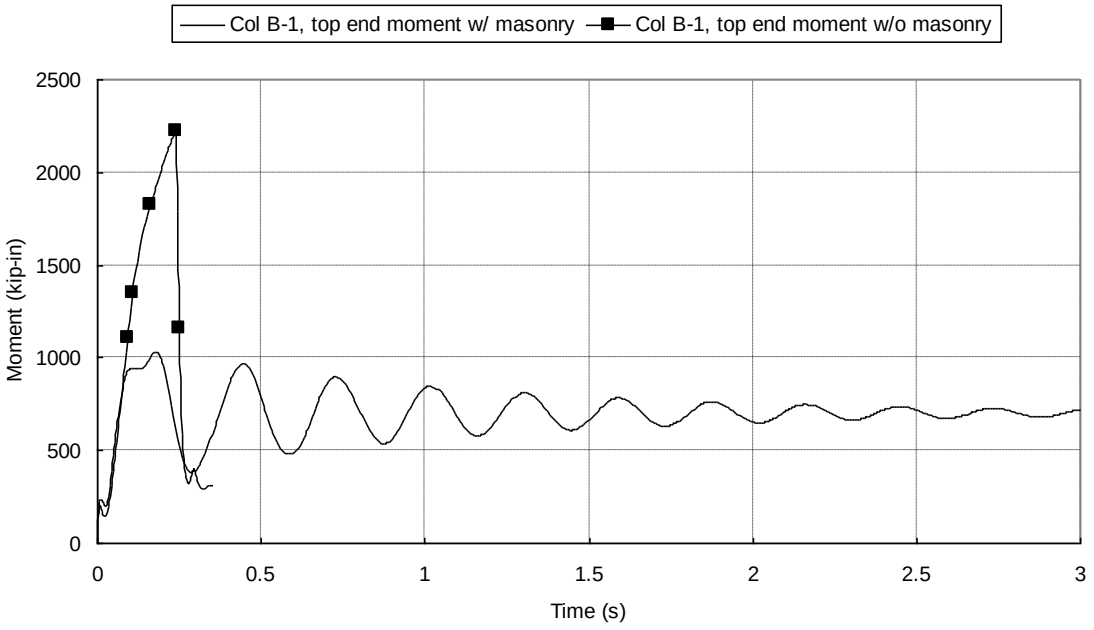

Figure 4.28 Moment in adjacent column B-1 after removal of column A-1

4.3.4 Summary

The robustness of a typical older steel framed building has been assessed in this section. The analysis results show that although the riveted connections are relatively weak, the frame can absorb the initial damages in the two stipulated scenarios with consideration of the composite behavior of the unreinforced masonry infills and the steel frame, and the contributions from encasements of connections and slab. The frame can survive in the first scenario even without taking into account of the effects of the infills, which is partly due to the shorter spans in older steel buildings. Therefore, older steel buildings similar to the one analyzed in this chapter can be considered to be robust in resisting disproportionate collapse.

CHAPTER 5 AN IMPROVED ENERGY-BASED STATIC ANALYSIS METHOD FOR ASSESSING VULNERABILITY TO DISPROPORTIONATE COLLAPSE

In the previous chapters, it has been shown that the connections (e.g., pre-Northridge moment-resisting connections, riveted connections) often are the most vulnerable components in steel building structures subjected to initial local damage. Furthermore, instability may occur in structures with strong connections (e.g., post-Northridge moment-resisting connections) or weak connections strengthened during rehabilitation or retrofit. In this chapter, a new energy-based static analysis method is developed. This method can be used as a simplified alternative tool to nonlinear dynamic analysis for identifying the potential for both connection failure and global instability of a structural system following local damage.

Energy-based methods that have been proposed recently (Dusenberry and Hamburger 2006; Izzuddin et al. 2008) have not considered the possibility that the damaged structural system might become unstable, a limit state which is known to be important in some cases (e.g., Ettouney et al. 2006). Following the sudden removal of one or more columns, the axial forces in the adjacent columns increase abruptly and dynamically. The sudden removal of a column generally results in an asymmetric residual structure, and causes an increase in the end moments of adjacent columns as a result of both the effect of asymmetry and dynamic effects. The stability of these adjacent columns and the overall remaining frame should be checked, along with the vulnerability of the beams (beam-column connections) in the spans directly above the

removed column, if an accurate assessment of structural system behavior following local damage is to be achieved.

This chapter proposes an energy-based method, denoted the Energy-based Partial Pushdown (EPP) method, for analyzing a structural system following local damage that addresses some of the above concerns. The method is illustrated using two three-story steel moment frames with fully restrained (FR) connections designed for different seismic requirements and one two-story frame with PR connections in which the design of the lateral force-resisting system is controlled by wind. Comparisons of the EPP analysis with the results of nonlinear time history analyses of the same frames establishes its validity for assessment of simple systems for design and preliminary evaluation of more complex systems.

The EPP method builds upon the approach of Izzuddin, et al. (2008) by considering, in addition to the deformation demand on beams and their connections, the possibility of column instability in the structure following local damage. Because of the need to consider system stability, we have opted to work with a model of the structural system as a whole, rather than following Izzuddin's approach of attempting to build a high-level structural model from low-level models of each component. Thus, the first step is to establish the modal response of the frame prior to and immediately following sudden removal of structural members. This modal analysis is aimed at identifying the system deformation mode(s) that are likely to be most significant for nonlinear static response. Based on the deformation patterns identified, a pushdown analysis then is conducted that involves only the portion of the structure immediately above the damaged column to determine whether new equilibrium states in the damaged structure are

possible and column stability can be maintained. It will be shown that the results of the EPP analysis compare favorably with the structural responses computed through NTHA of the same frames, and thus might be suitable for a preliminary assessment of vulnerability for structural design.

The EPP analysis procedure is illustrated using the three-story pre-Northridge steel moment frames designed for Seattle, WA, (SE3), and Boston, MA, (BO3), the floor plans and elevations of which are shown in Figure 4.1. All analyses, including static, dynamic and modal analyses, are performed using the computer program OpenSees (Mazzoni et al. 2009).

5.1 CHARACTERISTICS OF DYNAMIC RESPONSE AFTER SUDDEN COLUMN REMOVAL

The sudden removal of a column in a structure causes the damaged structure to vibrate vertically. This behavior is illustrated from the modal analysis of both the original and the damaged SE3 frames (Figure 5.1 and Figure 5.2) following removal of the quarter-point column (column D7 – see Figure 4.1) in the first level. Figure 5.1 compares the first four natural periods and mode shapes of the undamaged building frame to those modes for the frame following damage by sudden removal of column D7 of the first floor. Prior to the removal of column D7 (top row of Figure 5.1), the vertical modes are exclusively beam modes due to the large axial stiffnesses of the columns. Moreover, the first four mode shapes all involve the beams in the roof because the flexural stiffness of these beams is smallest. Floor vibration modes also occur at small periods, and have similar shapes but are not shown for brevity. Following removal of column D7, the first mode shape of the damaged structure (bottom row of Figure 5.1) becomes a global

vibration mode, in which all members supported by the removed column deform together. Note, however, that the second, third and fourth modes of the damaged structure are virtually identical to the first, second and third modes of the undamaged structure. In other words, the occurrence of damage to the structure is reflected in the introduction of a global mode that reflects that damage, but the remaining modes are essentially the same as in the undamaged structure. This development of a global mode in a damaged frame was also observed experimentally and analytically by Sasani (2008), whose study considered reinforced concrete frames. Figure 5.2 compares the first 20 natural periods of the undamaged and damaged frame, illustrating this effect in a slightly different manner. The periods are virtually same except for the first 'inserted' mode in the damaged frame.

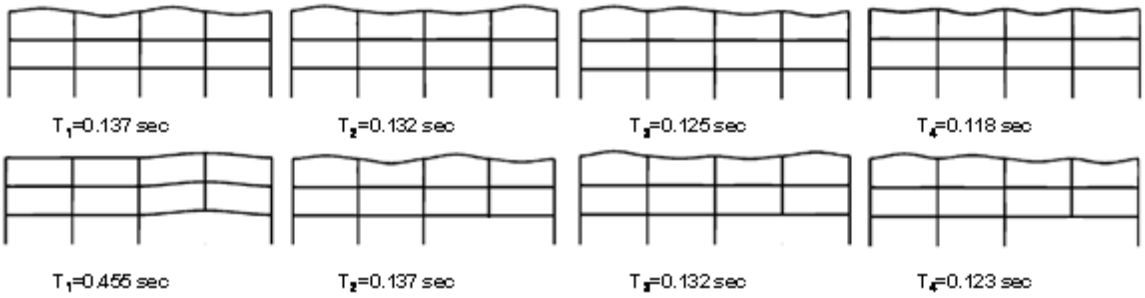

Figure 5.1 Comparison of the first four natural periods and modes in the undamaged (top row) and damaged structure (bottom row)

Following sudden removal of column D7, then, the dominant global mode contributes most to the deformation of the damaged structure, provided that the damaged structure deforms in the elastic range. Furthermore, the deflections of beams formerly

supported by the removed column become much larger under the same loads than the deflections of the remaining beams in the damaged structure as a result of the increase of beam spans. Similar behaviors were observed following sudden removal of corner column E7 in the first level of frame SE3.

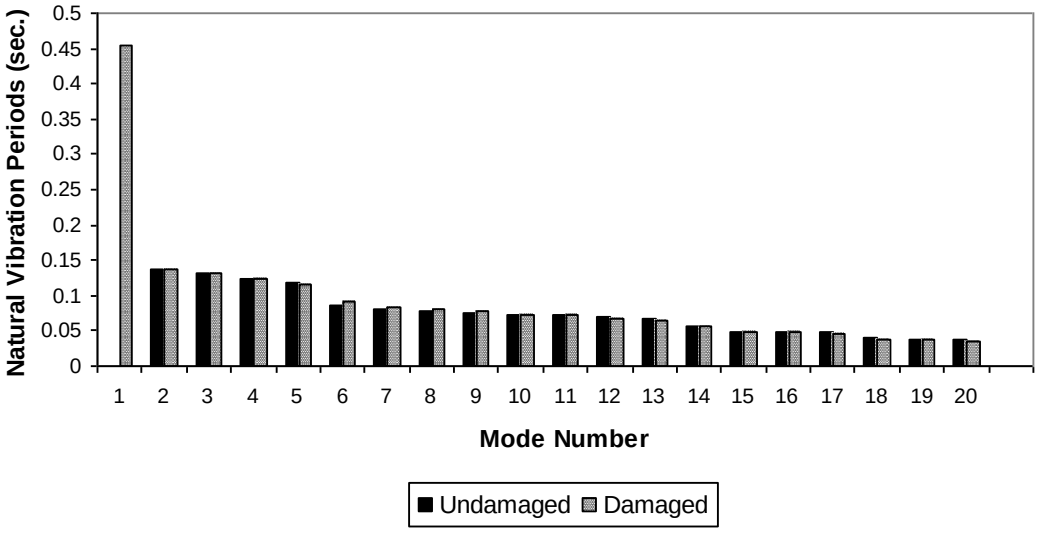

Figure 5.2 Comparison of natural periods between the undamaged and the damaged frame (modes of the undamaged structure shifted right by 1)

5.2 PARTIAL PUSHDOWN ANALYSIS OF ELASTIC STRUCTURES

The elastic response of a structural system modeled with N degrees of freedom (DoF) to sudden failure of one or more structural members is determined by the equation of dynamic equilibrium:

$$\mathbf{m}\ddot{\mathbf{u}} + \mathbf{c}\dot{\mathbf{u}} + \mathbf{k}\mathbf{u} = -\mathbf{m}\iota g \tag{5-1}$$

where $\mathbf{m}$, $\mathbf{c}$ and $\mathbf{k}$ are the mass, damping and stiffness matrices of the system, $\mathbf{u}$ is the vector of node vertical displacements of the system relative to the ground; all elements of vector ι are 1; and g is the acceleration due to gravity. The spatial distribution of the effective gravity forces is defined by

$$\mathbf{s} = \mathbf{m}\iota \tag{5-2}$$

This force distribution can be expanded as a summation of modal forces, $\mathbf{s}_n$:

$$\mathbf{m}\iota = \sum_{n=1}^{N} \mathbf{s}_n = \sum_{n=1}^{N} \Gamma_n \mathbf{m}\phi_n \tag{5-3}$$

where $\Gamma_n = \dfrac{L_n}{M_n}$; $L_n = \phi_n^T \mathbf{m}\iota$; $M_n = \phi_n^T \mathbf{m}\phi_n$ (5-4)

and ϕ_n is the nth natural vertical vibration mode of the structure. The contribution of the nth mode to $\mathbf{m}\iota$ is

$$\mathbf{s}_n = \Gamma_n \mathbf{m}\phi_n \tag{5-5}$$

If the system remains elastic, the displacements $\mathbf{u}$ can be expressed as the superposition of the modal displacements:

$$\mathbf{u}(t) = \sum_{n=1}^{N} \phi_n q_n(t) \tag{5-6}$$

where $q_n(t)$ is the nth modal coordinate, which is governed by

$$\ddot{q}_n + 2\zeta_n \omega_n \dot{q}_n + \omega_n^2 q_n = -\Gamma_n g \tag{5-7}$$

Let $q_n = \Gamma_n D_n(t)$ (5-8)

in which $D_n(t)$ = displacement of the SDOF system corresponding to the n[th] mode. Substituting Equation (5-8) into (5-7), one obtains:

$$\ddot{D}_n + 2\zeta_n \omega_n \dot{D}_n + \omega_n^2 D_n = -g \tag{5-9}$$

The solution to Equation (5-9) describes the response of a SDOF system to a step force with intensity g:

$$D_n(t) = e^{-\zeta_n \omega_n t}(A\cos\omega_D t + B\sin\omega_D t) - \frac{g}{\omega_n^2} \tag{5-10}$$

where the constants A and B are determined from the initial conditions.

When one or more structural members are suddenly removed, the gravity loads formerly carried by those members are applied to the remaining structure almost instantaneously as step loads. There are two different types of initial conditions for the beams in the frame. The beams in the spans directly above the removed column are at rest before the step force is applied. The initial (static) displacements due to the service loads on the structure are trivial compared to the peak dynamic responses, which are the response quantities of interest. Hence, the initial displacement can be assumed to be zero. Using $\dot{D}_n(t) = D_n(t) = 0$ and assuming that $\zeta_n = 0$, the peak response of each SDOF system is

$$D_{no} = -2\frac{g}{\omega_n^2} \tag{5-11}$$

The peak value of the n[th] mode response r_{no} is given by

$$r_{no} = r_n^{st} A_n \tag{5-12}$$

where r_n^{st} is the modal static response due to external force $\mathbf{s}_n$, and

$$A_n = \omega_n^2 D_{no} = -2g \tag{5-13}$$

Using the complete-quadratic-combination (CQC) modal combination rule (Kiureghian 1981), the peak value of the total response is determined by

$$r_o \approx \left(\sum_{i=1}^{N}\sum_{n=1}^{N} \rho_{in} r_{io} r_{no}\right)^{0.5} \tag{5-14}$$

where ρ_{in} is a correlation coefficient, which is a function of mode frequencies.

The peak modal response, r_{no} also can be estimated from a sequence of static pushdown analyses of the structure subjected to the vertical modal load distributions

$$\mathbf{f}_{no}^1 = -2\Gamma_n \mathbf{m}\phi_n g \tag{5-15}$$

Due to the dominance of the global vibration mode, it can be assumed that all modes reach their maximum responses approximately when the dominant mode reaches its maximum response. Accordingly, all modal load distributions derived from modal analysis can be summed prior to performing the pushdown analysis. The summation of all applied load distributions is

$$\mathbf{f}^1 = -2\mathbf{m}\iota g \tag{5-16}$$

Note that twice the actual gravity loads (GL) should be statically applied to these beams to get the peak responses.

In contrast to the beam spans immediately above the damaged column, the modal analysis of the damaged SE3 structure reveals that the vibration characteristics of the beams in the remaining spans are not affected by that column's removal. Accordingly,

each SDOF system transformed by the modal analysis initially is at rest at its static equilibrium position prior to column removal. Hence, these SDOF systems remain in their equilibrium positions without vibrating after column removal and there is no dynamic effect. The summation of applied modal loads is

$$\mathbf{f}^2 = -\mathbf{m}\iota g \tag{5-17}$$

The original gravity load distributions should be applied to the beams in these spans.

According to Equations (5-16) and (5-17), the static pushdown analysis need only be performed on the portion of structure in the spans directly above the removed column. The static partial pushdown analysis procedure of elastic structures is illustrated in Figure 5.3.

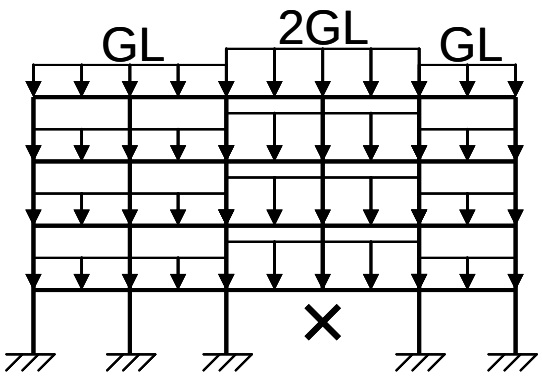

Figure 5.3 Partial pushdown analysis of elastic structures

5.3 ENERGY-BASED PARTIAL PUSHDOWN (EPP) ANALYSIS – INELASTIC STRUCTURAL SYSTEMS

Equation (5-16) shows that twice the gravity load should be used in the pushdown analysis to yield accurate results in the elastic range. If the partial pushdown analysis

involves response in the nonlinear range, however, the calculated deformations usually will be much larger than those obtained from a nonlinear dynamic analysis. The reason can be seen from the analysis of an inelastic SDOF system, which is summarized in Figure 5.4. There is a large difference between the displacements u_d from dynamic analysis and u_s from static analysis of the same inelastic SDOF system because a small increase in load leads to a large increase in displacement after yielding. As shown in Figure 5.4, when the SDOF system reaches the maximum displacement, the external work must equal the strain energy stored in the system. When one or more structural members are suddenly removed, the gravity loads formerly carried by those members are applied to the remaining structure almost instantaneously as step loads. As the structure deflects, the external work done by the gravity loads is transformed into strain energy stored in the remaining structural members. When the external work equals the strain energy, the structure reaches a new state of equilibrium and its maximum deflection, as if the structure behaves like a SDOF system.

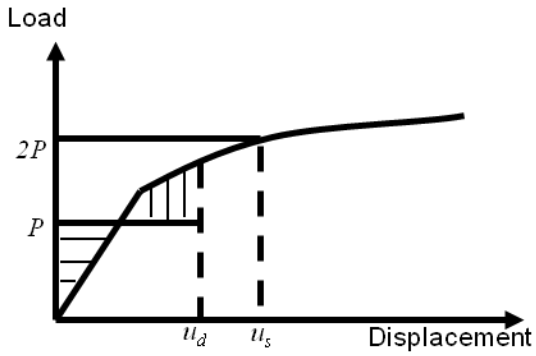

Figure 5.4 Displacement of a SDOF system

In the EPP method, amplified gravity loads are applied to the beams in the bays immediately adjacent to and above the removed column, but the gravity loads on the beams in the other spans remain unchanged. The work done by the gravity loads and strain energy in the beams in the span directly above the removed column are calculated according to the deflected structural shape. The difference between strain energy and external work is checked at the end of each step of the EPP analysis procedure, and a new equilibrium configuration is achieved if and when the energy balance is reached. The displacements from the EPP analysis procedure reasonably approximate the displacements obtained from a NTHA because the portion of structure in the bays immediately adjacent to and above the removed column behaves like a SDOF system.

The EPP analysis procedure (illustrated in Figure 5.5) can be summarized as follows:

1. Preload the damaged structure except the portion directly above the removed column with the actual gravity (dead plus live) loads.
2. Perform a nonlinear static pushdown analysis on the portion of the structure in the spans directly above the removed column with the incremental loads according to the gravity load distribution on those spans. Record the analysis information $\mathbf{W}_i$, $\mathbf{u}_i$ and r_i at step i of the analysis. $\mathbf{W}_i$, $\mathbf{u}_i$ and r_i are the external pushdown load vector, displacement vector in the spans directly above the removed column and the response of interest (e.g. axial force or moment of a column).
3. Calculate the strain energy at step i:

$$SE_i = SE_{i-1} + (\mathbf{W}_i)^T (\mathbf{u}_i - \mathbf{u}_{i-1}) \quad (5\text{-}18)$$

where $\mathbf{u}_0 = \mathbf{0}$, $SE_0 = 0$ and the work done by gravity loads is

$$W = (\mathbf{m}\iota)^T \mathbf{u}_i g \quad (5\text{-}19)$$

4. Stop the calculation if $SE \geq W$ (denoted as step j) or a preset deformation or force limit is reached. If $SE \geq W$, the displacements $\mathbf{u}_j$ are the target displacements. The response of interest r_j is also obtained accordingly. The target pushdown load is $\mathbf{W}_j$ (i.e., αGL in Figure 6 in the case of uniformly distributed gravity loads, where α is the gravity load ratio, and $1 < \alpha \leq 2$).

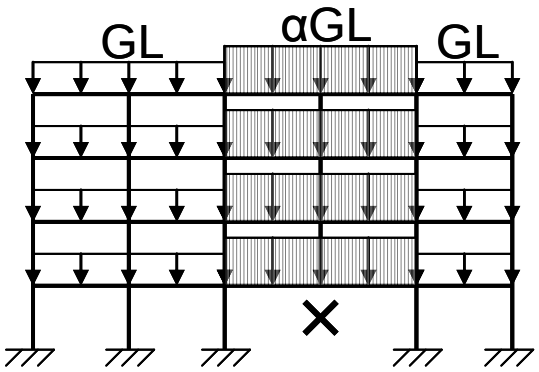

Figure 5.5 Energy-based partial pushdown analysis procedure

Note that it may not be possible to achieve an energy balance in step 4 if the collapse-resisting capacity of the structure is quite small compared to the collapse demand. In this case, a deformation or force limit representing the maximum reasonable deformation or force can be set and the calculation is stopped when a preset deformation

or force limit is reached. In this case, the implication is that the analyzed structure cannot resist disproportionate collapse.

5.4 ILLUSTRATION OF THE EPP METHOD

Three steel frames are analyzed with the EPP method and the forces and deformations developed are compared with those determined from a NTHA of the same frames. The first two frames have FR beam-column connections connections similar to those described in Chapter 3, a type of construction that is usually found used in areas of high or moderate seismicity. The third frame is constructed with PR connections, which transfer only a portion of the moment capacity of the beams. In the examples that follow, the collapse potential of the structures is checked by the removal of columns of the first floor, consistent with the requirements in the *UFC*. The robustness of structures undergoing sudden failure of columns of other floors could also be checked, as explained in the previous section. Information about the deformation limits of strong or strengthened weak beam-column connections during collapse currently is limited, and the failure of beam-column connections following damage is not considered.

5.4.1 Analysis of FR Frames

The aforementioned FR frames SE3 and BO3 are evaluated by both the EPP analysis procedure and NTHA under three column removal scenarios. The first scenario involves the removal of the quarter-point column D7 of the first floor (column D7-1) considered in the previous section, while in the second scenario column E7 at the corner of the first floor (E7-1) is removed. The third scenario involves instantaneously removal of two structural members - two columns of the first floor (C7-1 and D7-1) – to create a

damage scenario in which development of column instability might become apparent. In all cases, the responses determined from the NTHAs provide the benchmarks against which the accuracy of the approximate EPP is compared. The NTHA are performed with (modal) structural damping ratios equal to 0% and 5% in order to investigate the error from the assumption (made previously) that damping effects can be neglected. Stiffness-proportional damping is used in the analyses.

The dynamic displacement history of the nodes immediately above the removed columns of frame SE3, the numbers of which are identified in the frame elevation in Figure 4.1, are shown in Figure 5.6 for the first two scenarios and Figure 5.7 for the third scenario. In the case of failure of column D7-1, the maximum displacement of node 24 is 4.26 in (108.20 mm) if the structure is modeled with 5% damping, while it is 4.61 in (117.09 mm) if damping is neglected, an increase of only 8.22%. Similarly, the neglect of damping increases the maximum displacement of node 25, following the sudden failure of column E7-1 by 8.13%, from 6.27 in (159.26 mm) to 6.78 in (172.21 mm). All maximum displacements are reached in the first half-cycle of vibration, a result that is consistent with the findings of other investigators (Izzuddin et al. 2008; Sasani 2008). In the third scenario, which involves the sudden failure of two columns, the maximum displacements of nodes immediately above the removed columns also are reached in the first half-cycle of vibration, as in the single-column damage scenarios. The corresponding maximum displacements of nodes 23 and 24 are 17.23 and 16.45 in (437.64 and 417.83 mm) respectively. If damping is neglected, the maximum displacements increase by approximately 10%.

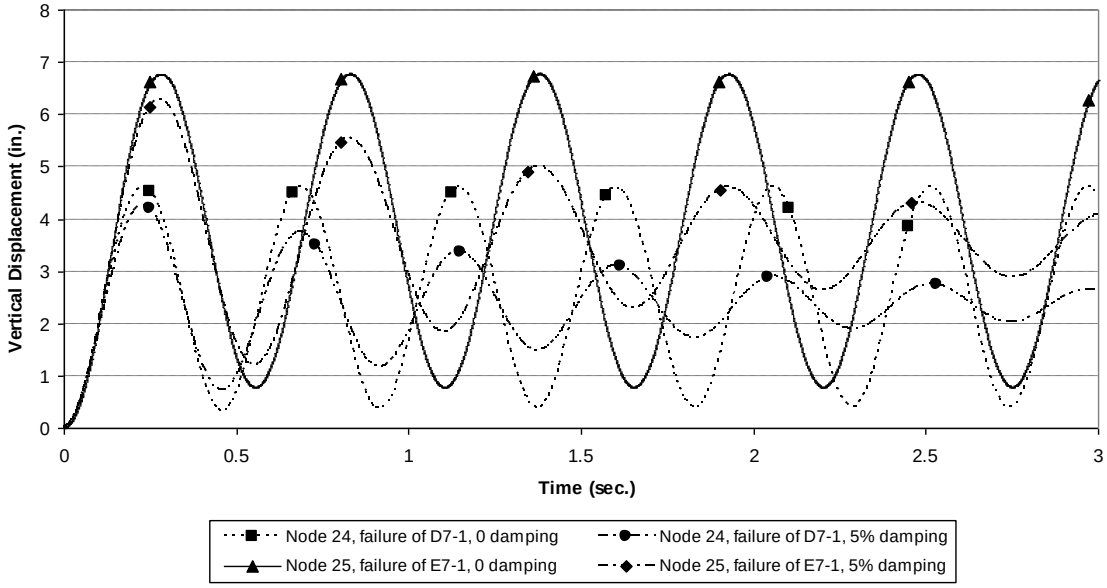

Figure 5.6 Dynamic responses of nodes after removal of one column of frame SE3

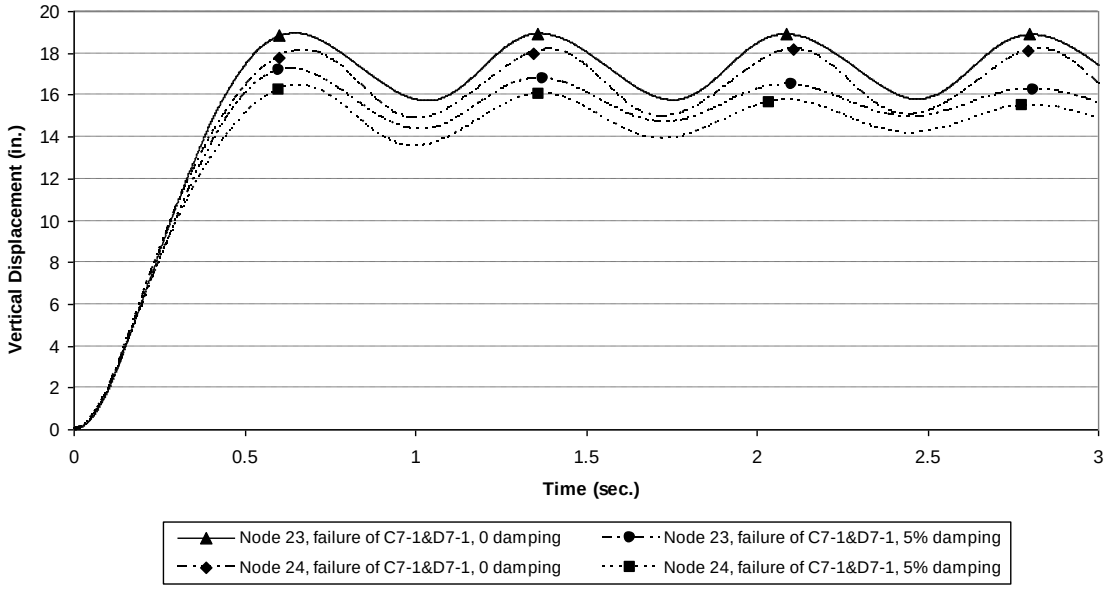

Figure 5.7 Dynamic responses of nodes after removal of two columns of frame SE3

For frame BO3, the dynamic displacement histories of the nodes immediately above the removed columns are shown in Figure 5.8 and Figure 5.9. The displacements obtained from NTHA when damping is neglected are nearly 10% larger than those with 5% damping in the cases involving removal of one column, while the differences are approximately 4% in the scenario involving sudden removal of two columns. The maximum displacements of nodes 23 and 24 following the sudden removal of columns C7-1 and D7-1 are quite large in comparison with the corresponding displacements in frame SE3 because the girders in frame BO3 are relatively more flexible.

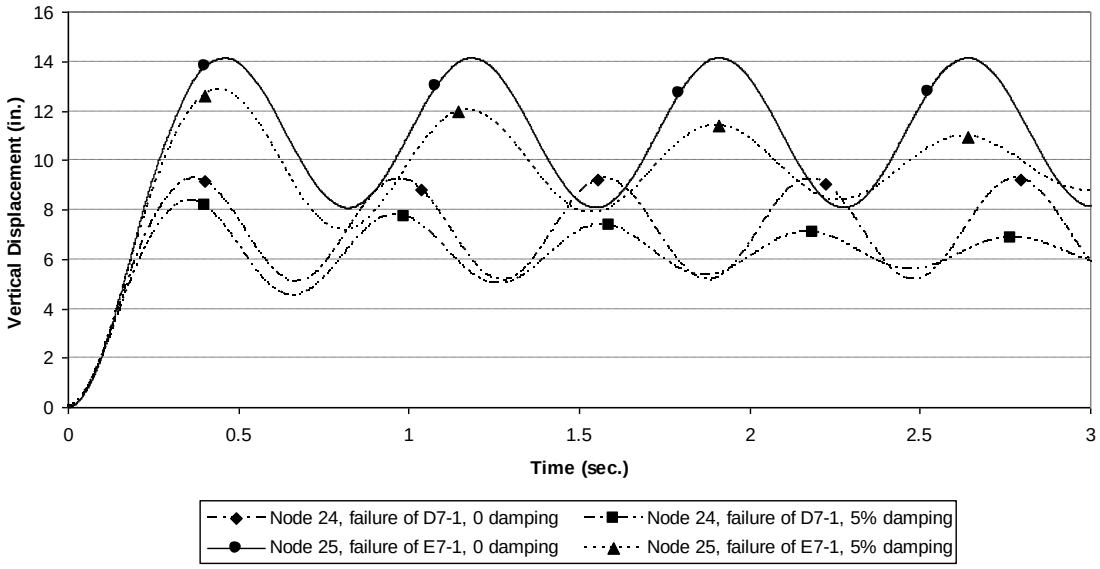

Figure 5.8 Dynamic responses of nodes after removal of one column of frame BO3

Figure 5.10 and Figure 5.11 compare the maximum displacements obtained from the EPP analysis with the displacements obtained from NTHA for frames SE3 and BO3, respectively. The EPP analysis yields displacements that are very close to the

corresponding results from NTHA when damping is neglected. The differences between the results of the EPP analysis and NTHA with 5% damping are within 10% or less in most cases. Hence, the EPP analysis appears to be sufficiently accurate to evaluate the deformation demands on the vulnerable beam-column connections in the spans directly above the removed columns for these and similar frames.

Figure 5.12 and Figure 5.13 compare the peak axial forces developed in the adjacent undamaged columns following sudden column removal in all scenarios calculated by EPP analysis and NTHA. The axial forces obtained from the EPP analysis and NTHA are very close in all cases. The maximum moments in the undamaged columns all occur at the top ends except that in column E7-1 of frame BO3 following failure of both column C7-1 and D7-1, which occurs at the bottom of the column. The maximum moments of the vulnerable columns of frames SE3 and BO3 following removal of columns are shown in Figure 5.14 and Figure 5.15, respectively. The columns in frame SE3 do not buckle when the gravity load redistributes following initial column failure; frame SE3 is a strong-column/weak-beam frame designed to withstand seismic effects. However, columns in building frames in regions of low-to-moderate seismicity may be susceptible to buckling during disproportionate collapse. Frame BO3 is a case in point; the maximum axial force and moment in column E7-1 following the sudden removal of both column C7-1 and D7-1 are 274 kips (1,219 kN) and 9,668 kip-in (1,092 kN-m), respectively. According to the *Specification for Structural Steel Buildings* (AISC 2005), Equation (H1-1b), column E-1 will buckle immediately following sudden removal of columns C7-1 and D7-1. The horizontal and vertical maximum displacements

of node 25 at the top end of column E7-1 are 17.38 and 1.35 in (441.45 and 34.29 mm), respectively.

The results presented in Figure 5.12 through Figure 5.15 indicate that the EPP analysis is sufficiently accurate to assess the vulnerability (instability) of the remaining columns near or adjacent to the removed column. Hence, the EPP analysis procedure can be used as a tool to evaluate the potential for instability of a structural frame with moment-resisting connections.

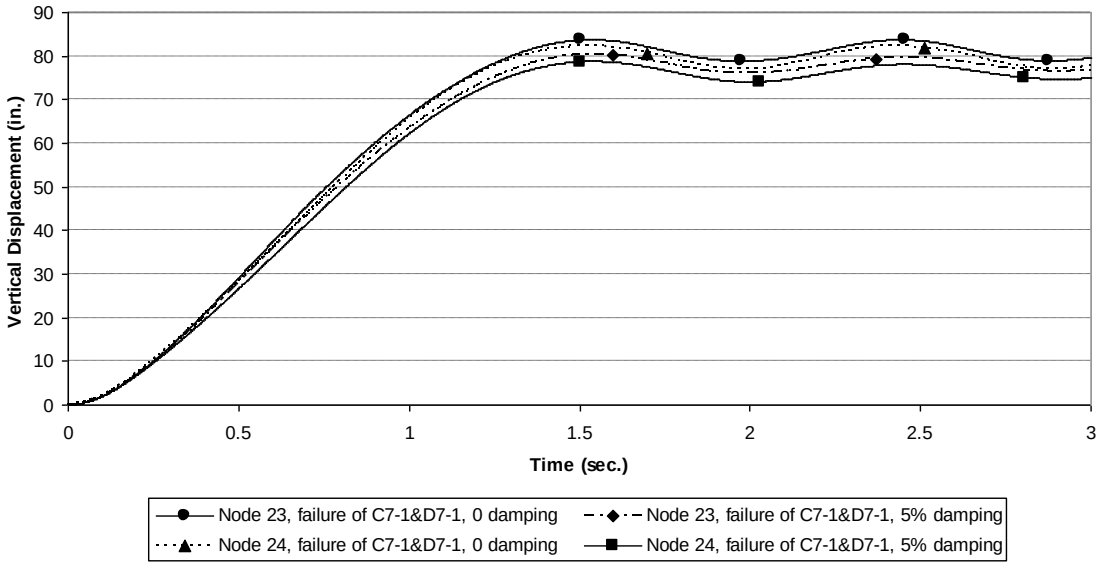

Figure 5.9 Dynamic responses of nodes after removal of two columns of frame BO3

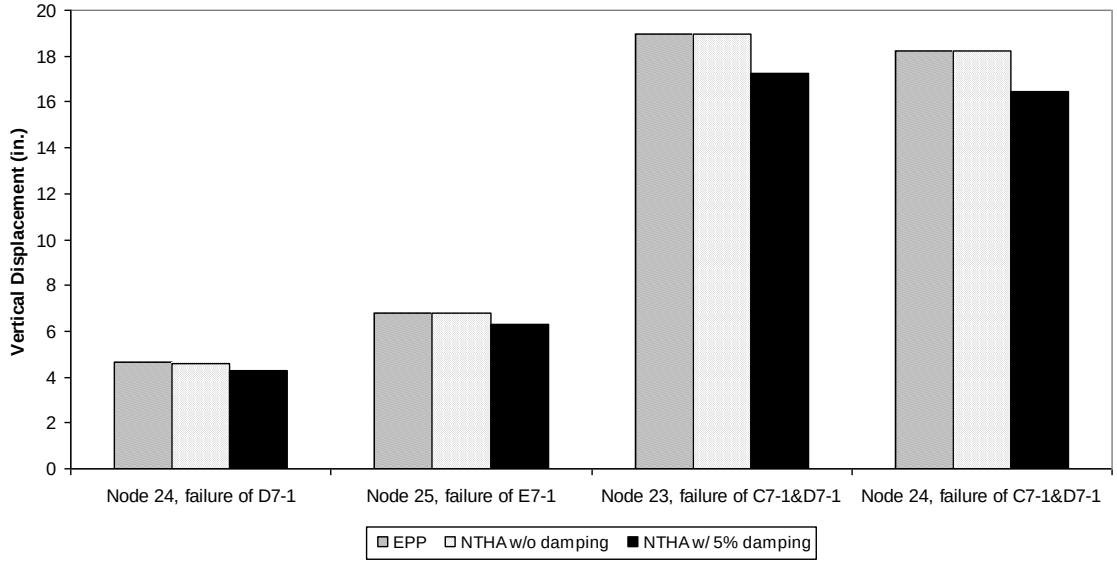

Figure 5.10 Comparison of peak displacements from EPP and NTHA analyses following removal of columns of frame SE3

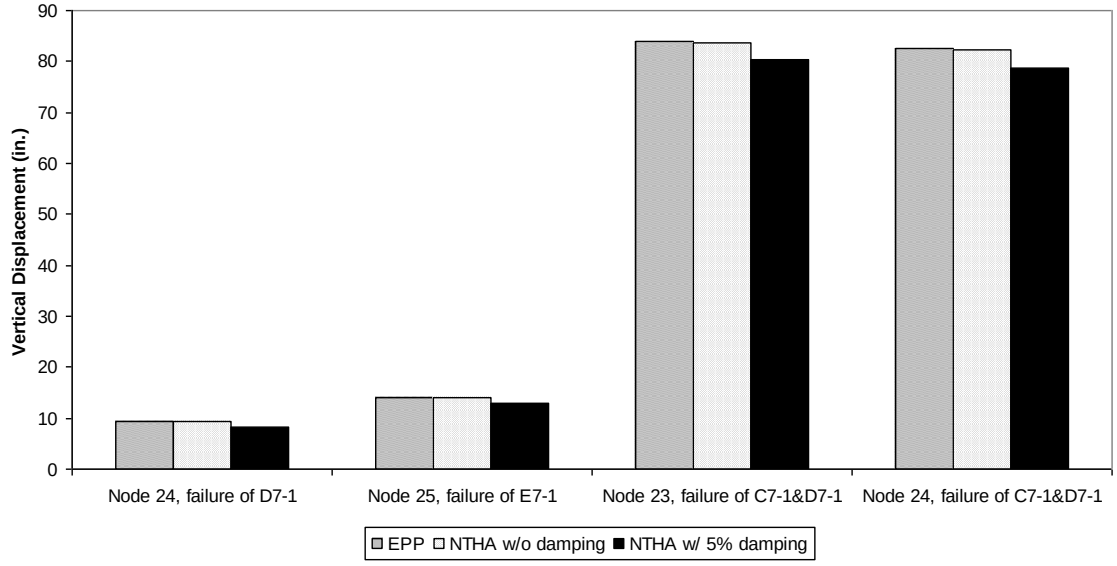

Figure 5.11 Comparison of peak displacements from EPP and NTHA analyses following removal of columns of frame BO3

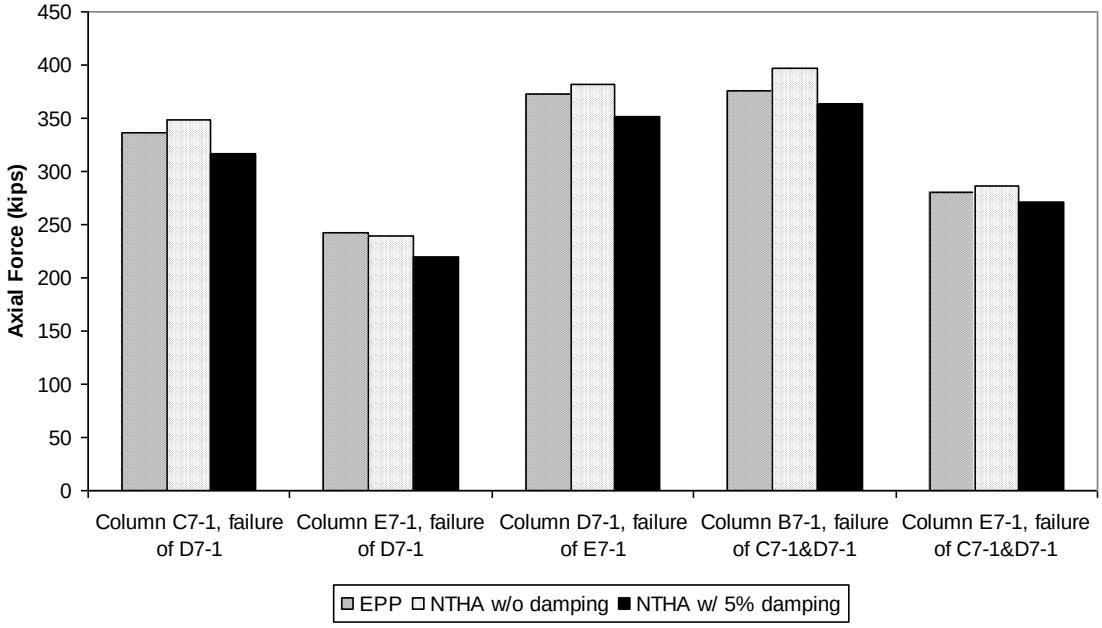

Figure 5.12 Comparison of peak axial forces of vulnerable columns from EPP and NTHA analyses following removal of columns of frame SE3

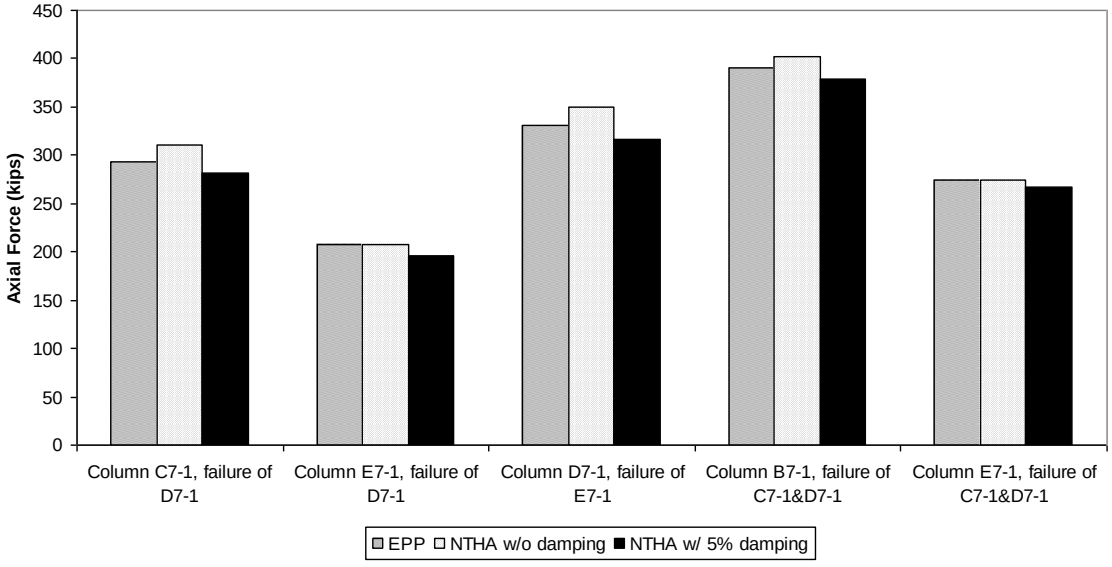

Figure 5.13 Comparison of peak axial forces of vulnerable columns from EPP and NTHA analyses following removal of columns of frame BO3

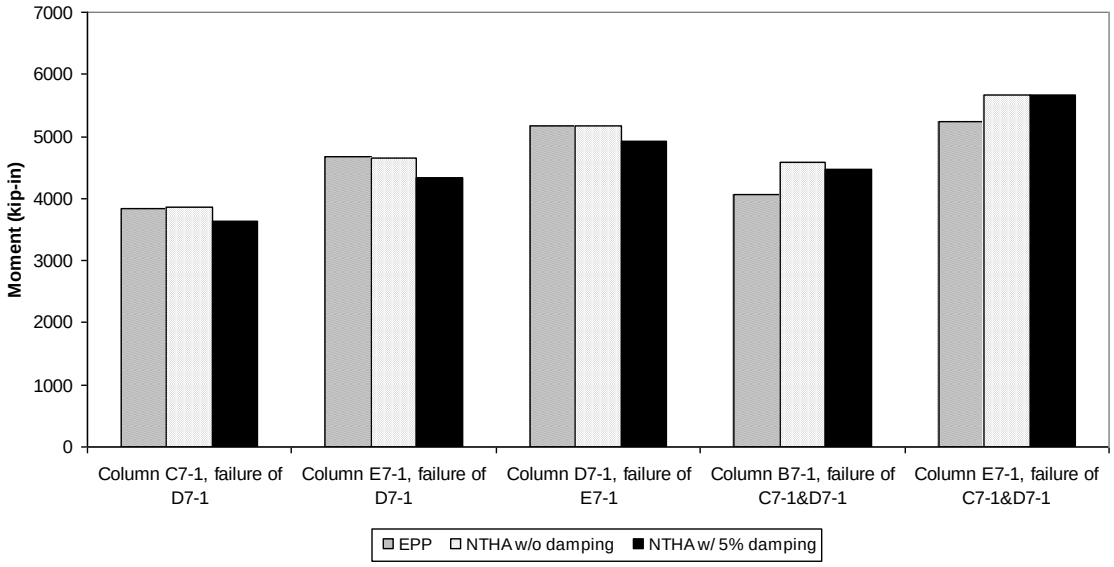

Figure 5.14 Comparison of peak end moments of vulnerable columns from EPP and NTHA analyses following removal of columns of frame SE3

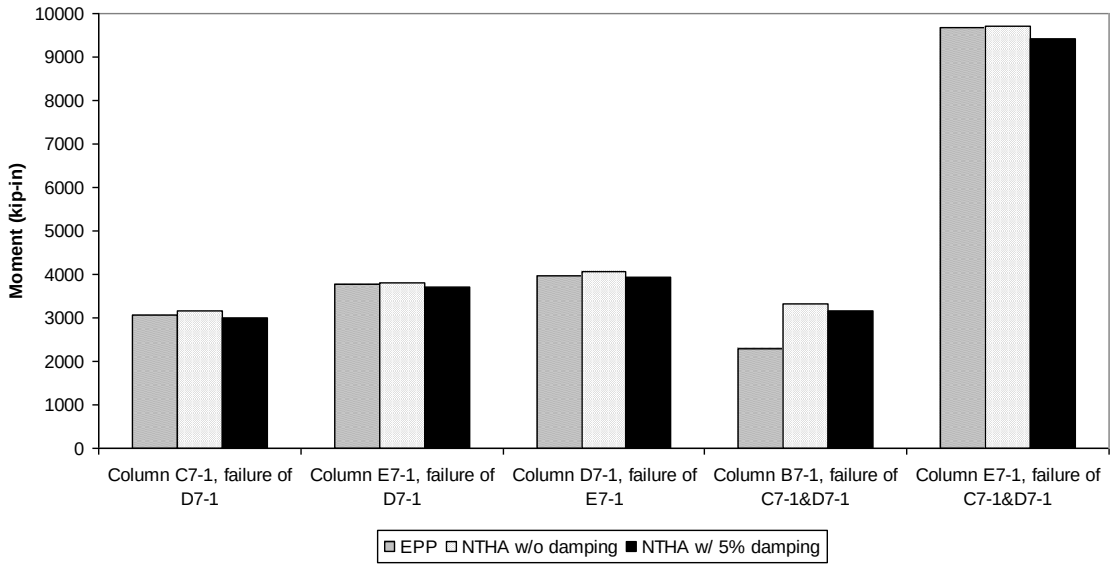

Figure 5.15 Comparison of peak end moments of vulnerable columns from EPP and NTHA analyses following removal of columns of frame BO3

5.4.2 Analysis of PR Frame

The frame with PR connections, designated 2ST-PR in the following, is a two-story, four-bay frame, one of a series of interior frames spaced at 25 ft (7.62 m) in the out-of-plane direction. A typical elevation is shown in Figure 5.16. It is an older frame, which was designed according to the *AISC Specification, 1978 Edition* (Barakat and Chen 1991). The lateral force requirements were governed by wind load, and seismic loading was not considered, leading to a strong beam-weak column configuration. All members bend about their strong axes. The design dead loads for the floor and roof are 68 psf (3.3 kPa) and 20 psf (0.96kPa), respectively. The design live loads are 40 psf (1.9 kPa) for the floor and 12 psf (0.57 kPa) for the roof. All column and beam sections were Grade A36 steel, with the mean yield strength equal to 40 ksi (276 MPa).

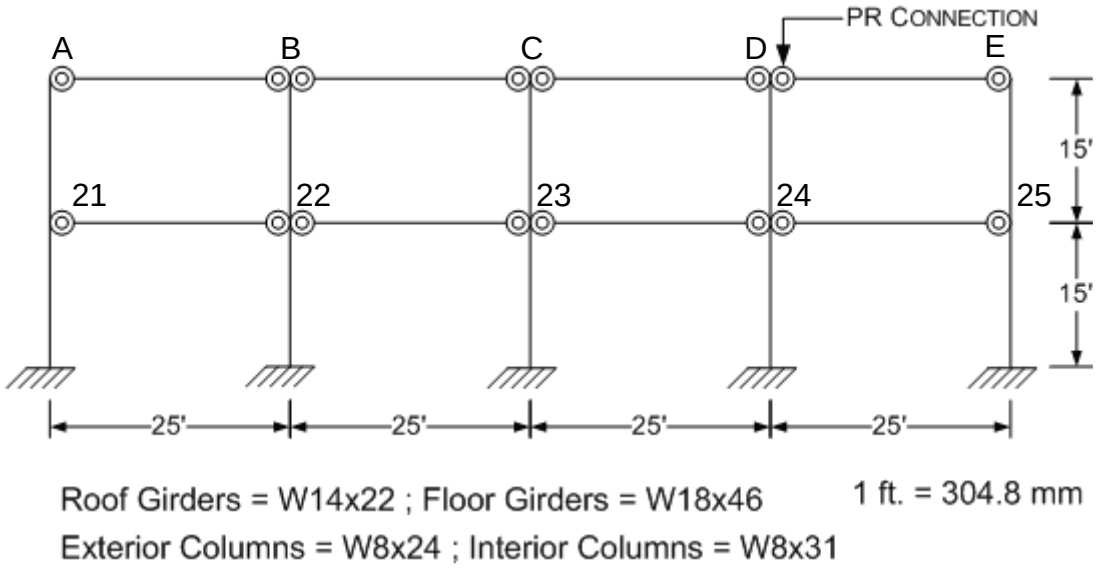

Figure 5.16 Elevation view of frame 2ST-PR (Barakat and Chen, 1991)

The PR connections consisted of top and bottom flange angles and web angles. Essentially the same structural modeling procedure as used for the frames SE3 and BO3 was applied, except that the connections were modeled explicitly with rotational springs. The moment-rotation relationship (backbone curve) of the connections presented in Figure 5.17 was developed from test data (Azizinamini et al. 1985), as discussed in Kinali (2007). Once the rotation exceeds 0.04 rad, the moment-resisting capacity of the connections drops rapidly from 65% of the full plastic moment (M_p) of the beam section to 15% of M_p (residual capacity).

In contrast to frames SE3 and BO3, frame 2ST-PR cannot withstand the instantaneous damage of a perimeter column due to the relatively weak connection capacity of its connections. Accordingly, only one interior column removal scenario involving instantaneous damage to column D-1 of the first floor (Figure 5.16) is considered. The EPP analysis of frame 2ST-PR in the assumed damage scenario shows that the axial force and top end moment of the adjacent column, E-1, is 39.5 kip (175.7 kN) and 909.2 kip-in (102.7 kN-m), respectively when the gravity load ratio α (cf Figure 5.5) is increased to 0.255. Substitution of these forces in Equation (H1-1b) of the *Specification for Structural Steel Buildings* indicates that column E-1 is likely to buckle before the energy balance can be achieved. At the same time, connections at nodes 23, 25, and 33 – 35 in the spans directly above the removed column have nearly reached the rotation limit (i.e. 0.04 rad), which means that these connections are at a state of incipient failure as well. This assessment indicates that this PR frame is vulnerable to disproportionate collapse. Even if the residual capacity of the connection can be maintained for large connection rotation, the instability problem will lead to collapse of

the frame. This conclusion is confirmed by a NTHA of the same damage scenario, summarized in Figure 5.18. In particular, the horizontal displacement of node 25 increases rapidly and reaches 10 in (0.254 m) at 0.5 s, which is an obvious sign of column buckling.

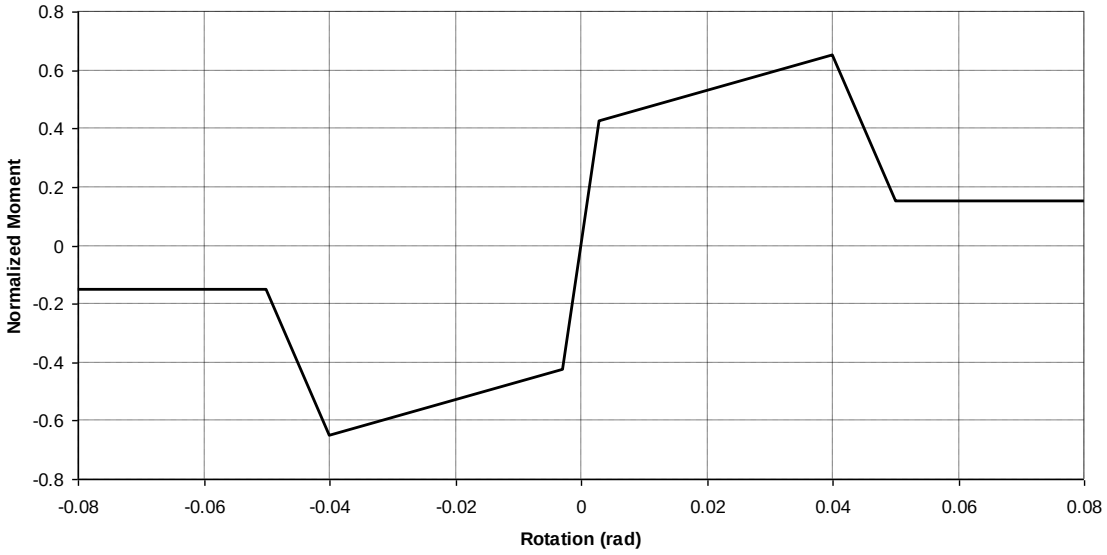

Figure 5.17 Moment-rotation relationship for the PR connections in frame 2ST-PR

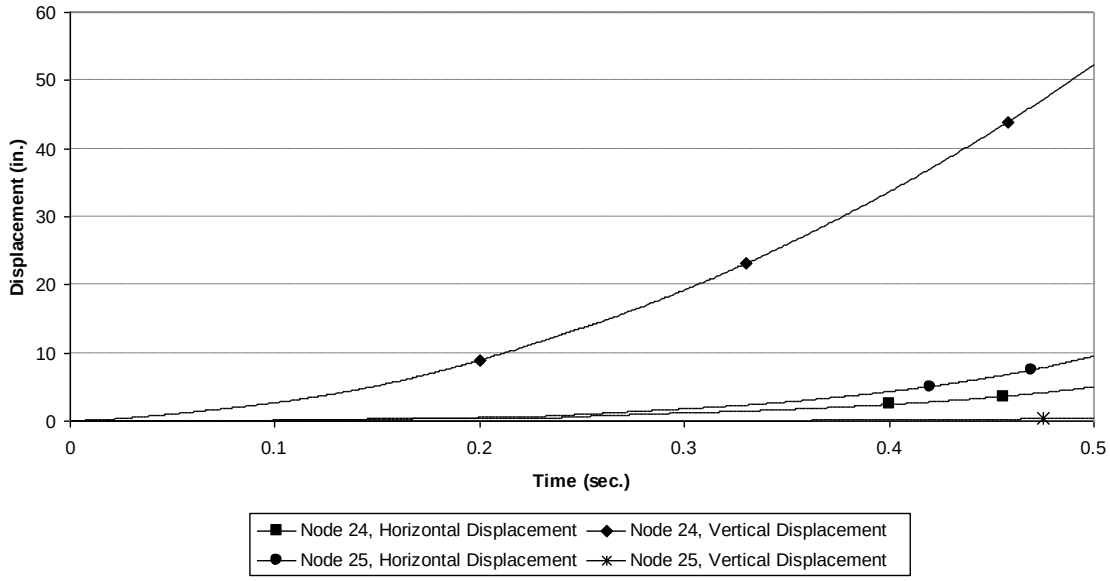

Figure 5.18 Dynamic responses of nodes after removal of column D-1 of frame 2ST-PR

5.5 DISCUSSION

The EPP analysis is aimed at providing an alternative method of static analysis of disproportionate collapse vulnerability that can be used as a design and assessment tool for regular building frames suffering local damage and to suggest where more involved NTHA methods might be warranted. In the new *Unified Facilities Criteria* (2009), the dynamic increase factor for the nonlinear static analysis option has been changed from its previous (2005) value of 2 to a value that depends on the structure type and plastic rotation limit. The information needed to obtain the value of the dynamic increase factor for a specific structure also can be derived from the simple procedure proposed in this study. A comparison of the results of the EPP and NTHA analyses for damage scenarios

in several frames with either FR or PR connections showed that the EPP analysis yields reasonable assessments of the vulnerability of these frames to disproportionate collapse. Compared to frames with FR connections, frames with PR connections usually have weaker beams and columns, which are susceptible to both connection failure and column buckling. Both failure modes can be captured by the EPP method.

Although the EPP analysis procedure was developed for planar frames, it can be easily extended and used in 3D structure analysis (with or without consideration of the effect of floor or roof slabs) for cases in which the damage scenario involves sudden removal of one column and a dominant vertical vibration mode usually exists. The areas affected by the sudden removal of a column can be pushed down by increasing gravity loads from zero until an energy balance is reached. Areas other than those immediately adjacent to the bay in which damage occurs can be preloaded with gravity loads before pushdown.

The EPP analysis procedure, as developed in this chapter, is limited to regular building frames and damage scenarios involving removal of one or two columns where a dominant vibration mode exists in the damaged structure. If two or more primary load-bearing elements including beams (beam-column connections) are damaged suddenly, the assumption of one dominant vibration mode may not be valid. Moreover, in the nonlinear range, the effect of mode coupling can be significant. Finally, the impact of uncertainties in strength of the structure in its damaged state has not been taken into account. Further research is needed to investigate the limitations of the EPP method to irregular frames and to account for such uncertainties in practical design.

CHAPTER 6 SUMMARY, CONCLUSIONS AND FUTURE WORK

6.1 SUMMARY AND CONCLUSIONS

Structural models for modeling the behavior of steel building structures during collapse, a simplified method for structural robustness assessment, and assessments of robustness of typical steel building frames against disproportionate collapse have been presented in this dissertation.

The behaviors of three types of connections, which are typical of steel building construction – partially restrained T-stub connections, moment-resisting connections, and riveted connections typical in older buildings subject to retrofit - were studied with different modeling methods. A macro-model for bolted T-stub connections was developed by modeling the connection components (i.e. T-stub, shear tab and panel zone) with a series of rigid elements and connecting springs, in which element properties were developed by analysis and were subsequently calibrated to experimental data. A model for pre-Northridge moment-resisting connections was developed which considers the uncertainties in the collapse demands. The dominant connection failure mode, which involves fracture of the weld connecting the beam and column flanges, under scenarios involving sudden column loss, was developed using a J-integral formulation of fracture demand and was characterized probabilistically. This connection behavior model was validated using connection test data from the SAC project on steel frames conducted following the Northridge earthquake. Finally, riveted connections in older buildings were modeled with an improved experimental method to take advantage of available

experimental data from tests of earthquake-resistant connections and to model unequal compressive and tensile stiffnesses and catenary effects.

The connection models developed were integrated into structural models of typical steel building structures to analyze their inherent capacities to withstand disproportionate collapse following local damage stipulated by the new *Unified Facilities Criteria* (2009). For the performance following damage to load-bearing columns in steel frames with PR connections fabricated from bolted T-stubs, two prequalified T-stub connections were considered, one of which is intended to develop the full moment capacity of the beam. The evaluation was conducted for various floor plans of typical office buildings. The analysis indicated that the frames with typical strong full-strength T-stub connections can resist collapse in damage scenarios involving notional removal of one column, while the robustness of the frames with typical weak partial strength T-stub connections was questionable.

The robustness of two three-story pre-Northridge moment-resisting steel frames designed in the SAC project was assessed with nonlinear dynamic analysis utilizing (a) the requirements in the new *Unified Facilities Criteria* and (b) a system reliability analysis. In the system reliability analysis, the uncertainties in gravity loadings were also taken into account, besides the uncertainties in the capacity of the structures. The robustness assessment revealed that steel moment frames with connections similar to those found in pre-Northridge building construction may not meet the *UFC* requirements for general structural integrity following notional column removal. It was also found that uncertainties in connection behavior and gravity loads had little effect on the performance of the structures considered during collapse. Hence, a mean-centered deterministic

analysis is appropriate for the robustness assessment of similar structures in accordance with the *UFC* requirements.

Finally, the robustness of a typical older steel building was assessed The contribution from the unreinforced masonry infills, which often are found in older buildings, was considered. The building was also assessed without taking into account the effects of the unreinforced masonry infills for comparison. The analysis results showed that although the riveted connections were relatively weak, the frame can absorb the initial damages in the two stipulated scenarios when the composite behavior of the unreinforced masonry infills and the steel frame and the contributions from encasements of connections and slab are considered. The frame can survive following the removal of one interior column of the first floor even when the effects of the infill panels are neglected, which was partly due to the shorter spans in older steel buildings. Therefore, the older steel buildings similar to the building considered herein can be considered to be robust against disproportionate collapse.

To provide an alternative method of static analysis of disproportionate collapse vulnerability that can be used as a preliminary assessment tool for regular building frames suffering local damage, an energy-based nonlinear static pushdown analysis procedure was developed. Dominant vibration modes first were identified through modal analysis of a structure following sudden column loss. Following this identification of the vibration characteristics, the damaged structure was divided into two parts, each of which can be reasonably described by a SDOF system. The method was then derived based on the assumption that the system could be modeled as a SDOF system and imposing the proper boundary conditions. The predictions from the EPP analysis procedure were

sufficiently close to the results of a NTHA that the method would be useful for disproportionate collapse-resistant design and robustness assessment of buildings with regular steel framing systems.

6.2 RECOMMENDATIONS FOR FUTURE RESEARCH

Several disproportionate collapse research issues have been successfully addressed in this study. However, further investigations are still needed on some topics as follows.

The annual mean occurrence rate of a specific type of extreme event impacting a building is related to the occupancy of that building and its importance and prominence in the community. For instance, government buildings are at higher risk of terrorist attack than residential buildings; conversely, residential buildings have a higher risk of fire or gas explosion than government buildings. However, the annual mean occurrence rate of terrorist attack of residential buildings near government buildings may be higher than for other residential buildings. The annual mean occurrence rate can be important to the disproportionate collapse risk assessment of a specific type of buildings, because small variations in λ_H in Equation (2-1) may have a significant impact on which risk mitigation strategy – nonstructural or structural - is most cost-effective. Hence, the purpose, location, size, occupancy, and etc. of the building must be considered when the incidence of extreme events is evaluated.

When assessing disproportionate collapse risk, tone must decide "how safe is safe enough." The *de minimis* threshold, expressed in terms of annual frequency less than 10^{-6} per year, may be a reasonable criterion for an individual risk, below which no actions

need to be taken (Pate-Cornell 1994). However, the public response and social impact also should be considered to decide the *de minimis* threshold for each individual risk. It is possible that the *de minimis* threshold for terrorist attack (e.g. bomb blast) is smaller than the thresholds for hazards that are more familiar to the public. A consistent way of measuring risk between competing alternatives remains to be established. Furthermore, the consequence of disproportionate collapse should be included in the risk acceptance criteria; up to the present time, this has not been done (NIST 2007). At the same risk level, the extreme event that can be addressed most economically should receive the highest priority. These issues have not been addressed in any significant way.

The disproportionate collapse risks of typical steel building structures in the United States exposed to multiple-abnormal loads including fire, natural gas explosions, vehicular collision, and bomb blast should be benchmarked to identify the scope of the problem for the building population and to suggest future avenues of research and code implementation. Recent studies of vulnerability of steel buildings to disproportionate collapse (Grierson, et al, 2005; Foley, 2006) have been strictly deterministic. The comparison of the risk corresponding to each individual extreme event is necessary to identify the most "dangerous" extreme event to a specific type of building. Also, the total risk should be calculated and compared with the target criterion to illustrate the vulnerability of existing steel building structures subjected to abnormal loads.

Cost-benefit analyses should be conducted to identify effective methods for reducing the disproportionate collapse risk for a specific building subjected to multiple hazards. Furthermore, actions may be required to prevent disproportionate collapse for a group of buildings . A group of buildings of same type (e.g. bank buildings) needs to

protected against multiple hazards within budgetary limitations. Such analyses have yet to be performed, despite their importance to risk-informed decision making.

REFERENCES

AISC. (2005). *Specification for Structural Steel Buildings*, American Institute of Steel Construction, Chicago, IL.

Alemdar, B. N., and White, D. W. (2005). "Displacement, Flexibility, and Mixed Beam--Column Finite Element Formulations for Distributed Plasticity Analysis." *Journal of Structural Engineering*, 131(12), 1811-1819.

ASCE. (2006). *Minimum design loads for buildings and other structures (ASCE Standard 7-05)*, American Society of Civil Engineers, Reston, VA.

Astaneh-Asl, A. (2003). "Progressive prevention in new and existing buildings." *Proc., 9th Arab Structural Engineering Conf., UAE Univ., Abu Dhabi, U.A.E., 1001–1008.*

Astaneh-Asl, A., Madsen, E., McCallen, D., and Noble, C. (2001). "Study of catenary mechanism of cables and floor to prevent progressive collapse of buildings subjected to blast loads." *Rep. to Sponsor: General Services Administration*, Dept. of Civil and Environmental Engineering, Univ. of California, Berkeley.

ATC. (1992). *Guidelines for Cyclic Seismic Testing of Components of Steel Structures, ATC-24.*, Applied Technology Council , Redwood City, California.

Azizinamini, A., Bradburn, J., and Radziminski, J. (1985). *Static and cyclic behavior of semi-rigid steel beam-column connections*, University of South Carolina.

Azizinamini, A., Bradburn, J. H., and Radziminski, J. B. (1987). "Initial stiffness of semi-rigid steel beam-to-column connections." *Journal of Constructional Steel Research*, 8, 71-90.

Baker, J. W., Schubert, M., and Faber, M. H. (2008). "On the assessment of robustness." *Structural Safety*, 30(3), 253-267.

Barakat, M., and Chen, W. F. (1991). "Design Analysis of Semi-Rigid Frames: Evaluation and Implementation." *Engineering Journal, AISC*, Second Quarter, 55-64.

Barsom, J. M., and Rolfe, S. T. (1999). *Fracture and Fatigue Control in Structures: Applications of Fracture Mechanics*, ASTM International; 3 edition.

Bartlett, F. M., Dexter, R. J., Graeser, M. D., and Jelinek, J. J. (2003). "Updating Standard Shape Material Properties Database for Design and Reliability." *AISC Engineering Journal*, 40(1), 2-14.

Batho, C., and Lash, S. D. (1936). *Further Investigations on Beam and Stanchions Connections, Including Connections Encased in Concrete; Together with Laboratory Investigations on a Full-Scale Steel Frame*, Final Report of the Steel Structures Research Committee, pp 276-363, Department of Scientific and Industrial Research, His Majesty's Stationery Office, London.

Beall, C. (1984). *Masonry design and detailing: for architects, engineers, and builders*, Prentice-Hall.

Beremin, F., Pineau, A., Mudry, F., Devaux, J.-C., D'Escatha, Y., and Ledermann, P. (1983). "A local criterion for cleavage fracture of a nuclear pressure vessel steel." *Metallurgical and Materials Transactions A*, 14(11), 2277-2287.

BOCA. (1993). "National Building Code." *12th Edition*, Building Officials & Code Administrators International, Inc.

Boe, W. A. (1952). *Wind Stresses by the K-Percentage Method*, M. S. Thesis, University of Minnesota, Minneapolis.

Breen, J. E., and Siess, C. P. (1979). "Progressive collapse-Symposium summary." *ACI Journal*, 76(9), 997-1004.

Chi, W.-M., Deierlein, G. G., and Ingraffea, A. (2000). "Fracture Toughness Demands in Welded Beam-Column Moment Connections." *Journal of Structural Engineering*, 126(1), 88-97.

Computers & Structures Inc. (2002). "SAP2000." Computers & Structures Inc., Berkeley, Calif.

Crisfield, M. A. (1991). *Non-linear finite element analysis of solids and structures*, Wiley, New York.

Department of Defense (DoD). (2009). *Unified Facilities Criteria (UFC): Design of Structures to Resist Progressive Collapse*, Washington, D.C.

Dusenberry, D. O., and Hamburger, R. O. (2006). "Practical Means for Energy-Based Analyses of Disproportionate Collapse Potential." *Journal of Performance of Constructed Facilities*, 20(4), 336-348.

Ellingwood, B., MacGregor, J., Galambos, T., and Cornell, C. (1982). "Probability-based load criteria: Load factors and load combinations." *J. Struct. Div. ASCE*, 108(5), 978-997.

Ellingwood, B. R. (2006). "Mitigating Risk from Abnormal Loads and Progressive Collapse." *Journal of Performance of Constructed Facilities*, 20(4), 315-323.

Ellingwood, B. R., and Dusenberry, D. O. (2005). "Building Design for Abnormal Loads and Progressive Collapse." *Computer-Aided Civil and Infrastructure Engineering*, 20(3), 194-205.

Ellingwood, B. R., and Leyendecker, E. V. (1978). "Approaches for design against progressive collapse." *J. Struct. Div.*, 104(3), 413-423.

Ettouney, M., Smilowitz, R., Tang, M., and Hapij, A. (2006). "Global System Considerations for Progressive Collapse with Extensions to Other Natural and Man-Made Hazards." *Journal of Performance of Constructed Facilities*, 20(4), 403-417.

Federal Emergency Management Agency (FEMA). (1995). *FEMA 267: Interim guidelines: Evaluation, repair, modification and design of welded steel moment frame structures.*, Washington, D.C.

Federal Emergency Management Agency (FEMA). (1997a). *FEMA 273: NEHRP Guidelines for the Seismic Rehabilitation of Buildings*, Washington, D.C.

Federal Emergency Management Agency (FEMA). (1997b). *FEMA 289: Connection Test Summaries*, Washington, D.C.

Federal Emergency Management Agency (FEMA). (2000a). *FEMA 355C: State of the Art Report on Systems Performance of Steel Moment Frames Subject to Earthquake Ground Shaking*, Washington, D.C.

Federal Emergency Management Agency (FEMA). (2000b). *FEMA 355D: State of the Art Report on Connection Performance*, Washington, D.C.

Flanagan, R. D., and Bennett, R. M. (1999). "In-Plane Behavior of Structural Clay Tile Infilled Frames." *Journal of Structural Engineering*, 125(6), 590-599.

Flanagan, R. D., and Bennett, R. M. (2001). "In-Plane Analysis of Masonry Infill Materials." *Practice Periodical on Structural Design and Construction*, 6(4), 176-182.

Foley, C. M., Martin, K., and Schneeman, C. (2006). "Robustness in structural steel framing systems." *Rep. No. MU-CEEN-SE-06-01*, Marquette Univ., Milwaukee, Wis.

Forcier, G. P., Leon, R. T., Severson, B. E., and Roeder, C. W. (2002). "Seismic performance of riveted connections." *Journal of Constructional Steel Research*, 58(5-8), 779-799.

Fricke, K. E., and Flanagan, R. D. (1995). *Compressive strength of masonry (f'_m) for the Oak Ridge Y- 12 Plant Hollow Clay Tile Walls*, Oak Ridge Y-12 Plant, TN.

General Services Administration (GSA). (2003). *Progressive collapse analysis and design guidelines for new federal office buildings and major modernization projects*, Washington, D.C.

Grierson, D. E., Xu, L., and Liu, Y. (2005). "Progressive-Failure Analysis of Buildings Subjected to Abnormal Loading." *Computer-Aided Civil and Infrastructure Engineering*, 20(3), 155-171.

Gross, J. L. (1998). "A connection model for the seismic analysis of welded steel moment frames." *Engineering Structures*, 20(4-6), 390-397.

Gupta, A., and Krawinkler, H. (1999). "Seismic demands for performance evaluation of steel moment resisting frame structures." *John A. Blume Earthquake Engrg. Ctr. Rep. No. 132,* Dept. of Civ. Engrg., Stanford University, Stanford, Calif.

Hallquist, J. (2005). "LS-DYNA." Livermore Software Technology Corp., Livermore, Calif.

Hamburger, R. O., and Whittaker, A. (2004). "Design of steel structures for blast-related progressive collapse resistance." *Proc., North American Structural Steel Conference, American Institute of Steel Construction*, Chicago, IL. pp. 43-53.

Hamburger, R. O. C., Ashok S. (1993). "Methodology for Seismic Capacity Evaluation for Steel-frame Buildings with Unreinforced Masonry Infills." *Proc. 1993 National Earthquake Conference, Memphis, Tennessee*, 173-182.

Hool, G., and Johnson, N. (1920). *Handbook of building construction: data for architects, designing and constructing engineers, and contractors*, McGraw-Hill Book Company, inc.

Izzuddin, B. A., Vlassis, A. G., Elghazouli, A. Y., and Nethercot, D. A. (2008). "Progressive collapse of multi-storey buildings due to sudden column loss -- Part I: Simplified assessment framework." *Engineering Structures*, 30(5), 1308-1318.

Joh, C., and Chen, W.-F. (1999). "Fracture Strength of Welded Flange-Bolted Web Connections." *Journal of Structural Engineering*, 125(5), 565-571.

Kaewkulchai, G., and Williamson, E. B. (2004). "Beam element formulation and solution procedure for dynamic progressive collapse analysis." *Computers & Structures*, 82(7-8), 639-651.

Kaufmann, E. J., and Fisher, J. W. (1997). "Failure analysis of welded steel moment frames damaged in the Northridge earthquake." NISTIR 5944, National Institute of Standards and Technology, Gaithersburg, Md.

Khandelwal, K., and El-Tawil, S. (2007). "Collapse Behavior of Steel Special Moment Resisting Frame Connections." *Journal of Structural Engineering*, 133(5), 646-655.

Khandelwal, K., El-Tawil, S., Kunnath, S. K., and Lew, H. S. (2008). "Macromodel-Based Simulation of Progressive Collapse: Steel Frame Structures." *Journal of Structural Engineering*, 134(7), 1070-1078.

Kim, K. (1995). "Development of analytical models for earthquake analysis of steel moment frames," PhD Dissertation, The University of Texas at Austin.

Kinali, K. (2007). *Seismic Fragility Assessment of Steel Frames in the Central and Eastern United States*, Ph.D. Thesis, Georgia Institute of Technology, Atlanta, GA.

Kinali, K., and Ellingwood, B. R. (2007). "Seismic fragility assessment of steel frames for consequence-based engineering: A case study for Memphis, TN." *Engineering Structures*, 29(6), 1115-1127.

Kishi, N., and Chen, W.-F. (1990). "Moment-Rotation Relations of Semirigid Connections with Angles." *Journal of Structural Engineering*, 116(7), 1813-1834.

Kiureghian, A. D. (1981). "A response spectrum method for random vibration analysis of mdf systems." *Earthquake Engineering & Structural Dynamics*, 9(5), 419-435.

Krawinkler, H. (1978). "Shear in Beam-Column Joints in Seismic Design of Steel Frames." *AISC Engineering Journal*, 15(3).

Leyendecker, E. V., and Burnett, E. (1976). "The incidence of abnormal loading in residential buildings." Building science Series No. 89, National Bureau of Standards, Washington, D.C.

Liu, Y. (2007). "Progressive-Failure Analysis of Steel Building Structures under Abnormal Loads," Ph.D. thesis, University of Waterloo, Waterloo, Canada.

Mainstone, R. J., and Weeks, G. A. (1970). "The influence of bounding frame on the racking stiffness and strength of brick walls." *Proc., 2nd Int. Conf. on Brick Masonry*, 165–171.

Marjanishvili, S., and Agnew, E. (2006). "Comparison of Various Procedures for Progressive Collapse Analysis." *Journal of Performance of Constructed Facilities*, 20(4), 365-374.

Marjanishvili, S. M. (2004). "Progressive Analysis Procedure for Progressive Collapse." *J. Perform. Constr. Facil.*, 18(2), 79-85.

Matos, C. G., and Dodds, R. H. (2001). "Probabilistic modeling of weld fracture in steel frame connections part I: quasi-static loading." *Engineering Structures*, 23(8), 1011-1030.

Mazzoni, S., McKenna, F. T., Scott, M. H., and Fenves, G. L. (2009). *Open System for Earthquake Engineering Simulation User Command-Language Manual*, <http://opensees.berkeley.edu/OpenSees/manuals/usermanual/index.html>.

McKay, M. D., Beckman, R. J., and Conover, W. J. (1979). "A Comparison of Three Methods for Selecting Values of Input Variables in the Analysis of Output from a Computer Code." *Technometrics*, 21(2), 239-245.

Mudry, F. (1987). "A local approach to cleavage fracture." *Nuclear Engineering and Design*, 105(1), 65-76.

National Institute of Standards and Technology (NIST). (2007). *Best Practices for Reducing the Potential for Progressive Collapse in Buildings*, Gaithersburg, Md.

National Institute of Standards and Technology (NIST). (2008). *Final Report on the Collapse of World Trade Center Building 7*, Gaithersburg, Md.

Pate-Cornell, M. E. (1994). "Quantitative safety goals for risk management of industrial facilities." *Structural Safety*, 13(3), 145-157.

Poh, K. W. (2001). "Stress-Strain-Temperature Relationship for Structural Steel." *Journal of Materials in Civil Engineering*, 13(5), 371-379.

Popov, E. P., Yang, T.-S., and Chang, S.-P. (1998). "Design of steel MRF connections before and after 1994 Northridge earthquake." *Engineering Structures*, 20(12), 1030-1038.

Powell, G. (2005). "Progressive collapse: Case studies using nonlinear analysis." *Proc., ASCE/SEI Structures Conf., New York.*

Rex, C. O., and Easterling, W. S. (1996). "Behavior and modeling of single bolt lap splice connections." Report No. CE/VPI-ST 96/15, November.

Rex, C. O., and Easterling, W. S. (2003). "Behavior and Modeling of a Bolt Bearing on a Single Plate." *Journal of Structural Engineering*, 129(6), 792-800.

Rice, J. R. (1968). "A Path Independent Integral and the Approximate Analysis of Strain Concentration by Notches and Cracks." *Journal of Applied Mechanics*, 35, 379-386.

Righiniotis, T. D., and Imam, B. (2004). "Fracture reliability of a typical Northridge steel moment resisting connection." *Engineering Structures*, 26(3), 381-390.

Roeder, C. W., Knechtel, B., Thomas, E., Vaneaton, A., Leon, R. T., and Preece, F. R. (1996). "Seismic Behavior of Older Steel Structures." *Journal of Structural Engineering*, 122(4), 365-373.

Roeder, C. W., Leon, R. T., and Preece, F. R. (1994). "Strength, Stiffness and Ductility of Older Steel Structures Under Seismic Loading." University of Washington.

SAC. "SAC Connections Database." http://www.sacsteel.org/connections/, SAC.

Sadek, F., El-Tawil, S., and Lew, H. S. (2008). "Robustness of Composite Floor Systems with Shear Connections: Modeling, Simulation, and Evaluation." *Journal of Structural Engineering*, 134(11), 1717-1725.

Sasani, M. (2008). "Response of a reinforced concrete infilled-frame structure to removal of two adjacent columns." *Engineering Structures*, 30(9), 2478-2491.

Smallidge, J. M. (1999). "Behavior of Bolted Beam-to-Column T-Stub Connections Under Cyclic Loading," Master Thesis, Georgia Institute of Technology, Atlanta, GA.

Stafford Smith, B. (1966). "Behavior of square infilled frames." *J. Struct. Div.*, 92(1), 381-403.

Stewart, M. G. (2008). "Cost Effectiveness of Risk Mitigation Strategies for Protection of Buildings against Terrorist Attack." *Journal of Performance of Constructed Facilities*, 22(2), 115-120.

Stewart, M. G., and Netherton, M. D. (2008). "Security risks and probabilistic risk assessment of glazing subject to explosive blast loading." *Reliability Engineering & System Safety*, 93(4), 627-638.

Swanson, J. A. (1999). "Characterization of the strength, stiffness, and ductility behavior of T-stub connections," PhD Thesis, Georgia Institute of Technology, Atlanta, GA.

Swanson, J. A., and Leon, R. T. (2000). "Bolted Steel Connections: Tests on T-Stub Components." *Journal of Structural Engineering*, 126(1), 50-56.

Swanson, J. A., and Leon, R. T. (2001). "Stiffness Modeling of Bolted T-Stub Connection Components." *Journal of Structural Engineering*, 127(5), 498-505.

UBC. (1994). "Structural Engineering Design Provisions." *Uniform Building Code*, Vol. 2, International Conference of Building Officials.

Whitmore, R. E. (1952). "Experimental investigation of stresses in gusset plates." University of Tennessee Engineering Experiment Station, Bulletin No. 16, May

Xu, G., and Ellingwood, B. R. (2011). "Disproportionate collapse performance of partially restrained steel frames with bolted T-stub connections." *Engineering Structures*, 33(1), 32-43.

Zhou, Q., and Yu, T. X. (2004). "Use of High-Efficiency Energy Absorbing Device to Arrest Progressive Collapse of Tall Building." *Journal of Engineering Mechanics*, 130(10), 1177-1187.